JOURNAL OF APPLIED PHYSICS

JOURNAL
OF
APPLIED PHYSICS

JUNE, 1942 Vol. 13, No. 6

In This Issue

Page

First Report of the War Policy Committee 345

Explosives and Their Military Applications R. H. KENT 348

Frictional Phenomena. X ANDREW GEMANT 355

Contributed Original Research

X-Ray Study of Carbon Black
J. BISCOE AND B. E. WARREN 364

Cause of High Voltage Surges in Rectifier Circuits
ALBERT W. HULL AND FRANK R. ELDER 372

Eddy Current Type Flaw Detectors for Non-Magnetic Metals IRWIN VIGNESS, J. E. DINGER, AND ROSS GUNN 377

Transient Temperatures in the Anode of an X-Ray Tube
F. R. ABBOTT 384

Vector Potential and Inductance of a Circuit Comprising Linear Conductors of Different Permeability
THOMAS JAMES HIGGINS 390

Improved X-Ray Tube for Diffraction Analysis
R. R. MACHLETT 398

Rubber in Vibration S. D. GEHMAN 402

In Every Issue

Calendar of Meetings 354

New Books 361

Here and There 363

New Instrument Booklets 413

Index to Advertisers x

BOARD OF EDITORS

ELMER HUTCHISSON,
Editor

Associate Editors

FRANCIS BITTER
W. F. BUSSE
S. H. CALDWELL
ROBLEY D. EVANS
MORRIS MUSKAT
FREDERICK SEITZ
B. E. WARREN
J. B. WHITEHEAD

Publication of the American Institute of Physics

ADMINISTRATIVE STAFF

HENRY A. BARTON,
Director

MADELINE M. MITCHELL,
Publications Manager

JOHN T. TATE,
Adviser on Publications

GOVERNING BOARD

PAUL E. KLOPSTEG,
Chairman
GEORGE B. PEGRAM,
Secretary
R. B. DOW
L. A. DUBRIDGE
FLOYD A. FIRESTONE
HARVEY FLETCHER
R. C. GIBBS
K. S. GIBSON
ARTHUR C. HARDY
GEORGE R. HARRISON
HERMANN MARK
A. G. WORTHING
JOHN T. TATE
N. W. TAYLOR
WALLACE WATERFALL

The JOURNAL OF APPLIED PHYSICS, published monthly at Prince and Lemon Sts., Lancaster, Pa., is devoted to physics in its role as the science basic to other natural sciences and to the arts and industries. Previous to 1937 this publication was known as PHYSICS. It aims to be of service not only in physical laboratories, but also in the laboratories of industrial, chemical, geological, geophysical, meteorological, radio, and similar concerns. The JOURNAL OF APPLIED PHYSICS publishes editorials, news of physicists and reviews, as well as technical papers of applied physics.

Manuscripts should be submitted to Elmer Hutchisson, Editor, American Institute of Physics, 175 Fifth Avenue, New York, New York.

Subscriptions and orders for back numbers should be addressed to Prince and Lemon Streets, Lancaster, Pa. or to the American Institute of Physics, 175 Fifth Avenue, New York, N. Y.

SUBSCRIPTION PRICE

	U. S. AND CANADA	ELSEWHERE
To members of scientific societies	$5.00	$5.70
To all others	7.00	7.70

Single copies are $.70 each.

Changes of address and proofs should be addressed to the Publications Manager.

Advertising rates supplied on request. Orders, advertising copy and cuts should be sent to the American Institute of Physics.

Entered as second class matter at the Post Office at Lancaster, Pennsylvania, under the Act of March 3, 1897.
Accepted for mailing at the special rate of postage provided for in the Act of February 28, 1925, authorized May 2, 1932.

Copyright 1942, by the American Institute of Physics.

Journal
of
Applied Physics

Volume 13 June, 1942 Number 6

First Report of the War Policy Committee of The American Institute of Physics, New York, N. Y. May 1, 1942

REPRESENTATIVES of United States Government agencies, institutions of learning, the press, and various national associations are turning more and more frequently to the American Institute of Physics for information, advice, and cooperation from physicists as a national group. These appeals present opportunities for national service. It falls within the designated scope of the American Institute of Physics to grasp such opportunities, but in order to do so the Institute must first clearly understand the place of the science and the profession in the affairs of the nation and the world. Then it must accept the responsibility of speaking with authority about physics, of reflecting truly the wise consensus of physicists.

The war has brought new problems and rapid changes. It has placed physics in an important position; in fact, the present and potential contributions of physics may well have a profound effect on the course if not the outcome of the war. The Institute has thereby acquired the responsibility of keeping abreast of changes, and of presenting to those concerned with the applications of physics and the use of physicists in the war effort, a currently valid and accurate portrayal of the science and the profession.

To meet these necessities the Institute established a War Policy Committee for Physics, with power to direct the "external" activities in which the Institute engages on behalf of the profession. The members of the Committee are: Dr. Oliver E. Buckley, President of the Bell Telephone Laboratories; Dr. Karl T. Compton, President of Massachusetts Institute of Technology; Dr. Homer L. Dodge, Dean of the Graduate College, University of Oklahoma; Dr. R. C. Gibbs, Chairman of the Department of Physics, Cornell University; and Dr. Paul E. Klopsteg, President of the Central Scientific Company, Chairman. Dr. Henry A. Barton, Director of the

"NEW tools of war have been devised which can swing the tide of victory. They utilize results of research in electronics, electric waves, acoustics, mechanics, and optics. Physicists have devised these new tools, engineers have shaped them for manufacture, and manufacturers are producing them. Men are needed to make the best use of them, to test and maintain them, to improve them, and to devise new ones. These men are of many kinds, from high school graduates to doctors of philosophy, but one thing they must have in common—knowledge of the fundamental laws of physics on which the operation of these tools depends.

"Training in physics for all of these operations and at all of these levels is urgently needed."

This and other subjects of great interest to physicists in this time of national emergency are covered in the accompanying report of the War Policy Committee.

Institute, is Secretary of the Committee.

There follows a report of certain conclusions and recommendations of the Committee:

1. PROFESSIONAL STATUS OF PHYSICISTS

Recent developments in technical and industrial trends have brought physicists into a position of importance in industry not heretofore existing. The present situation requires a more clear cut definition of "physicist." The War Policy Committee has adopted the following definitions as a basis and guide for its work and they are recommended to the Founder Societies for adoption:

(a) A *physicist* is one whose training and experience lie in the study and applications of the interactions between matter and energy in the fields of mechanics, acoustics, optics, heat, electricity, magnetism, radiation, atomic structure, and nuclear phenomena.

(b) To qualify as a *professional physicist* one must have had at least eight years of training and experience in physics. Toward this experience four years of formal collegiate education with major emphasis on physics may be credited, year for year, if it leads to a bachelor's degree, five years if it leads to a master's degree, and seven years if it leads to a doctor's degree, from a recognized institution. Years of teaching of physics in a recognized institution may be credited as years of experience in physics. By a *recognized institution* is meant one which appears in the list of institutions approved by the Association of American Universities.

2. TRAINING IN PHYSICS FOR THE WAR

New tools of war have been devised which can swing the tide of victory. They utilize results of research in electronics, electric waves, acoustics, mechanics, and optics. Physicists have devised these new tools, engineers have shaped them for manufacture, and manufacturers are producing them. Men are needed to make the best use of them, to test and maintain them, to improve them, and to devise new ones. These men are of many kinds, from high school graduates to doctors of philosophy, but one thing they must have in common—knowledge of the fundamental laws of physics on which the operation of these tools depends.

Training in physics for all of these operations and at all of these levels is urgently needed.

3. EMPHASIS UPON THE STUDY OF PHYSICS

Even before the war the place of physicists in industry was becoming increasingly recognized. This is made evident by available statistics concerning the growing number of physicists employed in industrial laboratories, and the expanding membership lists of national societies in the field of physics. In the last two years, as a result of war requirements, the need for physicists, as compared with other professions, has grown very rapidly. Recent estimates indicate that the need is now growing at the rate of 1500 to 2000 per year, and that the current annual supply from schools is no more than 500. The need referred to applies to individuals having five or more years experience in physics in the sense of Section 1 (b) above (i.e., at least one year of study or experience after the bachelor's degree). It does not include the much larger need for individuals well enough prepared in mathematics and physics for training in technical war operations. This need has been officially estimated at more than 100,000. The War Policy Committee considers this a very conservative estimate.

Accordingly, it is urged upon officers and faculty members of high schools, colleges, and universities to recommend immediately that students enroll in courses in fundamental physics and their prerequisites in mathematics, whatever the stage in the student's educational career. The recommendation should be made only to students who possess natural aptitude for these studies. Such guidance for the student will to a marked degree increase his value to his country in this critical time.

Advisers of students may wish to point out to the latter that the study of physics (irrespective of any postwar career) is immeasurably helpful in any walk of life, because such study improves the ability to understand the new physical environment which man is creating for himself, and which far more even than now, is bound to exert a major influence upon social, political, and economic trends.

Moreover, great new developments now ap-

pearing behind the veil of war secrecy are, beyond all possibility of doubt, establishing the basis for unprecedented peacetime applications of physics in industry. Some of the greatest of these are along lines not yet developed as branches of engineering. They give promise of opening large and fruitful fields for the useful and profitable employment of those well equipped with a broad, fundamental training in physics.

The Committee recommends to high schools that they emphasize mathematics through trigonometry, and that in teaching physics the aim should be to give a well-planned, thorough course in the fundamentals of the subject. Unless the high school is properly equipped to offer specialized training in the applications of physics, it should leave this to the higher institutions.

To colleges and universities the Committee recommends making provision for the most advanced courses for which students are qualified and, where facilities are suitable, the establishment of intensive courses, with laboratory practice, in electronic devices and high frequency circuits.

4. SPECIAL TRAINING OF PHYSICISTS

Since the demand for physicists exceeds the supply which can be expected from the normal operations of schools and colleges, this Committee endorses the program of special agencies operating to supplement this supply.

5. USE OF PHYSICISTS

The need for physicists in the total war effort is so vital, and the demand so greatly exceeds the supply, that it is essential that every available individual trained in physics be placed in a position in which full use is made of that training. The Committee therefore would strongly endorse the adoption of any policies and regulations by the Selective Service System, personnel divisions of the Armed Services, and other government agencies concerned, to achieve this end more effectively.

RESEARCH'S biggest job is to discover frontiers. Our economy doesn't work on perpetual motion. If we have any idea of continuing the prosperity we have enjoyed for the last hundred years, we are going to have to come to a recognition of the fact that the business of seeking for new frontiers in the form of new industries is one of our major jobs. I doubt if anyone was conscious of creating a new industry at the time it was started. Certainly, Oersted didn't know he was creating the electrical power industry when he held an electric wire over a compass needle and saw it swing into the line of flux. Alexander Graham Bell had no idea of creating the telephone industry when he started his experiments to improve the telegraph. The fact I am calling attention to is that these new industries were *created.*

I am an optimist. I have every confidence in the future. If we had a universal diary in which the people wrote down what they thought of the world for every year since the beginning of history, and opened it at random to any page, we would find that all the entries would read pretty much the same. "We have progressed a long way from where our forefathers were," it would say, "but we don't see how people in the future are going to go much further than we have." Unimaginative people have always complained about the lack of frontiers. Always the human race has found new frontiers and new opportunities. Nobody can look at the record without gaining renewed confidence in the fact that we are going ahead. The world isn't finished. The day of discovery has not passed. There will always be new frontiers.

CHARLES F. KETTERING in "Prospecting for Knowledge" in the *Bakelite Review*, January, 1942

Explosives and Their Military Applications*

BY R. H. KENT

Ballistic Research Laboratory, Aberdeen Proving Ground, Maryland

AN explosive is a substance or mixture of substances which is likely, on the application of heat, friction, or a blow to a small portion of the mass, to be converted in a very short interval of time into other more stable substances largely or entirely gaseous. A considerable amount of heat is also invariably evolved, and consequently there is a flame. The very sudden or violent transformation of the explosive into the more stable gases is called an explosion.

Explosions are usefully divided into two classes depending upon the manner of propagation of the explosive reaction from one part of the explosive substance to the other. The explosion may be propagated relatively slowly by the conduction or radiation of heat from the burnt part to the unburnt part. This is called deflagration or more simply burning. Such an explosion occurs in the burning of propellant powders in a gun. The outside surfaces of the solid grains are heated by the primer gases to a temperature of some 400°C, at which temperature a reaction occurs producing hot gases. These hot gases in turn raise the newly exposed surfaces to the ignition point and they are transformed in turn into gas. The rate of propagation of such a burning or deflagration is relatively slow. Even at the high pressure of 100,000 lb./in.^{2}, the rate is only, approximately, 2 ft./sec.

If a sufficiently powerful blow or impact is imparted to certain explosives, they will detonate instead of burn. In a detonation the reaction is propagated not by heat conduction but by wave action. A pressure wave of great violence is produced which travels at high speed through the explosive substance compressing and heating each layer of the substance it reaches. Under the influence of the wave, the unstable explosive breaks down into a gas. The successive layers are thus suddenly converted into more stable compounds, mostly gaseous. The rate of propagation in a detonation in nitroglycerin by wave action is sometimes as great as 5 mi./sec. Because of the much greater suddenness with which the explosive is converted into gases in a detonation than in a deflagration, the effects of a detonation on nearby structures and on personnel are much greater than the effects produced by a deflagration or burning. Twenty-five lb. of powder burning in a 155-mm G.P.F. gun will impart a velocity of 2400 ft./sec. to the 95-lb. projectile but will leave the gun unharmed. Twenty-five lb. of powder detonated in the G.P.F. gun would smash the gun and projectile into thousands of pieces.

Although the deflagration of explosives is a subject of great importance for interior ballistics, which deals with the motion of the projectile and gases in a gun, in this paper our further attention will be confined to the explosive substances which are intended to be detonated and the phenomena accompanying the detonation. Among such substances having military or industrial uses or both may be listed: trinitrotoluol or T.N.T., picric acid, tetryl, nitroglycerin, ammonium nitrate, and ammonium picrate.

In an explosive intended for military uses, there are three properties of great practical importance. These are (1) insensitiveness, (2) blasting power, (3) shattering power or brisance. Inasmuch as both blasting power and shattering power depend upon definite physico-chemical properties of the explosive, these latter properties will be discussed before discussing the blasting power and the shattering power themselves.

Some of the physico-chemical properties of explosives have an important bearing on their military usefulness. Among these are (1) sensitiveness, (2) force or product of gas volume and gas pressure, (3) rate of detonation, (4) density, (5) pressure, and (6) energy.

SENSITIVENESS

By the sensitiveness of an explosive is meant the ease with which it can be detonated by a shock or blow. Some explosives like lead azide,

* Released for publication by the Bureau of Public Relations, War Department, Washington, D. C.

or mercury fulminate can be easily detonated by a light blow from a hammer or firing pin. Such a sensitive explosive while very useful in fuzes to set off other less sensitive explosives, would be extremely hazardous if used as a bomb or shell filler. There would not only be a likelihood of an explosion during transportation but a shell filled with such an explosive would certainly burst in the gun. Other explosives like T.N.T. and ammonium picrate are extremely insensitive and require a most violent blow or shock to detonate them especially if they are pressed to a high density. Ammonium picrate is commonly used as a filler of armor piercing projectiles. Even the violent shock of impact against armor 12″ thick or more is insufficient to set it off. However many other desirable properties an explosive may possess, unless it is distinctly insensitive it should not be used as a bomb or shell filler because fatal nerve and morale shattering accidents will result from its use.

FORCE

The force of an explosive is roughly an index of the weight lifting or heaving ability. Suppose the explosion takes place in a large closed chamber with rigid walls. If v is the volume of the chamber and p is the steady pressure produced by the explosive gas as it fills the chamber, the force of the explosive is defined to be the product of p and v per unit weight of explosive. If the chamber volume is not too small, i.e., if the perfect gas law holds approximately, this product is approximately independent of the volume for a given explosive. If an explosive detonates in a confined space, this definition is no longer useful since the density is so high that the perfect gas law is no longer a good approximation. For such cases, one takes the force as proportional to the product of the number of gram molecules per gram and the temperature. It is evident that if the density is small this definition of force is equivalent to the one previously given.

The forces of a number of explosives obtained when the explosive is deflagrated or burned have been measured but no reliable direct measurements of forces produced by detonations have been obtained. However, it is possible to calculate the forces from thermo-chemical data. Some of these data are obtained by an analysis of the band spectra of the various molecules concerned by quantum-mechanical methods to obtain the specific heats and equilibrium constants as functions of the temperature. Others are obtained

FIG. 1. Detonation of American 600-lb. demolition bomb, reproduced by courtesy of Army Ordnance.

TABLE I. Forces of explosives.

Explosive	Force at 100,000 atmospheres inch lb./lb.
T.N.T.	3,627,000
Tetryl	4,728,000
Picric acid	3,999,000
Blasting gelatin	4,974,000

from direct measurements of the heats of formation of the various gases and substances from their elements. The results obtained by these rather complicated processes indicate that values of the forces of deflagrating or burning explosives as calculated from the thermo-chemical data agree fairly closely with the forces as obtained by direct measurement. In view of this result, one is warranted in placing a measure of confidence in the calculated results for detonating explosives.

In making such calculations, it is convenient to assume a pressure in the explosion since theory and experiment both indicate that the composition of the products of the explosion depends upon the pressure. For example, a very high pressure will tend to produce solid carbon or smoke as a high pressure on ice tends to make it melt. It is for this reason that a cloud of black smoke after an explosion of a charge of T.N.T. (Fig. 1) indicates that high pressure occurred and that therefore the charge detonated and did not merely burn which would produce a relatively low pressure. In Table I are given the forces of various explosives as calculated for a pressure of 100,000 atmospheres or approximately 1,500,000 lb./in.^{2}. The results are given in inch lb./lb. The weight lifting ability which a bomb possesses by virtue of the force of its explosive is exhibited by the crater shown in Fig. 2.

The chemical compositions of the products of explosions are of some interest. The principal products as calculated for the explosives mentioned above appear in Table II.

Certain defects in the methods used in obtaining these results should be pointed out. The equilibrium constants used in these calculations are those tabulated by Lewis and von Elbe[1] which were originally deduced by various physicists and chemists from analyses of spectral data according to methods developed by Nernst, Planck, Sackur and Tetrode, Ehrenfest and Trkal, G. N. Lewis, Giauque, Fowler, and others. These equilibrium constants, however, hold only for a perfect gas, and one may expect very important changes in these constants for the high densities which occur in detonations.

RATE OF DETONATION

If a bomb were dropped inside a building the most important characteristic of the explosion from a military point of view is probably the force as defined above. For a bomb of a given weight the outward thrust on the walls would depend mainly on the force of the explosive. Consider on the other hand a bomb dropped alongside a battleship or a submarine mine. In such a case the effect produced would depend not only on the force of the explosive but also on the rapidity with which the explosion takes place. Suppose the bomb is nose fuzed and the detonation begins at the nose. Compressional waves in the water will start at once from the nose and travel toward the battleship. The water waves from the base of the bomb will not start until the detonation has reached the base of the bomb. If this takes place after an appreciable delay, the water waves from the base of the bomb will not reach the battleship until some time after the waves from the nose. Thus the greater the

[1] B. Lewis and G. von Elbe, J. Am. Chem. Soc. **57**, 612 (1935); also their book, *Combustion, Flames, and Explosions of Gases* (Cambridge, 1938). For ammonia, the data were obtained from E. Justi, *Spezifische Wärme, Enthalpie, Entropie, Dissoziation technischer Gase* (Berlin, 1938). Apparently the data for ammonia are not very reliable.

TABLE II.

Explosive	Percentage products of explosion by weight*												
	CO_2	CO	H_2O	H_2	N_2	OH	NO	O_2	O	C	CH_4	NH_3	HCN
T.N.T.	7.3	59.7	3.2	0.7	16.2					5.7	3.5	1.2	2.5
Tetryl	8.4	59.8	4.8	.8	22.3						0.5	1.2	2.2
Picric acid	12.5	63.1	4.3	.5	17.0						.5	.7	1.4
Blasting gelatin	49.4	7.5	18.5	.1	16.8	2.2	2.7	2.7	0.1				

* I am indebted to J. R. Lane, D. Shanks, and H. Mark for these and other calculations.

delay in the arrival of the detonation at the base of the bomb the more gradual and less violent will be the blow delivered on the side of the battleship. For this reason the speed with which the reaction is propagated or the rate of detonation is of considerable military importance.

In Table III are listed the speeds of detonation of various explosives as given by Marshall.[2] It should be noted that these values are not very definite since the rate of detonation depends upon several factors such as the violence of the initiating explosion, the diameter of the explosive column, the material surrounding the explosive column, etc. The table gives the highest rates obtained under ordinary conditions.

TABLE III.

Explosive	Rate of detonation mi./sec.
Mercury fulminate $Hg(ONC)_2$	3.36
Lead azide N_6Pb	3.29
Gun cotton	4.54
Nitroglycerin	5.44
Blasting gelatin	4.85
T.N.T.	4.41
Tetryl	4.67
Picric acid	4.50
Amatol 80/20	3.23

DENSITY

Another very important characteristic of an explosive especially for submarine explosions such as those of mines, torpedoes, and of bombs dropped alongside a ship is the density of the explosive. If the volume in which the explosion occurs is large compared with the volume of the explosive substance the free space available for the motion of the molecules of the explosive gas is large compared with the volume of the molecules themselves. Under these conditions, the perfect gas law holds approximately, that is, the product of pressure p and volume v is approximately a constant, or it is approximately independent of the volume v. It follows that under these conditions with a given amount of explosive, the pressure is approximately proportional to $1/v$.

Consider now an explosion taking place in a confined space such as that of a bomb under water. Under these conditions the volume occupied by the gaseous molecules is no longer small compared with the total volume available and the perfect gas law no longer holds. However, the previous statement holds if a new definition of v is given. Accordingly v is taken not as the total volume but as the free volume available for the motion of the molecules. Since the space taken up by the molecules is approximately proportional to their number and since the number for ordinary explosives is approximately proportional to their weight, it follows that the space occupied by the molecules themselves is approximately proportional to the weight of the explosive.

Consider now two bombs of the same volume exploding under water. The bombs are filled with two different explosives having the same force as measured in inch lb./lb. but having different densities. Suppose the explosive of bomb No. 2 has twice the density of bomb No. 1 and thus its weight will be twice as great. Since the force per pound of the two explosives is the same the total force of the explosive of bomb No. 2 will be twice as great. In addition the denser explosive will in general have more molecules than the other and these will occupy more space. Since the pressure varies inversely as the free space which is the total space minus the space effectively occupied by the molecules, the pressure produced by the denser explosive should be considerably more than twice as great as that produced by the less dense explosive. In certain applications, especially submarine work, the magnitude of the pressure obtainable should be of great importance, hence the desirability of high density.

Table IV gives approximately the greatest density available with various explosives under practicable working conditions.

TABLE IV.

Explosive	Density g/cm³
Nitroglycerin	1.60
Blasting gelatin	1.63
T.N.T.	1.55*
Tetryl	1.65
Picric acid	1.69

* Average density cast in shell.

[2] A. Marshall, *Explosives* (London, 1932), volume 3, second edition.

PRESSURE

The pressures occurring in an ordinary military explosive at the instant of detonation are enormous. They are so great that so far as is known their direct measurement has not even been attempted. However, a knowledge of these pressures would be of great practical value in rating explosives. Although these pressures have never been directly measured, there is a certain phenomenon accompanying a detonation which enables us to assign an at least approximate lower limit to the pressure developed. This phenomenon is the black smoke composed of carbon particles produced by many detonations. (See Fig. 1.)

It is known on physico-chemical grounds, that at low pressures and high temperatures there would be no black smoke formed; all of the carbon would unite with oxygen or hydrogen. However, the total volume of the gas when no smoke is present is greater than when smoke occurs. If the pressure is great, it tends to reduce the volume, which entails the production of smoke.

From knowledge of the thermo-chemical data, one can compute approximately the pressure at which smoke begins to form for various explosives. Then if it is noted that smoke does form in appreciable quantities, there is reason to suppose that the actual pressures are greater than those computed on the above basis. It should be noted that it is assumed that the explosive gas has not been cooled appreciably, since the cooler the gas, the greater the amount of smoke for a given pressure.

It has been calculated that the smoke forming pressure for nitrocellulose is 1,100,000 lb./in.^{2}. Since it has been noted that this explosive forms smoke when detonated,* it is a reasonable inference that the pressure produced by the detonation is greater than that given. How much greater is not known.

ENERGY

To damage structures requires energy. Hence it is apparent that the energy of an explosive is one of its most important characteristics from the point of view of its military application. When a charge first detonates the gas is under a very high pressure, but is moving at a relatively low velocity. As the gas immediately begins to expand the heat energy is converted in part into kinetic energy of motion of the gas, while another part is used in pushing aside the atmosphere. At short distances from the point of explosion, the pressure in the expanding gases is very much reduced but the envelope has attained a velocity of the order of 10,000 or 15,000 ft./sec. A gas of high density moving at such a velocity is very destructive.

The energy of an explosive may be calculated by methods similar to those mentioned in computing the force of an explosive. The energies of a number of explosives as thus calculated follow:

Explosive	Energy cal./g.
T.N.T.	782
Picric acid	830
Tetryl	988
Blasting gelatin	1364

BLASTING POWER

Experiment and theory both indicate that the blasting power of an explosive, i.e., its ability to produce damaging blast effects, depends mainly on the high velocities attained by the exploding gases in the vicinity of the point of explosion. Since it requires energy to produce these high velocities it is evident that blasting power depends upon the energy of the explosive. In fact it is a plausible assumption that blasting power is proportional to the energy. On this basis the relative blasting powers of a number of explosives with T.N.T. taken as unity are listed below.

Explosive	Relative blasting power (estimated)
T.N.T.	1.00
Picric acid	1.06
Tetryl	1.26
Blasting gelatin	1.74

SHATTERING POWER OR BRISANCE

As has been seen, for closely confined explosives, the force, the rate of detonation, and the density are all of great importance. To obtain a means of rating confined explosives taking all three factors into account the well-known German authority, Kast, considers that their effectiveness is proportional to the product of the three, i.e., the product of force, rate of detonation,

FIG. 2. Crater from detonation of American 1100-lb. demolition bomb, reproduced by courtesy of Army Ordnance.

and density. Kast calls this product "brisance" which may be roughly defined as shattering power. It appears that the brisance as defined by Kast considerably underestimates the effect of density since it seems to ignore the increase in pressure produced by the reduction of free volume as the density increases.

The comparative brisances of various explosives are given below taking the brisance of T.N.T. as unity.

Explosive	Relative brisance
T.N.T.	1.00
Picric acid	1.23
Tetryl	1.47
Blasting gelatin	1.59

THE PHENOMENA ATTENDING AN EXPLOSION

Some of the important military characteristics of explosives such as insensitiveness, blasting power, and shattering power have been discussed. An attempt will now be made to describe in a general way what happens when an explosive explodes. Suppose a 2000-lb. bomb with a booster and a quick acting point detonating fuze hits the deck of a battleship or an airdrome. The fuze is so constructed that as its firing pin hits the target it is pushed back striking some sensitive priming mixture. The friction of the sharp point causes it to detonate. The wave from the priming mixture then hits the explosive in the booster. The booster explosive is less sensitive than the priming mixture but more sensitive as a rule than the T.N.T. or other explosive which constitutes the main charge of the bomb. The wave from the priming mixture initiates a more powerful detonating wave in the explosive charge of the booster which soon reaches the T.N.T. or other explosive of the bomb and causes it to detonate in turn. If the bomb is six feet in length and the rate of detonation is, for example, 18,000 ft./sec., it will require only about 1/3000 of a second for the solid T.N.T. to be converted into a dense gas at a pressure of the order of a million lb./in.^{2}. Under the influence of this enormous pressure, the steel case of the bomb is shattered into thousands of fragments and the gas somewhat retarded by the atmospheric inertia begins to expand rapidly. Within a distance of a few feet, the velocity of the outer envelope of the explosive gas mass attains a magnitude of some 10,000 or 15,000 ft./sec. while a velocity of about 3000 ft./sec. is imparted to the fragments. The fragments thus become lethal missiles and remain so until they have lost a good part of their velocity because of air resistance. As the velocity of the gas envelope increases, the pressure within the gas decreases to such an extent that at a distance of a few feet from the bomb it is only a small fraction of the original pressure. Although the pressure at say 10 ft. from the bomb is relatively low, the gases

by virtue of their velocity of 10,000 ft./sec. or more are enormously destructive. A wind of 100 or 150 mi./hr. is considered as very destructive. How much more destructive is a wind of 7000 mi./hr.! The blast effect often referred to is truly the effect of a blast in the original meaning of the word, a violent wind, but not in the sense sometimes associated with explosives, that is, a shattering effect. The blast is indeed a wind of terrific force.

As the gas continues to expand, it does work on the surrounding atmosphere and loses its kinetic energy until at a distance of approximately 50 ft. the velocity of the envelope of the gas becomes zero. By this time, however, the pressure within the gas mass has fallen to a point appreciably below atmospheric and the surrounding air rushes in to fill the partial vacuum. Previous to this, however, the expanding gas compresses the air surrounding it, producing pressures in excess of atmospheric and velocities of the order of that of the gaseous envelope. This excess of pressure and air velocity is transmitted as a wave of gradually decreasing amplitude to great distances.

The ensuing flow of the air into the partial vacuum surrounding the point of explosion causes a rarefaction of the air which is also transmitted as a wave. Thus at a point somewhat remote from the explosion there will arrive a wave of compression followed by one of rarefaction of smaller amplitude. The compressional wave will tend to push in roofs and windows, etc., while the wave of rarefaction will tend to suck them outwards. If the structure is strong enough to withstand the compression, it is frequently so weakened that it cannot withstand the effects of the rarefaction and will burst outward, a tendency which may be reinforced by the rebound from the previous wave of compression. Depending upon the violence of the explosion, the distance, and the type of construction, some structures will be crushed in and others will burst outward. According to eyewitnesses of the Lake Denmark explosion, this is what happened in that tremendous explosion.

Calendar of Meetings

June

8–11 American Society of Mechanical Engineers, Cleveland, Ohio
8–12 American Medical Association, Atlantic City, New Jersey
15–20 American Association for the Advancement of Science, Salt Lake City, Utah
16 American Association of Physics Teachers, Salt Lake City, Utah
18–20 National Colloid Symposium, Boulder, Colorado
22–26 American Society for Testing Materials, Atlantic City, New Jersey
22–26 American Institute of Electrical Engineers, Chicago, Illinois
25–27 American Physical Society, State College, Pennsylvania
25–27 American Association of Physics Teachers, State College, Pennsylvania
29–July 1 Institute of Radio Engineers, Cleveland, Ohio
29–July 1 American Society of Heating and Ventilating Engineers, St. Paul, Minnesota

July

11 American Physical Society, Pacific Coast, Berkeley, California
20–22 Optical Society of America, Cambridge, Massachusetts
22–24 American Society of Civil Engineers, Spokane, Washington

September

7– 9 Mathematical Association of America, Ithaca, New York
7–11 American Chemical Society, Buffalo, New York
8–11 American Mathematical Society, Ithaca, New York
9–11 American Institute of Electrical Engineers, Vancouver, B. C.

Frictional Phenomena. X

BY ANDREW GEMANT

The Detroit Edison Company, Detroit, Michigan

Chapter X. Lubrication

Abstract

THE application of the viscosity concept to this technically important field is presented. Discussed first is film lubrication which occurs when the film thickness is greater than 10^{-5} cm. This mechanism is chiefly controlled by the viscosity η of the liquid. The basic mathematical theory is developed, and it is shown how this adequately describes the experimental facts. Next boundary lubrication is discussed, a type occurring with stable layers less than 10^{-5} cm thick. This mechanism is essentially a plastic flow within the boundary layer. The chief experimental data are described together with their technical implications.

39. Film Lubrication

Because of the many extensive monographs available on the subject of lubrication, it will not be necessary to discuss it in detail. Its inclusion in the present discussion cannot, however, be completely avoided, since the technical problem involved is of great importance and, besides, is an excellent illustration of various viscous processes. In fact, there are three different frictional phenomena involved.

The problem is how to minimize frictional forces between two rubbing (gliding or rolling) solid surfaces as encountered in nearly any machinery. This type of friction is called *external solid friction*. Its peculiarities will be discussed in Chapter XV of this monograph.

Lubrication consists of bringing a small amount of a suitable liquid between the surfaces in question. Thus solid friction is eliminated and replaced by the *viscosity* of the liquid, as dealt with in the preceding chapters. This particular process, called perfect or film lubrication, will be dealt with in this section.

Lubrication can also be effected by such small amounts of liquid that a liquid flow in the usual sense cannot take place. A boundary layer of only submicroscopic thickness is present on the solid surface, the motion in that layer resembling in many ways the *plastic flow* of solids, to be dealt with separately in Chapter XI. Certain peculiarities of this so-called imperfect, or boundary, lubrication will be discussed in the following section.

The theory of perfect lubrication was developed by O. Reynolds and later by A. G. M. Michell. In the following, a brief deduction of the basic equations will be presented, particularly for the sliding type of motion. The treatment of the rolling motion, although in principle the same, is mathematically more involved.

Let us assume that the lower surface in Fig. 73 moves in the x direction with velocity u_0, and that the upper surface is at rest. One has to imagine that the upper surface carries a load, the pressure per unit surface of which is p_0.

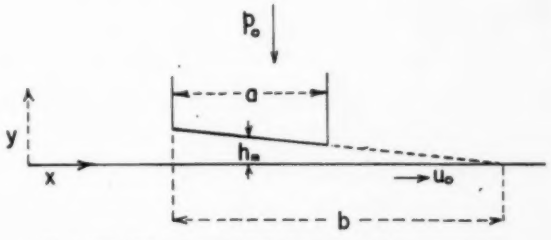

FIG. 73. Diagram of lubricated gliding contact.

If, now, lubricating oil is supplied to the interface, experience shows that:

(a) The load will lower the upper surface until an average separation h_m is attained, the latter decreasing with increasing load.

(b) The upper surface will assume an inclination towards the lower such that a kind of wedge is formed, into which the oil is being pulled by the moving surface. An analysis shows that the ratio a/b (a=width of slipper, b=measure of inclination, see Fig. 73) depends upon the position of the load—the farther to the right the latter, the stronger the inclination and the larger the ratio a/b. In actual devices, for instance the Michell thrust block (Fig. 74), the position of the load acting on the slipper is fixed; thus the ratio a/b is given. The angle

between the two surfaces then will decrease with increasing load, free pivoting of the slipper allowing the correct angle to be obtained.

The problem is now to obtain the film thickness h_m as a function of the apparatus constants a and b, the velocity u_0, the viscosity of the liquid η, and the applied pressure p_0. When h_m is computed, the frictional force will be known too.

In calculating[1] h_m one has to start from the fundamental differential equation

$$\eta(d^2u/dy^2)=dp/dx. \tag{108}$$

This equation is the same as that used in Section 7; the result of integration is, however, different because of the boundary conditions. Our conditions are now $u=u_0$ for $y=0$, and $u=0$ for $y=h$ (h being the variable height). With these conditions, the double integration with regard to y yields:

$$u=(dp/dx)(1/2\eta)(y^2-hy)+(u_0/h)(h-y). \tag{109}$$

Again, as in Section 7, the total volume V (breadth of slipper taken as unity) is given by $\int_0^h u\,dy$, thus

$$V=(u_0h/2)-(h^3/12\eta)(dp/dx). \tag{110}$$

Because of the continuity of the flow, V must be a constant with varying x. Hence, one has from Eq. (110) the differential equation for p

$$dp/dx=12\eta(u_0/2h^2-V/h^3), \tag{111}$$

where h is a function of x. Assuming a device as shown in Figs. 73 and 74, one has for this function:

$$h=\frac{b-x}{b-a/2}h_m. \tag{112}$$

Carrying out the integration of Eq. (111) by using (112), the integration constant will be given by the boundary condition that there is atmospheric pressure at the entrance of the film; $p=p_{at}$ for $x=0$. In writing $x=a$ in the integrated equation, p again must be p_{at}, since there is atmospheric pressure also at the rear of the film. This latter condition allows the quantity V to be computed and thus to be eliminated from the equation $p(x)$. The result of this computation will be

$$p=p_{at}+\frac{3\eta u_0x(a-x)}{h^2(b-a/2)}. \tag{113}$$

Equation (113) describes the change in pressure along the film. If h were constant along the film, the excess pressure $(p-p_{at})$ would start with zero, increase parabolically, reach a maximum in the middle of the slipper and fall off towards the rear in a symmetrical manner. This symmetry is disturbed by the variation with x of h, causing a shift of the maximum to the right from the middle. This is in agreement with the design of the thrust block shown in Fig. 74, the asymmetry, as pointed out before, being a function of a/b.

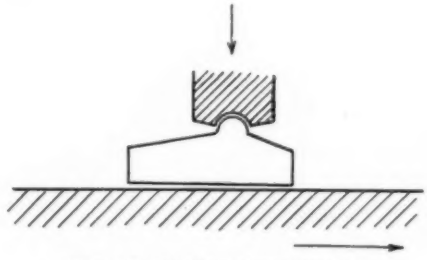

FIG. 74. Michell thrust block.

In replacing x in Eq. (113) by $a/2$, a value very nearly equal the maximum excess pressure is obtained. Since the pressure distribution is nearly parabolic, $\frac{2}{3}$ of the maximum value will give the mean value. But this must be equal to the applied average pressure p_0, as defined above. Thus

$$p_0=\eta u_0a^2/h_m^2(2b-a), \tag{114}$$

if h in Eq. (113) is replaced by its average value h_m. Solving for h_m,

$$h_m=[\eta u_0a^2/p_0(2b-a)]^{\frac{1}{2}}; \tag{115}$$

thus the required function is obtained. The thickness decreases with increasing pressure, as mentioned before; it further increases with increasing viscosity and speed.

The mean frictional force is evidently $\eta u_0/h_m$; as a closer analysis shows, this value is only an approximation, but it will suffice for our purpose. In replacing h_m by its value (115), the frictional force:

$$\left[\left(\frac{2b-a}{a}\right)\frac{\eta u_0p_0}{a}\right]^{\frac{1}{2}} \tag{116}$$

is obtained.

In the treatment of external solid friction it is usual to define the frictional force per pressure

unit as the coefficient of friction, evidently a dimensionless number. The coefficient of friction in case of film-lubricated gliding surfaces is

$$\left[\left(\frac{2b-a}{a}\right)\frac{\eta u_0}{a p_0}\right]^{\frac{1}{2}}. \qquad (117)$$

Expressions (116) and (117) show that the frictional force increases with the square root of the viscosity and the velocity. The order of magnitude of the coefficient of friction is 10^{-3}–10^{-2}. The order of the film thickness is around 10^{-4}–10^{-3} cm.

Rolling friction in journal bearings is dealt with similarly (Fig. 75). Instead of the quantities a, h, and b, the journal radius r, the clearance c between journal and bearing, and the eccentricity e of the journal will enter the equations.

Recently M. Muskat and co-workers[2] have done extensive work to improve the existing theories, the basic principle of which was just outlined. They developed analytical expressions for the plane slider for any position of the pivot. Experimentally determined coefficients on steel and brass sliders were mostly in excellent agreement with the theory. Another paper of a mathematical nature is that by A. Rosenblatt.[3]

Cowlin[4] in a recent paper deals with the practical aspects of lubrication in turbine-driven generators, particularly with the design and capacity of oil pumps, tanks, and pipes. McKee[5] considers the criteria of safe operation

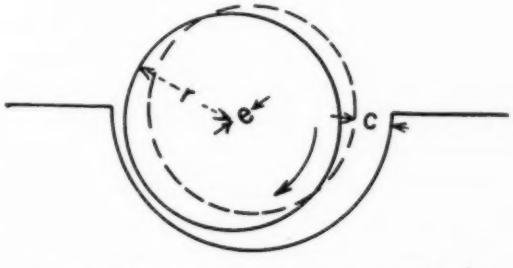

FIG. 75. Diagram of lubricated journal bearing.

of journal bearings; he derives them from thermodynamical and hydrodynamical relations that control thermal stability, and uses experimentally obtainable friction and heat dissipation data.

The technological aspects of film lubrication offer a vast field of activity to the chemical engineer; a few remarks, however, should suffice in this connection.

(1) Equation (117) indicates that low viscosity of the lubricant is desired. However, too low values are undesirable because such films might easily break down.

(2) A further important requirement is chemical stability against oxidation, particularly at elevated temperatures prevalent in the bearings. The requirements under (1) and (2) have led to the preferential use of medium viscosity mineral oils as lubricants.

(3) More specifically, the viscosity *vs.* temperature curve should not be too steep, in order not to obtain too low viscosities when the temperature rises. Spiers[6] showed that temperatures in bearings increase rapidly with decreasing clearance, and that oil cooling has little value in reducing these temperatures.

(4) Also the pressure variation of viscosity should be within certain limits. Muskat[7] recently investigated this question as well, showing that the exponent in the exponential viscosity-pressure relation (Section 22) should not exceed the value 2. The limiting load, therefore, can be made higher, by selecting lubricants of relatively flat viscosity-pressure curves.

The usefulness of different lubricants is often tested by investigating the wear/load characteristics of a given metal-lubricant combination.[8] A suitable apparatus for carrying out such tests is the 4-ball testing apparatus.[9] Clayton[10] uses the same test to investigate seizure of the lubricated surfaces, a phenomenon occurring when the film breaks down.

As was just pointed out, the chemical stability of lubricating oils is as essential as are their viscosity characteristics. Many tests have been carried out in order to study the oxidation rate of various oils. A recent extensive study by Fenske,[11] which included the determination of all volatile and non-volatile end products, should be mentioned. The present author[12] described a rapid test on the oxidation rate of oils, allowing conclusions to be drawn from the change of the volume of the gas phase in contact with the oil as plotted against time. Webber[13] discusses tests on soap greases, including corrosion tests, high temperature stability, and low temperature efficiency. A. C. Egerton[14] in his extensive

published studies on combustion engines deals also with lubricating oils; he showed, for instance, that nitrogen oxides formed in the fuel gases act as catalysts on the oxidation process and cause gumming of the oil.

The proper treatment of lubricating oils is an important side line of the whole problem. Stuart[15] points out that filtration, in addition to cleaning the oil mechanically, also acts on an adsorption basis. Worth[16] describes among other methods used for purification the electrostatic precipitation of impurities. Hansen[17] deals with mechanical, adsorption, and chemical methods of purification.

The effect of the metal upon the lubricating oil is also a point to be considered. Matthijsen[18] investigated the catalytic effect of ferrous and non-ferrous metals upon the aging of lubricating oils. Incidentally, bearings are made also of plastics instead of metal, and it is claimed[19] that when lubricated with oil, grease, or water they prove useful in many industries.

40. Boundary Lubrication

In the preceding section, films of 10^{-4}–10^{-3} cm thicknesses were considered, the viscous flow in which replaces the solid friction of the two surfaces. If the load increases, the thickness of the film decreases, until the layer becomes so thin that it breaks down and seizure of the surfaces occurs. This statement is correct for mineral oils used as lubricants. It will not hold, however, if other types of materials of chiefly dipolar nature, like alcohols, organic acids, and esters are used. Experience has shown[20] that extremely thin layers—indeed, even monomolecular ones—are sufficient to reduce the coefficient of friction to a considerable extent.

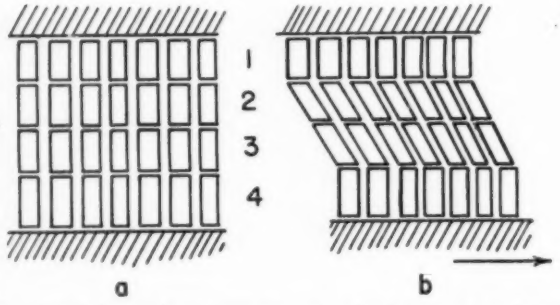

FIG. 76. Schematic picture of molecules in boundary lubrication: (a) surfaces at rest; (b) surfaces in motion.

It is evident that the mechanism of this type of lubrication must be entirely different from that discussed in the previous section. In fact, it cannot have any connection with the bulk viscosity (η) of the liquid.

The following qualitative picture of this so-called boundary lubrication is approximately correct. Figure 76(a) shows the two surfaces in contact, each covered with a thin layer, two molecules deep. The molecules in these layers show a definite orientation with regard to the surface, the nature and cause of which orientation will be explained below. When now the lower surface is moved in the right direction (Fig. 76(b)), layer 1 will still adhere to the top surface, just as layer 4 will adhere to the lower surface. The forces of attraction between subsequent layers become somewhat weaker with increasing distance from the surface; thus there will be moderate slippage between layers 1 and 2, and between layers 3 and 4, whereas a considerable slippage will take place between layers 2 and 3. Simultaneously, layers 2 and 3 will probably become tilted with respect to the normal to the surfaces.

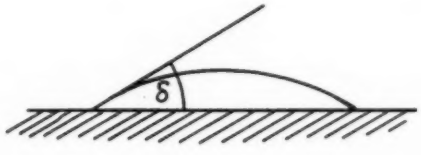

FIG. 77. Diagram showing contact angle.

The motion of these molecules is much more regular than that of molecules in a liquid; it resembles, as already mentioned, the plastic flow in solids. The peculiarities of this latter will be treated in Chapter XI, and accordingly we refer to that discussion. What remains to be dealt with here is, first, an explanation of the formation of boundary layers as described, and, second, the reporting of the chief experimental facts on this type of lubrication.

The formation of surface layers depends upon the attraction between the liquid and the solid, as measured by the so-called adhesion tension γ_{ad}. In Fig. 77 the contact angle between liquid and solid is shown, its value being given by the equation:

$$\cos\delta=(\gamma_{ad}/\gamma)-1, \qquad (118)$$

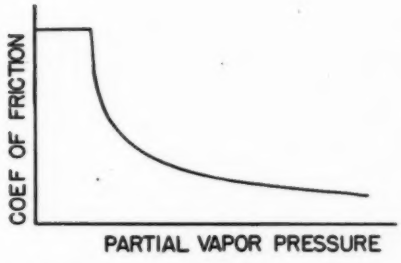

FIG. 78. Diagram showing effect of partial vapor pressure of lubricant on coefficient of friction in boundary lubrication.

where γ = surface tension of the liquid. If $\gamma_{ad} < \gamma$, then δ is obtuse and the liquid is not wetting the solid. If $\gamma_{ad} > \gamma$, then δ is acute and the liquid wets the solid. If $\gamma_{ad} = 2\gamma$, wetting becomes complete, and a stable layer is formed. For values of $\gamma_{ad} > 2\gamma$, the equation is no longer valid, but the stability of the layer, of course, increases with an increase in the ratio γ_{ad}/γ.

The adhesion tension is shown by experience to be particularly high for molecules containing polar groups, like OH, COOH, and the like. Thus mineral oils, which are best suited for film lubrication, have a relatively low wetting power on metals. This wetting property in connection with lubrication is often called oiliness in the literature. Thus it is said that vegetable oils exhibit a much higher degree of oiliness than mineral oils, the reason being that vegetable oils are chiefly esters, hence contain polar groups.

Because of the strong attraction of the polar group to the metal surface, the polar end of the molecule is nearest to the metal and the rest of the molecule, usually of the chain type, stands perpendicularly to the surface. The first complete monomolecular layer built on the surface now attracts more distant molecules and a next regular layer may be built, after that a third one, and so on. It is understandable that the rigidity of the first layer depends considerably on the nature of the metal; hence the structure also of the subsequent layers will be influenced in an indirect manner by the nature of the metal. This occurs in spite of the fact that the attraction forces decrease with a high (the sixth) power of the distance. A very extensive study of such layers has been carried out by Langmuir[21] and collaborators, clearly indicating how the orientation of each layer is determined by that of the directly preceding layer; thus showing that any influence of the metal upon further distant layers is an indirect one.

The experimental study on these lubricants allows a determination of the drop of the friction coefficient with increasing thickness of the boundary layer. A large number of these substances can be applied as vapor in contact with the metal, since a definite adsorption equilibrium will be established between the vapor phase and the metal, the thickness of the layer increasing with increasing partial pressure of the vapor. In carrying out such tests it was found that the coefficient of friction drops according to a curve indicated in Fig. 78. A definite amount of adsorbed material is required to cause a change in the value characteristic for the dry solid. Upon adsorption of the required amount this value first diminishes rapidly, and later slowly with increasing thickness of the layer.

It is quite likely that the point of sharp drop is that at which the first complete layer has been formed. Experiments of Langmuir and also Deveaux[22] have proved that monomolecular layers are sufficient to reduce the friction considerably. As to the upper limit of boundary layers, results of Bowden[23] seem to indicate that layers beyond 1000A thick are not stable.

Tests of the above-mentioned type carried out by Hardy[24] and co-workers show a definite influence of both the lubricant and the solid surface upon the value of the coefficient. Figure

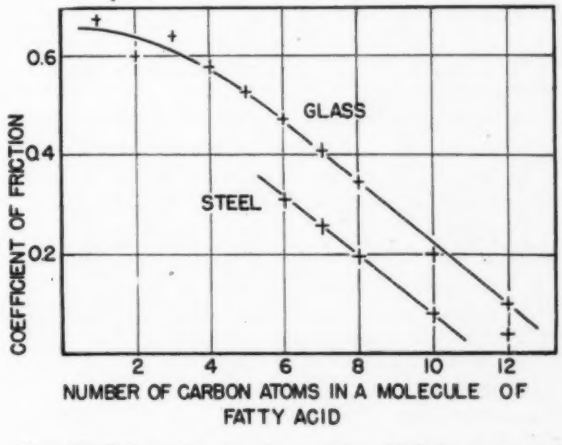

FIG. 79. Effect of molecular weight of lubricant on coefficient of friction in boundary lubrication (after W. B. Hardy).

79 gives an example for the series of fatty acids on steel and glass. The effect upon the coefficient increases linearly with the molecular weight, i.e., with the chain length. This will be understandable on the basis of Fig. 76(b), since slippage probably occurs the more easily with greater flexibility of the chains. Each layer of the total structure contributes additionally to the total friction, since slippage takes place between any two neighboring layers. Thus the interesting experimental fact, that the coefficient of friction between two different solid surfaces is an additive quantity, becomes explainable, since each solid will determine the rigidity of those layers that constitute its own adsorbed deposit. Hence the friction between steel and phosphorbronze for a given lubricant is the arithmetic average of the values between two steel and two phosphorbronze plates.

A mathematical theory of boundary lubrication does not yet exist, the whole field being still in the experimental stage. Bowden[25] in a recent paper tried to show that the behavior of such films is essentially controlled by their ability to withstand breakdown during sliding.

It is important from a practical standpoint that small additions, say 1 to 2 percent, of fatty acids to mineral oil improve the lubricating property of the latter appreciably. In these cases the oil acts not only as a viscous film lubricant, but independently by way of adsorption to form stable boundary layers of the fatty acids. The result is that at higher pressures when the oil film becomes too thin to remain stable, the acid layer still remains intact and the viscous action of the oil is then simply replaced by a plastic flow of the acid. The technical aspects of boundary lubrication are discussed in a recent paper by Fogg.[26]

Boundary lubrication may also be obtained by inorganic materials, a method that has many advantages. Such is the action of graphite, either alone or as a colloidal suspension in oil. Graphite forms flaky crystallites that are deposited parallel to the metal surface, and act in exactly the same manner as organic layers. Sometimes the action of inorganic materials is different. Thus Beeck[27] describes the use of phosphorus as a lubricant in that it forms metal phosphides upon the surface and lowers the melting point of the metal; in this manner the surface of the metal will maintain its polish, thus preventing wear. Atlee[28] suggests vaporizing metals like barium upon bearings of rotating anodes within x-ray tubes used for roentgenography. Alloys that act as a liquid lubricant are formed upon the base metal, which may be cobalt, chromium, or aluminum.

Bibliography for Chapter X

1. P. P. Ewald, Th. Pöschl, and L. Prandtl, *The Physics of Solids and Fluids* (Blackie, 1936).
2. F. Morgan, M. Muskat, and D. W. Reed, J. App. Phys. **11**, 541 (1940).
3. A. Rosenblatt, Comptes rendus **210**, 694 (1940).
4. F. J. Cowlin, Proc. Inst. Mech. Eng. **143**, 83 (1940).
5. S. A. McKee, J. Research Nat. Bur. Stand. **24**, 491 (1940).
6. J. Spiers, J. Inst. Auto. Eng. **9**, 7 (1941).
7. M. Muskat and H. H. Evinger, J. App. Phys. **11**, 739 (1940).
8. A. S. T. Thomson and R. Logan, J. Roy. Tech. Coll. Glasgow **4**, 696 (1940).
9. R. Schnurmann, Engineering **149**, 567 (1940).
10. D. Clayton, J. Inst. Petrol. **26**, 256 (1940).
11. M. R. Fenske et al., Ind. Eng. Chem. (Anal. Ed.) **13**, 51 (1941).
12. Andrew Gemant, Trans. Faraday Soc. **32**, 1628 (1936).
13. M. W. Webber, J. Inst. Petrol. **26**, 273 (1940).
14. T. K. Hanson and A. C. Egerton, Proc. Roy. Soc. **A163**, 90 (1937).
15. A. H. Stuart, Engineering **149**, 177 (1940).
16. T. C. Worth, J. Inst. Auto. Eng. **9**, 13 (1940).
17. S. S. Hansen, Power **85**, 70 (1941).
18. H. L. Matthijsen, J. Inst. Petrol. **26**, 72 (1940).
19. L. M. Tichvinsky, Trans. A. S. M. E. **62**, 461 (1940).
20. N. K. Adam, *The Physics and Chemistry of Surfaces* (Clarendon Press, Oxford, 1938).
21. I. Langmuir, J. Am. Chem. Soc., p. 284 (1936).
22. H. Deveaux, J. de phys. et rad. **5**, 84 (1924).
23. F. P. Bowden and S. H. Bastow, Nature **135**, 828 (1935).
24. W. B. Hardy, *Collected Papers* (Cambridge, 1936).
25. F. P. Bowden and L. Leben, Phil. Trans. Roy. Soc. **A239**, 1 (1940).
26. A. Fogg and S. A. Hunwicks, J. Inst. Petrol. **26**, 1 (1940).
27. O. Beeck, J. W. Givens, and E. C. Williams, Proc. Roy. Soc. **A177**, 103 (1940).
28. Z. J. Atlee, J. T. Wilson, and J. C. Filmer, J. App. Phys. **11**, 611 (1940).

New Books

Doctor Wood

By William Seabrook. Pp. 335+xiv, 15×22 cm. Harcourt, Brace and Company, New York, 1941. Price $3.75.

Few men ever gather about themselves in one lifetime such an aura of legend and anecdote as clings to that doughty experimental physicist from The Johns Hopkins University, the master of physical optics, R. W. Wood. Well-known to physicists for many years as the author of *How to Tell the Birds from the Flowers*, Wood is now given to the world in a biography of great human interest wherein are discovered all of the facts and fictions with which his person has become invested during a long and exciting career. Boswell, writing under the name of Seabrook, has given us Dr. Johnson, under the name of Wood, in a grand series of yarns that exude the woodsy aroma of their origin. It is no mean accomplishment to portray such a figure in print—a man who combines in one person so many of the interesting qualities of Michael Faraday, P. T. Barnum, Sherlock Holmes, and Tyll Eulenspiegel—and to follow that tenuous line which divides the serious scientist from the irrepressible prankster with all his subtle humor. Mr. Seabrook has succeeded in admirable fashion in accomplishing this difficult job and the finished product is a sort of symphonic rhapsody scored for wood-winds with solo passages for the English horn.

The biographer has captured much of the essential quality of the man and his work: Wood is portrayed as a daring experimenter and a vital personality, with a keen sense for the unusual and an unrestrained way of undertaking the unconventional. His experimental work has, in many instances, demonstrated superb technical skill; but he is perhaps best known for his ingeniously simple and uncommonsense attacks on problems. The emphasis which the biographer lays upon the foreign triumphs and acclaims which have been accorded R. W. Wood seems to hint that Wood has not been sufficiently appreciated in America. But Wood is scarcely another Josiah Willard Gibbs, for he has been well known to his countrymen for decades and he has gathered many of the scientific honors which America has to bestow. Wood is one of the great spirits of physics, and as such he has been enjoyed by his compatriots for a long time. We in America may be more accustomed to the unconventional than are the British, and we can take a man like Wood in our stride, enjoying his shrewd experiments and his imaginative pranks, and delighting in the man who performs them.

A slight clue to the pattern of international success that has attended Wood's career may be found in the bibliography of more than 250 of his scientific papers listed at the end of the book wherein one may discover something of the wide range of his interests and the further fact that the ratio of his English to American to German publication is approximately 5 : 3 : 1. Wood is unquestionably "as American as a hickory tree" but his branches have cast their shade over a wide area. Born in Concord, Massachusetts, doubtless in the very shadow of Debunker Hill, he has been an ardent exploder of scientific myths and hoaxes. Mr. Seabrook weaves the story of his exploits, from the spectroscopic analysis of boarding-house hash to the purloining of Tutankhamen's purple gold for scientific investigation, into a thoroughly readable account. Most of Wood's well-known feats are here described with all the authority of truth pertaining thereto that can be safely mustered without running the risk of spoiling a good story here and there. The reviewer has recently discovered that the book stands as a threat to the safety of his own household—and herein lies one of its strongest recommendations—for his two young sons have found out how interesting it is and they are prone to emulate some of Wood's more spectacular stunts.

Richard M. Sutton
University of Minnesota

The Methodology of Pierre Duhem

By Armand Lowinger. Pp. 184, 14½×22 cm. Columbia University Press, New York, 1941. Price $2.25.

Pierre Duhem was a versatile French physicist distinguished also in chemistry and in the history of science. His place in time is indicated by the fact that he was born in Paris in 1861, trained at the École Normale, spent most of his life as Professor of Theoretical Physics in the University at Bordeaux, and died in Aude, the southernmost department of France, in 1916.

In the volume under review, Mr. Lowinger undertakes the highly commendable task of putting into English Duhem's ideas concerning good scientific method. Such a task means the summarizing of *La Théorie physique*, one of Duhem's five or six outstanding volumes, and the one which bears most directly upon the various procedures which are employed in the discovery and formulation of scientific truth.

Mr. Lowinger's book consists of ten chapters, the first nine of which are devoted to the digest of *La Théorie physique* and the last is reserved for the author's own comments.

Duhem's first and fundamental problem is to discover what is to be understood by the word "explanation"; and here he distinguishes clearly between what he calls a *descriptive* explanation and an *explanatory* explanation. He insists that when one attempts to explain any physical phenomenon by referring it to an invisible ether or to any occult principle or to the geometrical points of Boscovick, he is already in the domain of metaphysics and, in the Greek sense of that word, beyond physics. Terms such as gravity, capillarity, chemical affinity, are to him mere "fig leaves to hide one's ignorance."

On the other hand, the one fruitful and sound physical theory is that based upon *descriptive* explanation. His evidence for this view is based upon the history of physics and is contained in the illustrations cited. Outstanding among his masters of sound method is Newton, who in the *Principia* gives the rules for computing the observable positions of the planets, but refuses even to guess at the

invisible mechanism by which one heavy body attracts another.

Kirchhoff is placed in this same school and his position is justified by citing the famous first sentence from his *Mechanik* where he insists that the problem of mechanics is "to describe the motions of nature *completely* and *in the simplest possible manner*." Another master of the *descriptive* explanation is Fourier who introduces his *Analytical Theory of Heat* with the following words: "Primary causes are unknown to us; but are subject to simple and constant laws, which may be discovered by observation, the study of them being the object of natural philosophy." Space permits the mention of only one more of his examples of the *descriptive*, as opposed to the *explanatory*, method; and that will be the great paper in which Ampère (1826) creates the science of electrodynamics and blazons his viewpoint in the very title of the paper: *Théorie mathématiques des Phénomènes Électrodynamiques uniquement déduite de l'Expérience*.

The dominating thought in Duhem's work is not unlike that which inspires Ludwig Boltzmann in his *Methods of Theoretical Physics*, published in the *Philosophical Magazine*, July 1893. Here again the essence of explanation is represented as the discovery of analogy. A phenomenon is explained when one finds a group of familiar phenomena in which the given one clearly belongs. The next step, after having found several small groups of similar phenomena, is to combine them into one larger group which shall constitute the physical theory of that field.

There are certain paragraphs in this book—too long to quote—which give one the impression of hair splitting and shadow boxing with reality; and there are other paragraphs where more care in translation would have clarified the English, e.g., on p. 72, the substitution of "either" for "whether." But these are small matters compared with the help which this translation renders to the student who is short on French or to whom the original is not available. One who has read the original can only wish that Mr. Lowinger had put the entire volume into English, and thus have done for Duhem what T. J. McCormack did so splendidly for Mach a half century ago.

HENRY CREW
Northwestern University

Benjamin Franklin's Experiments

EDITED BY I. BERNARD COHEN. Pp. 453, 16×22½ cm. Harvard University Press, Cambridge, 1941. Price $4.00.

All American physicists know that Franklin devised the one-fluid theory and that he flew a kite to demonstrate the identity of lightning and the electric spark. Few of them are well-acquainted with his other scientific contributions. One reason for this lack of knowledge is that no extensive edition of Franklin's writings has been published since 1774. Mr. Cohen is to be commended for his work in writing an excellent critical historical introduction and in bringing to light a great deal of material not included in the earlier edition. The book will repay the reader by giving him a better appreciation both of Franklin's scientific ability and of the difficulties of experimentation in pioneer days.

The reviewer was interested to read Franklin's arguments against the corpuscular theory of light on the grounds first that the corpuscles would exert forces on smoke particles and the like, and second that the sun's substance would be dissipated if it emitted particles. He reasoned also that the corpuscles would dislodge "electric fire" from a charged electroscope and tried to observe the photoelectric effect more than a century before Hertz succeeded in doing so.

It is interesting to learn how faulty were the theories on which his successful experiments were based. Of fifty-six "suggestions and suppositions" as to the causes of thunderstorms, only twenty-two would be accepted today. Franklin modestly recognizes his limitations as a theorizer, but writes "even a bad solution, read and its faults discovered, may often give rise to a good solution, in the mind of an ingenious reader."

OSWALD BLACKWOOD
University of Pittsburgh

Heating, Ventilating, Air Conditioning Guide 1942

Pp. 1160+xxiii+91, 16×23½ cm. Published by the American Society of Heating and Ventilating Engineers, New York, 1942. Price $5.00 (with thumb index $5.50).

In this twentieth edition of *Heating, Ventilating, Air Conditioning Guide*, approximately one-half of the chapters have been reviewed, nine being completely rewritten. Aside from the addition of a new chapter, Fundamentals of Heat Transfer, covering the basic equations for conduction, convection, and radiation, there has been no change in the order of presentation of subject matter.

In the chapter on thermodynamics of air and water mixtures, the Mollier diagram for moist air has been redrawn and a new volume diagram for moist air has been added. The data on physiological principles have been revised to include current knowledge on thermal interchanges taking place between the human body and the environment. The chapter on central systems for comfort air conditioning has been completely rewritten. Revisions of the chapters on air distribution, air duct design, sound control and fans provide new data on the design of air handling systems. A new air friction chart, developed at the A.S.V.H.E. Research Laboratory, is included in the chapter on air duct design.

The chapter on radiant heating has undergone major revisions and contains data essential for the design of radiant heating systems. A new duct chart has been added to the chapter on pipe and duct heat losses. Additional chapters which have been reviewed and revised include the following: Combustion and fuels; Radiators and convectors; Pipe, fittings, welding; Heat transfer surface coils; Air pollution; Air cleaning devices; Natural ventilation; and Water supply piping and water heating.

The Catalog Data section has again been revised and gives factual data on the latest types of equipment.

Here and There

Research Agreement

A cooperative agreement with the School of Engineering at Columbia University, New York City, to investigate the heat flow through various building walls, has been announced by the American Society of Heating and Ventilating Engineers. The research program will be carried on in the heat transfer laboratory at the University by means of a specially designed apparatus for transient heat flow, in accordance with a study jointly planned by Dr. F. C. Houghten, Director of the ASHVE Laboratory, Pittsburgh, and Dr. Victor Paschkis, Research Associate at the University, who will conduct the laboratory work.

★

Annual Meeting

The American Society for Testing Materials will hold its forty-fifth Annual Meeting at Chalfonte-Haddon Hall, Atlantic City, from Monday, June 22 through Friday, June 26. Some 18 separate technical sessions are scheduled at which technical reports and papers will be presented and discussed. Since the triennially published Standards Book is scheduled for appearance late in November, the various committees will attempt in their reports to bring specifications up-to-date. Two outstanding technical features will be the Symposium on Radiography, for which three sessions are scheduled, and a round-table discussion on Solvent Action of Water Vapor at High Temperature and Pressure.

★

National Registry of Rare Chemicals

In order to facilitate the procurement of rare chemicals by scientific workers engaged in the war effort, the Armour Research Foundation has undertaken to operate, under the name of the National Registry of Rare Chemicals, a clearing house for chemicals not listed in the catalogs of the major supply houses. The Registry will not store chemicals, but will maintain an indexed file of their sources. The file will not be open to general inspection, and individuals or organizations may remain anonymous to protect commercial secrets. In these cases, the Registry will act as intermediary in all transactions if desired.

It is essential to the success of the Registry that all workers in every branch of science using chemicals make available information on any rare materials held by them. When possible, the approximate number of grams, pounds, or tons available should be indicated. Manufacturers of chemicals should supply data on new additions until their next catalogs are issued, and the Registry should be notified when these have finally been printed in catalog form. Prices which may be asked for chemicals are of no concern to the Registry, but are matters of interest only to buyer and seller.

Communications should be addressed to the National Registry of Rare Chemicals, Armour Research Foundation, 35 West 33rd Street, Chicago, Illinois.

★

Tenth Annual Summer Conference on Spectroscopy and Its Applications

A Summer Conference on Spectroscopy and Its Applications, to be sponsored jointly by the Optical Society of America and the Massachusetts Institute of Technology, will be held in Cambridge at M.I.T. on July 20, 21, and 22, 1942.

A Symposium on Fluorescence and Phosphorescence is planned in connection with the Conference. Admittance to the Conference will be by reservation as usual. Further information and tickets can be obtained from Professor George R. Harrison, Massachusetts Institute of Technology, Cambridge, Massachusetts.

The usual courses in spectroscopy will not be given at the Massachusetts Institute of Technology this summer.

★

Honors and Awards

The Bowie Medal, highest honor in the field of geophysics, was presented at a recent meeting of the American Geophysical Union to Captain N. H. Heck of the U. S. Coast and Geodetic Survey. This is the fourth award of the Bowie Medal, which was founded as a memorial to the late Dr. William Bowie, famous for his researches on gravitational variations in and below the crust of the earth.

The following awards for 1942 have been made by the Franklin Institute:

The Franklin Medal to Dr. Jerome Clarke Hunsaker, General Coordinator of the Naval Research and Development Board and Chairman of the National Advisory Committee for Aeronautics, designer of the Shenandoah and the NC type flying boat, and to Dr. Paul Dyer Merica, Vice President of the International Nickel Company of Canada, for his development of a variety of alloys for commercial purposes;

The Elliott Cresson Medal to Dr. Claude S. Hudson of the National Institute of Health for studies on the chemistry of sugars, and to Dr. I. I. Rabi of Columbia University for the magnetic resonance method of nuclear investigation;

The Howard N. Potts medal to Dr. Bernard Lyot, French astronomer, for his method of studying the sun's corona, and to Dr. Jesse W. Beams of the University of Virginia for his work with ultra-high speed centrifuges.

Contributed Original Research

An X-Ray Study of Carbon Black

J. Biscoe and B. E. Warren
George Eastman Laboratory of Physics, Massachusetts Institute of Technology, Cambridge, Massachusetts
(Received February 16, 1942)

X-ray studies have been made of a number of carbon blacks, prepared under different conditions, and subject to various heat treatments. The patterns were made in evacuated cameras, using Cu $K\alpha$ radiation monochromated by reflection from rocksalt. The patterns consist of crystalline reflections ($00l$), and two-dimensional lattice reflections (hk). The structure is one of true graphite layers arranged roughly parallel and equidistant, but otherwise completely random. The dimensions within a layer are the same as in graphite; the layer separation is somewhat larger than in graphite. The effect of heat treatment is to increase the size of the parallel layer groups. At graphitization the material changes discontinuously to the crystalline graphite structure. The usual carbon black is not finely divided graphite. Small angle scattering studies indicate the existence of clusters a few hundred angstroms in size. It is these clusters which are measured by microscope counts, by the electron microscope, and by surface areas, rather than the much smaller parallel layer groups.

I. INTRODUCTION

X-RAY diffraction patterns of the fine carbon blacks usually consist of three rather broad diffuse peaks. It has long been recognized that the pattern is essentially a washed out graphite pattern. Most of the x-ray studies of carbon black have assumed at the outset that the patterns could be treated as crystalline powder patterns, and indexed in terms of the graphite structure.

In a previous x-ray study of carbon black,[1] the attempt was made to find out what definite conclusions could be drawn without any *a priori* assumptions of crystallinity. From a Fourier integral analysis of the scattering curve, it was found that the distribution of neighboring atoms was exactly that of the atoms in a single layer of the graphite structure. Although this result indicated strongly the existence of the single graphite layers in the carbon black structure, it was not possible to determine uniquely the relative arrangement of the layers. The question as to whether carbon black was finely divided graphite crystals, or was another form of carbon with a lower degree of order, could not be answered definitely.

The present study of heat-treated carbon blacks has now supplied a definite answer to this question. By heating a carbon black for an hour or two at say 2000°C, in the absence of air, the diffraction pattern sharpens up considerably, more peaks appear, and more precise conclusions can be drawn. Figure 1 shows the patterns of a carbon black, of the same black heated for two hours at 2000°C, and of graphite. The pattern of the heat-treated black shows a closer resemblance to the graphite pattern. If we attempt to index the pattern of the heat-treated black in terms of the graphite pattern, we find that only lines of the type ($00l$) and ($hk0$) appear, the general lines hkl are missing. These facts indicate a random layer structure, in which single graphite layers are stacked roughly parallel and equidistant, but with each layer having a completely random orientation with regard to rotation about the layer normal. As a necessary part of this investigation the theory of the random layer lattice powder pattern has been developed.[2]

In addition to the usual x-ray diffraction measurements, a small angle scattering study has been made of several carbon blacks. Such studies are of value in giving information about the existence and size of clusters of material much larger than the individual groups which determine the lines of the powder diffraction pattern.

[1] B. E. Warren, J. Chem. Phys. **2**, 551 (1934).

[2] B. E. Warren, Phys. Rev. **59**, 693 (1941).

II. THEORY OF RANDOM LAYER STRUCTURE PATTERNS

From the theory of the random layer lattice powder pattern,[2] the points of importance to the present study will be summarized. The carbon black structure will be described in terms of the hexagonal graphite axes. The distance of repetition within a graphite layer is called a, and twice the perpendicular distance between layers is called c. The term "parallel layer group" will be used to mean an assemblage of graphite layers roughly parallel and equidistant, but random in orientation about the layer normal. The assemblage can be likened to a deck of cards thrown down in disorderly fashion upon a table.

From a powder sample of parallel layer groups there will be two kinds of reflections: sharp crystalline reflections of type $(00l)$, and diffuse two-dimensional lattice reflections of type (hk). There will be no general (hkl) reflections. The position, integrated intensity, and line breadth of the $(00l)$ reflections are given by the usual powdered crystal theory. Typical two-dimensional lattice reflections are shown in Figs. 2 and 3. If $\sin\theta_0$ is the value of $\sin\theta$ for the corresponding crystalline reflection $(hk0)$, a two-dimensional lattice reflection rises sharply at approximately the position $\sin\theta_0$, and then falls off slowly toward larger angle. The distribution of intensity in a two-dimensional reflection is given by two equations covering regions which overlap.* For large a

$$P'_{2\theta}=\frac{KmF^2(1+\cos^2 2\theta)}{4\sin\theta(\sin^2\theta-\sin^2\theta_0)^{\frac{1}{2}}}. \qquad (1)$$

For small a

$$P'_{2\theta}=\frac{KmF^2(1+\cos^2 2\theta)}{2(\sin\theta)^{\frac{1}{2}}}\left(\frac{L_a}{\pi^{\frac{1}{2}}\lambda}\right)^{\frac{1}{2}}F(a), \qquad (2)$$

where

$$a=\frac{2\pi^{\frac{1}{2}}L_a}{\lambda}(\sin\theta-\sin\theta_0), \qquad (3)$$

m is the two-dimensional multiplicity, F^2 is the structure factor squared, L_a is the layer dimension parallel to the layer, and $F(a)$ is a function of the variable a given by (3) and tabulated, in reference 2.

The layer dimension in the plane of the layer can be calculated from the peak breadth at half the maximum intensity

$$L_a=1.84\lambda/B\cos\theta. \qquad (4)$$

The peak of a two-dimensional lattice reflection (hk) is displaced toward larger angle from the position of the corresponding crystalline reflection $(hk0)$ by an amount $\Delta(\sin\theta)$

$$\Delta(\sin\theta)=0.16\lambda/L_a. \qquad (5)$$

In calculating axes and interatomic distances

* It is unfortunate that F and a have been used in two senses in the following equations. The nomenclature has been retained to conform to reference 2.

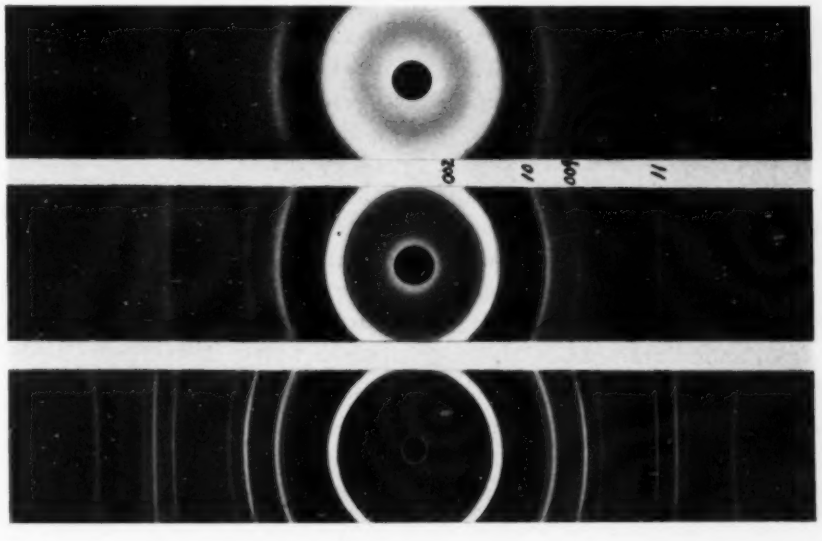

FIG. 1. X-ray diffraction patterns. (a) Spheron Grade 6 black unheated, (b) Spheron Grade 6 black, heated 2 hours at 2000°C, (c) graphite. Radiation Cu $K\alpha$.

from two-dimensional lattice reflections, allowance must be made for this displacement, otherwise erroneous conclusions about lattice contractions may easily result.

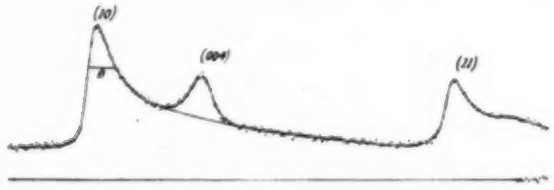

FIG. 2. Microphotometer record of the pattern of Spheron Grade 6 black, heated 2 hours at 2800°C.

III. EXPERIMENTAL TECHNIQUE

The x-ray patterns were made using extruded cylindrical samples (no binder) 0.6 mm in diameter, placed at the center of an evacuated cylindrical camera of radius 4.38 cm. Most of the patterns were made with Cu $K\alpha$ radiation $\lambda = 1.539$A monochromated by reflection from a rocksalt crystal. The films were microphotometered and intensity curves plotted from the microphotometer traces. For calculations which required subtracting the Compton modified scattering from the observed intensity curves, the experimental curves were fitted at large angle to the calculated total independent scattering per atom. The modified part of the scattering could then be subtracted off.

IV. DESCRIPTION OF SAMPLES

The carbon blacks employed in the present investigation are widely used in the rubber and paint industries. All samples, with the exception of the heat-treated blacks, were taken from standard production lots.

P-33

This material is produced by the thermal decomposition of natural gas.[3] While it is not generally recognized as a rubber reinforcing carbon, it is widely used in rubber compounding, particularly where a resilient, pliable stock is desired, as for example, in the production of footwear and inner tubes. This black has the largest particle size† of all the carbon blacks listed in Table I. Dark field observation with the optical microscope gives a value of 1590A for the average diameter.[4] An electron microscope value for the smallest particles in *P*-33 has been given as 1000A.[5] A more recent study[6] reports a considerably smaller diameter of 740A.

Acetylene Black (Shawinigan)

This black is produced by the thermal decomposition of acetylene. Like other "furnace" blacks, it produces a soft resilient stock when compounded in rubber. Surface area and electron microscope values[7] give a diameter of around 500A for acetylene black. It does not compare with channel carbon black in its ability to reinforce rubber. It is unique, however, in its extremely low electrical resistance both in the dry state and when compounded in rubber.[6]

Spheron Grade 6

This is a standard rubber reinforcing carbon black produced by the channel process. In this process, natural gas flames burning in incomplete supply of air, impinge and deposit carbon on slowly reciprocating metal surfaces. The bulk of the world's supply of carbon black is produced by this method. The average particle of this carbon black is around 300A in diameter.[7]

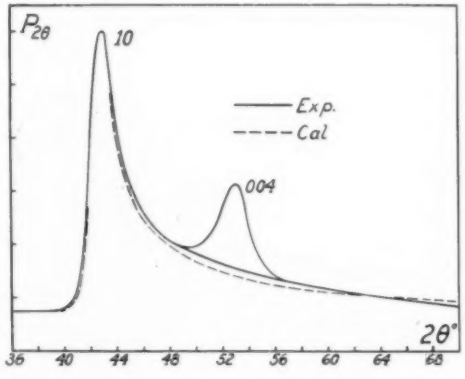

FIG. 3. Comparison of experimental and calculated intensity curves for the two-dimensional lattice reflection (10). Spheron Grade 6 black, heated 2 hours at 2800°C.

[3] Moore, Ind. Eng. Chem. **24**, 21 (1932).
† Particle size as used here refers to the diameter of the working particle as illustrated in Fig. 8.

[4] Gehman and Morris, Ind. Eng. Chem. Anal. Ed. **4**, 157 (1932).
[5] Heering *et al.* Kautschuk **5**, 55 (1941).
[6] Wiegand, India Rubber World **105**, 270 (1941).
[7] Smith, Thornhill, and Bray, Ind. Eng. Chem. **33**, 1304 (1941).

TABLE I. Results for a series of carbon black samples.

Sample	Heat treatment	L_c	L_a	a	c from (002)	c from (004)
P-33	none	16.8A	28.0A	2.45A	7.10A	6.98A
CK-3	none	12.1	19.5	2.45	7.1	6.85
Carbolac 1	none	13.1	18.6	2.46	6.95	6.7
Acetylene black (shawinigan)	none	26.6	47.5	2.42	7.0	6.86
Spheron Grade 6	none	12.7	20.0	2.45	7.10	6.82
Spheron Grade 6	760°C 2 hr.	14.4	22.6	2.42	7.05	6.86
Spheron Grade 6	1040°C 2 hr.	14.9	28.0	2.46	(7.3)	6.94
Spheron Grade 6	1500°C 2 hr.	24.9	44.2	2.44	6.95	6.90
Spheron Grade 6	2000°C 2 hr.	32.3	55.8	2.44	6.92	6.88
Spheron Grade 6	2800°C 2 hr.	40.0	65.2	2.46	6.90	6.88
Spheron Grade 6	2000°C 10 hr.	35.5	60.5	2.43	6.94	6.86
Spheron Grade 6	1040°C 28 hr.	14.9	29.8	2.43	7.10	6.92
Graphite				2.456	6.697	

CK-3

This material is a foreign product produced by a flame process very similar to the channel process. The raw material, however, is naphthalene or anthracene residue. These materials are vaporized and carried to the burner tips in a stream of air or inert gas. The rubber reinforcing properties of this black are about the same as those of a typical American gas black, such as the Spheron Grade 6 material described above. Its particle size[7] is also nearly identical with that of the rubber reinforcing channel blacks.

Carbolac 1

This carbon black, produced by the channel process from natural gas, is used in the paint and lacquer industry. It is one of the most finely divided carbon blacks commercially available. The best value for the diameter of the average particle lies between 30 and 50A.[7]

The heat treatments of the Spheron Grade 6 blacks were given by placing the material in graphite crucibles and heating in an induction furnace.** Samples were taken from different parts of the charge to check that there was no contamination from the walls.

V. POWDER PATTERN RESULTS

Figure 1 shows a set of typical diffraction patterns. Figure 1a is the pattern of the Grade 6 channel black, and is a typical pattern of a fine particle rubber reinforcing black. Figure 1b is the pattern of the same material heated 2 hours at 2000°C. The crystalline reflections (002) and (004) which fall off rapidly on the large angle side are readily distinguished from the two-dimensional lattice reflections (10) and (11) which fall off slowly toward larger angle. Figure 1c is the pattern of graphite.

Figure 4 shows the intensity curves obtained from the microphotometer records for three samples having different heat treatments. For each curve the Compton modified scattering has been subtracted off. Figure 2c is sufficiently sharp to distinguish readily the crystalline reflections 002, 004, and 006 from the two-dimensional lattice reflections (10) and (11). The vertical dashed lines marked (100) and (110) indicate the positions where the crystalline reflections (100) and (110) of graphite would occur. Notice that the peaks of the two-dimensional lattice reflections are displaced toward larger angle. The amount of this displacement is greater the smaller the layer dimension L_a. From Table I the layer dimensions for these three samples are $L_a = 20$, 44, and 65A. In calculating the distance of repetition within the layer (length of a axis) from the positions of the (10) and (11) reflections it is necessary to apply the correction for this displacement as given by Eq. (5). As an example consider Fig. 2a with a particle dimension $L_a = 20$A.

$$\Delta(\sin\theta) = 0.16\lambda/L_a = (0.16 \times 1.54/20) = 0.0123.$$

For the reflection (10) $\sin\theta_0 = 0.362$ and the displacement correction amounts to 3.4 percent. If the correction were not made, the erroneous conclusion would be drawn that there was a 3.4 percent contraction in the length of the a axis.

** We are indebted to Professor Chipman of the Department of Metallurgy for the heat treatments of the samples.

Figure 2 is part of the microphotometer record of the Grade 6 material heated 2 hours at 2800°C. The two-dimensional reflection (10) with the crystalline reflection (004) superimposed, is clearly shown. The layer dimension L_a is calculated by Eq. (4) from the breadth at half the maximum intensity.

$$L_a = 1.84\lambda/B\cos\theta$$
$$= (1.84\times1.54)/(0.0468\times0.932) = 65\text{A}.$$

Since the reflections (10) and (11) have been interpreted as two-dimensional lattice reflections, it is of interest to make a direct comparison of the observed intensity distribution with that calculated for a two-dimensional reflection. Figure 3 shows the experimental (10) intensity curve derived from the microphotometer record of Fig. 2. The calculated curve has been computed for a layer dimension $L_a = 65$A, the incoherent background of about 0.75 unit is assumed to be constant over the range plotted, and the maximum intensities of the two curves are matched. The curve was calculated using Eq. (2) for 2θ up to 46° and Eq. (1) for 2θ greater than 46°. Within the limits of the approximations, and the accuracy of microphotometering, the agreement is satisfactory. The two-dimensional lattice character of some of the carbon black reflections has been recognized by a number of previous investigators.[8–10] Recent electron diffraction studies of carbon black[11] have thoroughly confirmed the random two-dimensional lattice structure of the material.

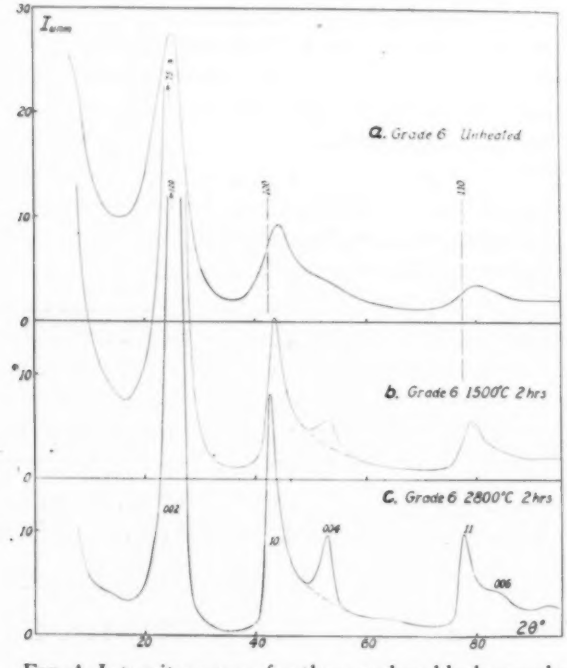

FIG. 4. Intensity curves for three carbon black samples. (a) Spheron Grade 6 black, unheated, (b) same black, heated 2 hours at 1500°C, (c) same black, heated 2 hours at 2800°C. Radiation Cu $K\alpha$. For all three curves, the Compton modified scattering has been subtracted.

The results for a series of carbon black samples are presented in Table I. L_c is the dimension of the parallel layer group perpendicular to the graphite layers. It is obtained from the width of the (002) reflection and from (004) when present, by using the ordinary crystalline particle size equation

$$L = 0.89\lambda/B\cos\theta.$$

The (002) reflection is somewhat influenced by the intense small angle scattering, and may consist in small part of the carbon-carbon interaction of the closest carbons in two adjacent parallel layer groups.

L_a is the effective dimension of the graphite layers in the plane of the layer. The values are calculated by Eq. (4) from the widths of the (10) and (11) reflections. From the hexagonal symmetry of the layer it can be assumed that the individual layers are approximately disk-shaped.

Using the hexagonal axes of graphite, a is the distance of repetition within the layer. The values are calculated from the (10) and (11) reflections with the correction for displacement given by Eq. (5). The values of c have been calculated from (002) and (004). The value from (004) is probably the more accurate when this reflection is well defined, since (002) is influenced by small angle scattering and the carbon-carbon interferences of regions of groups in contact.

The axial lengths for graphite were determined for a sample of very pure graphite (less than 0.1 percent impurity) using filtered Cu $K\alpha$ radiation, and copper powder as a calibration substance. The values obtained are in good agreement with those of Hofmann and Wilm.[8] The x-ray values give a calculated graphite density $\rho = 2.262$.

The average of the a values is about 0.5 percent less than that for graphite, but there is no

[8] U. Hofmann and D. Wilm, Zeits. f. Elektrochem. **42**, 504 (1936).
[9] H. Arnfeld, Arkiv f. Mat. Astron. Fys. **B23**, 1 (1932).
[10] E. Berl, K. Andress, L. Reinhardt, and W. Herbert, Zeits. f. physik. Chemie **A158**, 273 (1932); **A166**, 81 (1933).
[11] A. White and L. Germer, J. Chem. Phys. **9**, 492 (1941).

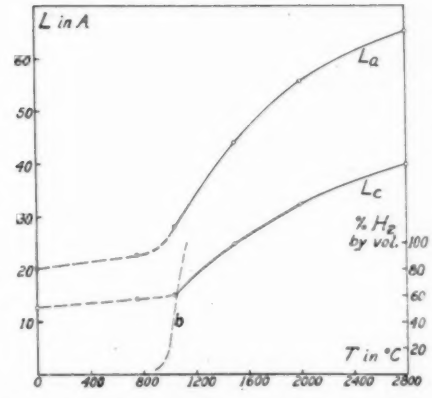

FIG. 5. (a) The dimensions L_a and L_c of the parallel layer groups in Spheron Grade 6 black, heated for 2 hours at various temperatures, (b) percent by volume of H_2 in gas evolved at various temperatures.

systematic trend and the difference is within the experimental error. We conclude that within this limit, there is no appreciable difference in the *a* axis dimensions of the graphite layers in carbon black and graphite. The *c* axis lengths for carbon black are appreciably greater than the graphite value. This is exactly what should be expected. In crystalline graphite, each layer sets itself precisely in the best position with respect to the neighboring layer on either side, and the minimum spacing is therefore achieved. In the random stacking together of layers in carbon black, the exact settings corresponding to minimum energy are not achieved, and a larger average spacing results.

For the unheated blacks the two dimensions of the parallel layer groups L_a and L_c have about the same values as found by other investigators. There is a fairly constant ratio for these two dimensions. Picturing the parallel layer group as a disk, the thickness of the disk is around one-half to two-thirds of the breadth. In a recent x-ray study of carbon black by Clark and Rhodes,[12] the conclusion was reached that the two particle dimensions L_a and L_c were roughly equal. However, their L_a values were calculated from two-dimensional reflections using the ordinary crystalline particle size equation. This would result in L_a values which were too small.

Figure 5 shows the L_a and L_c values for Grade 6 black heated for 2 hours at various temperatures. The parallel layer groups appear to grow at about the same rate in both directions—that is, the individual graphite layers grow in size, and more layers stack themselves parallel. The curves indicate a fairly definite temperature of around 1000°C, at which the rapid growth sets in. This temperature can perhaps be correlated with the sharp rise in the curve[13] 5*b*, which shows the percent of H_2 in the gas evolved at different temperatures. If the hydrogen content of the sample is chemically bonded around the edges of the graphite layers, it could presumably act as an effective barrier toward growth of the layers. Only at temperatures high enough to drive off this hydrogen can growth of the graphite layers take place.

As the material is carried to higher temperatures, the individual layers acquire greater thermal movement, and it should become easier for each layer to rotate with respect to neighboring layers into the graphite configuration. However, the size of each layer L_a increases with temperature, and the larger the layer, the more difficult for the layers to rotate into the graphite structure. If the temperature could be raised so rapidly that there were no time for appreciable increase in L_a, graphitization might set in at a lower temperature. Figure 6 shows patterns made in a small cylindrical camera of samples of Spheron Grade 6 heated 2 hours at 2800°C and 3300°C. The 2800°C pattern is still definitely the random layer pattern, showing the two-dimensional reflections, while the 3300°C pattern is the complete graphite pattern. For the Grade 6 material, and our rate of heating, graphitization has taken place somewhere between 2800° and 3300°C.

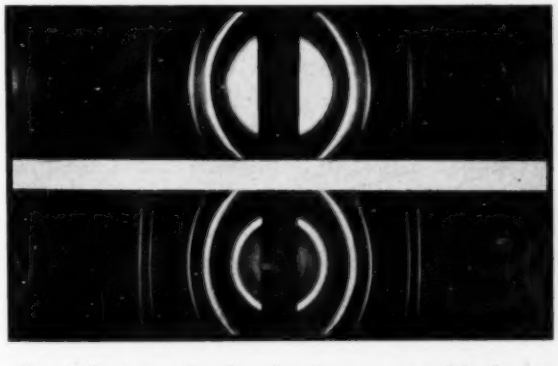

FIG. 6. Patterns showing the change to graphite by heat treatment. (Above) Spheron Grade 6 black heated 2 hours at 2800°C, (below) same black heated 2 hours at 3300°C.

[12] G. L. Clark and H. D. Rhodes, Ind. Eng. Chem. Anal. Ed. **12**, 66 (1940).

[13] Unpublished data from W. R. Smith.

The x-ray studies of the heat-treated blacks allow us to draw the clear and unambiguous conclusion that *carbon black is not small graphite crystals*. Up to the temperature of graphitization, the patterns show the two-dimensional reflections characteristic of the random stacking together of layers, and the higher the temperature of heat treatment the more definite is the pattern and the conclusion. When graphitization sets in, there is a discontinuous change from the pattern containing two-dimensional reflections, to the completely crystalline graphite pattern. Since the heat treatment at higher temperatures produces a more orderly structure, we can infer with certainty that the original unheated material had the same random layer structure, even though the patterns of the unheated material are too diffuse to allow any such definite conclusion to be drawn. The Fourier integral analysis of carbon black proved the existence of individual graphite layers, and the study of the heat-treated blacks proves that the layers are not packed together in the orderly fashion of crystalline graphite.

What should carbon black be called? It is not completely amorphous since there is a definite two-dimensional repetition within each layer, and yet it does not have the three-dimensional repetition of graphite. Carbon black is a simple and definite example of an intermediate form of matter, which is distinctly different from both the crystalline and the amorphous states. The term "turbostratic" (unordered layers) is suggested as a name for this particular class of mesomorphic solids. The carbon black structure would then be described as consisting of turbostratic groups, each group consisting of a number of graphite layers stacked together roughly parallel and equidistant, but with each layer having a completely random orientation about the layer normal.

A simple model of a turbostratic structure is readily obtained by shaking and rotating a bag full of penny-sized disks which have been coated with an adhesive. The agitation is suddenly stopped and the adhesive allowed to set. Examination will then show that the disks tend to be arranged in parallel groups with an average of about five parallel disks to a group. If the penny-sized disks were replaced by disks of the same thickness but say twice the diameter, and the experiment repeated, the average number of parallel disks in a group would presumably be greater. The rough proportionality between the two dimensions L_a and L_c which is shown by Fig. 5, is probably to be explained in this way.

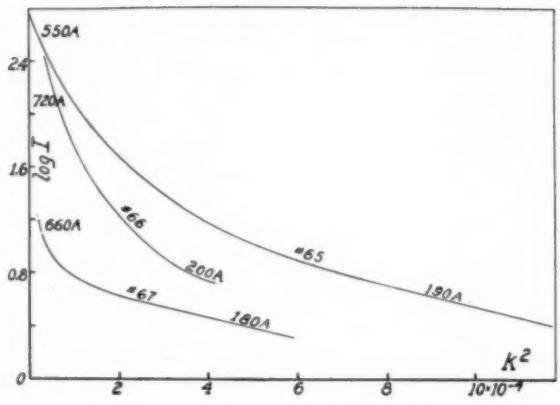

FIG. 7. Small angle scattering plots for three carbon black samples. #65 standard production Grade 6 channel black; #66 P33, large particle thermal decomposition black; #67 Carbolac 1 (extremely fine particle size channel black). Particle diameters are recorded on each curve.

VI. SMALL ANGLE SCATTERING STUDIES

Carbon black produces an extremely strong small angle scattering, the intensity increasing rapidly with decreasing angle. A material consisting of clusters, with gaps or voids between them, will give rise to small angle scattering. From the shape of the small angle scattering curve, a rough calculation of the cluster dimensions can be made. If the parallel layer groups in carbon black are packed together to form clusters, line broadening measurements will give the group dimensions. An x-ray determination of the cluster dimensions can be made only from the small angle scattering curves.

A number of small angle scattering studies on carbon black have been carried out.[14–16] The method has been highly developed by Guinier, who has applied it to a number of materials. The following simplified treatment will suffice to indicate the principle of the method. Consider a sample made up of spherical clusters of radius R, the clusters packed loosely together with empty gaps between them, and no definite center to center distances between clusters. At small angles

[14] P. Krishnamurti, Ind. J. Phys. **5**, 472 (1930).
[15] B. E. Warren, Phys. Rev. **49**, 885 (1936).
[16] M. A. Guinier, Thesis, Faculty of Science, University of Paris (Paris, 1939).

the scattering power can be taken as continuous within any one cluster. The amplitude scattered by one spherical cluster is then given in electron units by

$$E=\int_0^R 4\pi r^2\rho\frac{\sin kr}{kr}dr=N\Phi(kR),$$

where $k=4\pi \sin\theta/\lambda$, ρ = electron density, N = no. of electrons in a spherical particle, and

$$\Phi(x)=\frac{3}{x^2}\left\{\frac{\sin x}{x}-\cos x\right\}.$$

The diffracted intensity from a single particle is then given by

$$I=N^2\Phi^2(kR).$$

If the particles are sufficiently widely and randomly separated to produce incoherency in the radiation from the individual particles, the total intensity will be proportional to the intensity from a single particle.

$$I=C\Phi^2(kR).$$

For practical application it is convenient to approximate the curve $\Phi^2(x)$ by the error curve $\exp -[0.221x^2]$ which has the same height and same area.

$$I=C\exp -[0.221(kR)^2].$$

Taking logarithms

$$\ln I=\ln C-0.221R^2k^2.$$

A plot of $\ln I$ against k^2 should therefore give a straight line whose slope is $-0.221R^2$. Since only the logarithm of the intensity is involved in the plot, the intensity can be determined in arbitrary units.

The small angle scattering patterns were made in a large evacuated camera, with a sample to film distance of 47.6 cm. The radiation used was Cu $K\alpha$ monochromated by reflection from calcite, and collimated by very narrow slits. The patterns were made by transmission through thin slabs pressed together without a binder. Plots of log I *vs.* k^2 for three carbon black samples are shown in Fig. 7.

As is generally the case, the plots are not straight lines. In general the assumptions underlying the above derivation will not be fulfilled. The particles may not be spherical in shape and may not all have the same size, so that a straight line is seldom to be expected. There is the additional ambiguity that small angle scattering measurements can equally well be considered as giving the size of the material particles or the size of the holes between them. Strictly, the small angle scattering measurements give only the magnitude of the average scale of inhomogeneity in the sample. Since the lines are not straight, the slope has been measured at each end, and corresponding diameters of assumed spherical particles calculated. The values are recorded on each curve. Over the range through which the small angle scattering could be observed the effective particle diameters fall in the range 200–800A. Although small angle scattering measurements are not nearly as definite as those from line broadening, the results seem to indicate that in carbon black there is a clustering of the material, and that these clusters are of the magnitude of a few hundred angstroms. These cluster dimensions are of the same magnitude as the sizes determined by microscope counts and by the electron microscope.

Figure 8 illustrates schematically the structure

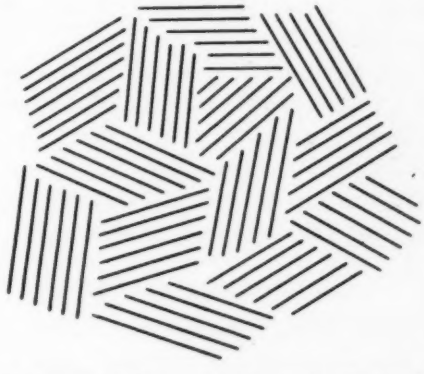

FIG. 8. A speculative and schematic illustration of a carbon black cluster. Each set of parallel lines represents a parallel layer group.

of a single carbon black cluster as suggested by the x-ray studies. The cluster as a whole is a few hundred angstroms in size. The groups of parallel lines represent the parallel layer groups, each line representing a graphite layer. The group dimensions L_a and L_c are the dimensions parallel and perpendicular to the sets of parallel lines.

We wish to acknowledge the financial assistance by Godfrey L. Cabot, Inc. which made this study possible, and to express our thanks to Dr. W. R. Smith, Chief Research Chemist of Godfrey L. Cabot, Inc., for his generous help and advice.

The Cause of High Voltage Surges in Rectifier Circuits

ALBERT W. HULL AND FRANK R. ELDER
Research Laboratory, General Electric Company, Schenectady, New York
(Received March 25, 1942)

It is shown that high voltage surges are produced in apparatus associated with gas discharge devices when, and only when, the demand for current exceeds the current-carrying capacity *of the gas* (or vapor). Cathode spot extinction and sputtering of hot cathodes cause only slight disturbances which do not produce high voltage in practical circuits. Experimental data on surge limits, i.e., the maximum currents that can be carried without surges, are given for four types of mercury vapor tube. These data lead to a single set of values of maximum current density as a function of vapor pressure, which may be used for the safe design of apparatus.

1. INTRODUCTION

ONE of the earliest complaints against mercury arc rectifiers was that they caused surges[1] which broke down the insulation of transformers and other apparatus connected to them. Temporarily the symptoms were cured, by surge arresters and stronger insulation; but the cause remained. Hence, it is not surprising that the symptoms have reappeared frequently in phanotron and thyratron circuits, and that they have a tendency to recur with each new type of application.

In the course of a study of the current-carrying capacity of ionized gas[2] we have discovered the cause of these surges and the means of avoiding them. This paper contains a discussion of surge production and experimental data on surge conditions in hot cathode tubes.

2. CAUSE OF SURGES

The surges are caused by *gas limitation* in the tube. They are produced, as will be shown, when, and only when, the demand for current is greater than the current carrying capacity of the *gas or vapor path*. This has a definite value, dependent only on the product of vapor density and cross section of path. The limit is reached when in some portion of the current path all the available atoms of the gas are ionized and are serving to neutralize space charge.[3] An unstable condition results. The ions move to the walls, under the influence of the potential difference between space and walls that always exists, because of the higher mobility and temperature of the electrons as compared to the ions. This leaves the space momentarily almost gas free, thus interrupting the supply of ions and hence the flow of current. The ionized atoms lose their charges at the walls and return to the space, with a time constant between 10^{-6} and 10^{-5} second, dependent on dimensions, to be again ionized and again swept out. Thus the process repeats itself indefinitely, unless the discharge path is short-circuited by a failure of the insulation or formation of a cathode spot on the tube wall near the anode. It has been used successfully as a source of high frequency oscillations.

Surges are also caused by *cathode extinction;*

[1] A. W. Hull and H. D. Brown, "Mercury arc rectifier research," Elec. Eng. **50**, 788 (1931).
[2] A. W. Hull, "Fundamental electrical properties of mercury vapor and monatomic gases," Elec. Eng. **53**, 1442 (1934).
[3] Irving Langmuir and Harold Mott-Smith, "Studies of electrical discharges in gases at low pressures," Part. 4, Gen. Elec. Rev. **27**, 769 (1924).

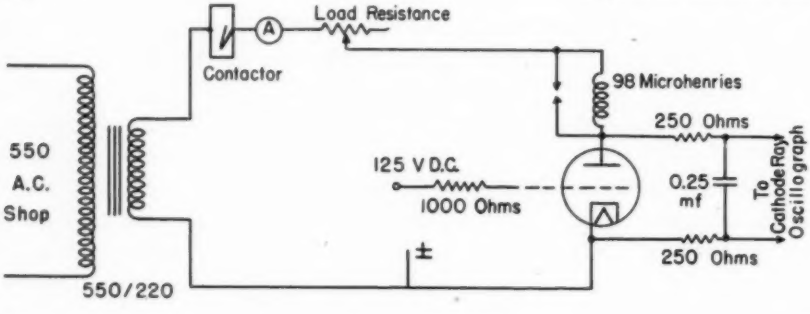

FIG. 1. Circuit for studying surges in thyratrons. The current is increased gradually until surges are seen on the oscillograph or spark gap.

i.e., the sudden extinction of the cathode spot on a mercury pool cathode or a "sputtering" hot cathode, or on an anode that is acting as cathode during arcback. But the energy of such surges is very small compared to that of the gas limit surges. The relative magnitudes can be estimated from the fact that cathode extinction occurs at the *smallest* current at which a cathode spot is stable, while gas limit extinction occurs at the *largest* current which the tube can carry. The former limit lies between 0.5 and 5 amperes, and is usually less than 2 amperes. The latter is several times the full load rating of the tube; in large mercury arc rectifiers it lies between 20,000 and 50,000 amperes. The speed of interruption is about the same for the two types of extinction, the time lying between 1 and 100 microseconds, depending on dimensions, for complete interruption. Hence, the magnetic energy $\frac{1}{2}$ Li^2 of the two types of surges is in the ratio $(20{,}000/2)^2 = 10^{10}$. When this is transformed by the interruption into electrostatic energy $\frac{1}{2}$ CV^2 across the tube and the circuit elements adjacent to it, including the first two or three turns of the transformer winding, the relative electrostatic energies will be in this same ratio. The voltages V will be in the ratio of the interrupted currents, *viz.*, 10,000/1. Experimentally it is found that the gas surges, when not limited by breakdown of the tube or insulation, are of the order of 100,000 volts, while extinction surges seldom reach 100 volts.

Commercial rectifiers and thyratrons are designed to carry their rated currents, including liberal overloads, without surges. Gas limitation and the resulting surges set in only when these ratings are exceeded. This may occur in one of two ways: (1) The vapor pressure may be allowed to fall below its specified value, thus decreasing the current capacity; or (2) excessive current may be passed through the tube. The commonest cause is the excessive currents which flow under short circuit conditions. The occurrence of such surges and the consequences which follow them are caused primarily by neglect of short-circuit considerations in the design of equipment. Surges will not occur if equipment is designed so that the maximum current demand, including short circuit, does not exceed the overload rating of the tubes.

3. EXPERIMENTAL TESTS

Surge limits, i.e., the limiting values of the tube current below which surges never occurred at the given vapor pressure, and above which they always occurred, were determined in the circuit shown in Fig. 1. Power was taken from the 550-

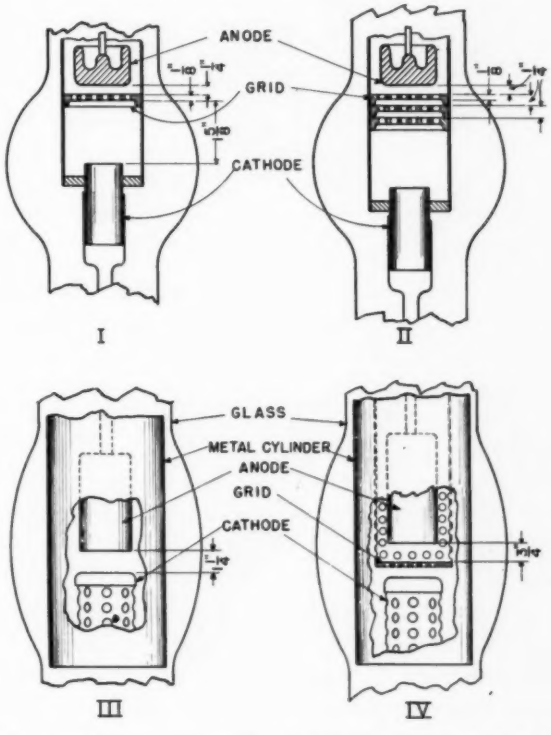

FIG. 2. Outline structures of tubes studied. I. FG-41; II. FG-118; III. FG-44; IV. FG-45.

volt, a.c. shop supply through a step-down transformer. Included in series with the tube under test were a contactor, an ammeter, a variable load resistance, and a small air-core inductance. In order to fix the mercury vapor pressure, the lower end of the tube was placed in an oil bath maintained at the desired temperature.

Currents of gradually increasing amount were passed through the tube for short periods, about $\frac{1}{10}$ second, just long enough to allow the trace of cathode-anode voltage to be observed on the oscillograph. When the current reached the limit of the tube, set by gas pressure, an attempt to increase it beyond this point first raised the tube voltage drop. A further slight decrease of the series resistance produced surges, which could be observed on the oscillograph, or evidenced by a

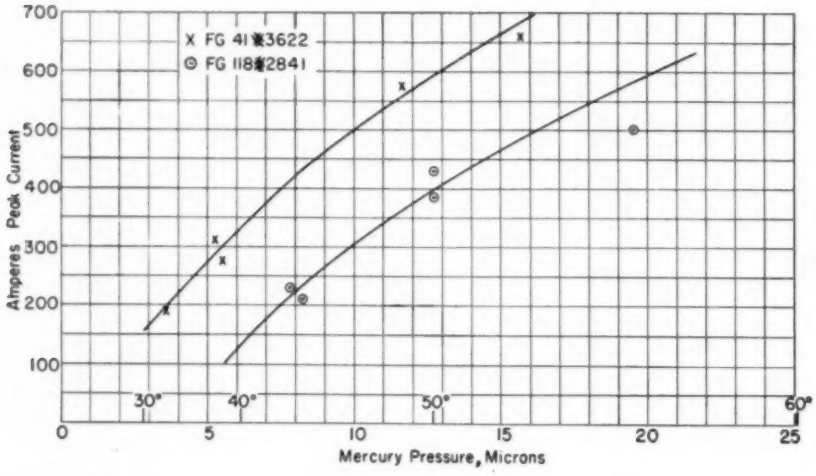

FIG. 3. Overload currents at which surges were observed in FG-41 and FG-118 thyratrons.

spark in the gap across the inductance. The capacity-resistance filter in the oscillograph leads protected the oscillograph from sparkover when the surges occurred.

Tests were made on four types of tube, *viz.*, FG-41, FG-118, FG-44, and FG-45. The outline structures and dimensions of these tubes are given in Fig. 2. The dimensions of the current paths shown in Fig. 2 will be discussed in Section 4, in connection with the interpretation of the results.

The results are shown in Figs. 3 to 6. Figure 3 gives the data for the FG-41 and FG-118 tubes. The ordinates are the currents at which surges were observed; the abscissas, the mercury vapor pressure in microns. The mercury temperatures are also given for convenience.

The FG-118 tube was a new one, and its cathode was capable of furnishing the maximum current demanded (500 amp.) at normal cathode temperature. The FG-41 was an old tube and was low in emission, but was made to furnish 650 amperes without sputtering by operating the cathode at 6.5 volts instead of the normal 5 volts. It will be shown later that cathode sputtering does not cause surges, but that "cathode spot" emission, which constitutes sputtering,* has a slightly lower surge limit than normal emission, presumably because not all of the tube's cross section is available for use when the current originates at a spot.

* The cathode sputtering referred to here might be called "cathode spotting," to differentiate it from disintegration by positive ions. It is an erratic formation and extinction of cathode spots, caused by the rise in voltage drop resulting from insufficient emission.

Figure 4 shows the values of current at which surges were observed in an FG-45 thyratron which had been in service for 12,000 hours. The upper curve represents data taken with a cathode heater voltage of 6.0. At this temperature (approx. 920°C) the cathode was able to furnish the 1600-amp. load current without sputtering.

The points on the middle curve were taken with cathode voltages of 5.0 and 5.5, respectively. Under these conditions, emission limitation occurred before the surge limit was reached. The emission limit was evidenced first by an increase in cathode-anode voltage drop; the cathode-ray oscillograph trace, which at low currents was flat, indicating a constant voltage drop throughout the half-cycle, bowed up in the center when the emission limit was exceeded slightly. As the current was increased further, this bowing of the CRO trace became more pronounced until a break in the trace occurred. If the limitation in current was caused by lack of emission, the trace merely dropped and remained flat after the break, which was interpreted as the formation of a cathode spot. Increasing the current demand still further caused this break to occur closer and closer to the beginning of the cycle but did not change its form. The trace is generally ragged just before the break, indicating formation and extinction of several cathode spots. The lower curve in Fig. 4 shows the values of current at which these emission limits were observed.

A second bowing up, in the middle of the cycle, appeared as the vapor pressure limit was approached; this broke into a jagged surge when the limit was reached, and increased rapidly in vio-

lence with further increase of current. At the lower vapor pressures these two phenomena sometimes overlapped, when the two limitations occurred at nearly the same current; but in general they were well separated.

Figure 5 gives similar data for an FG-44 phanotron. This tube was an old one, which had been in continuous operation for 30,000 hours. The two lower curves give the emission limits at the cathode voltages at which the surge data were taken. They show that a considerable part of the larger currents was furnished by cathode spots, so that the surge limits observed were those corresponding to this condition, and are to be compared with the 5.0- and 5.5-volt values in Fig. 4.

Figure 6 shows a comparison of the surge limits for thyratrons and phanotrons. It contains the data of Figs. 4 and 5, and similar data for two additional thyratrons which had had the same 30,000 service as phanotron No. 551. It is seen that the limits are the same for the phanotron and the thyratrons; and that the values all fall on a single curve, with the exception of the 6-volt

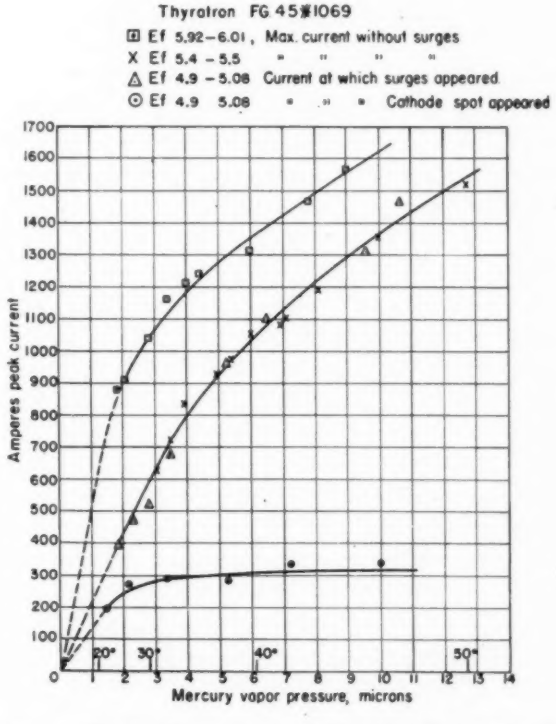
Thyratron FG 45 #1069
⊡ Ef 5.92–6.01, Max. current without surges
X Ef 5.4 – 5.5 " " " "
△ Ef 4.9 – 5.08 Current at which surges appeared
⊙ Ef 4.9 5.08 " " " Cathode spot appeared
Amperes peak current
Mercury vapor pressure, microns
20°
30°
40°
50°

FIG. 4. Overload currents at which surges were observed in FG-45 thyratron. The lower curve represents the limit of cathode emission with heater voltage 5.0.

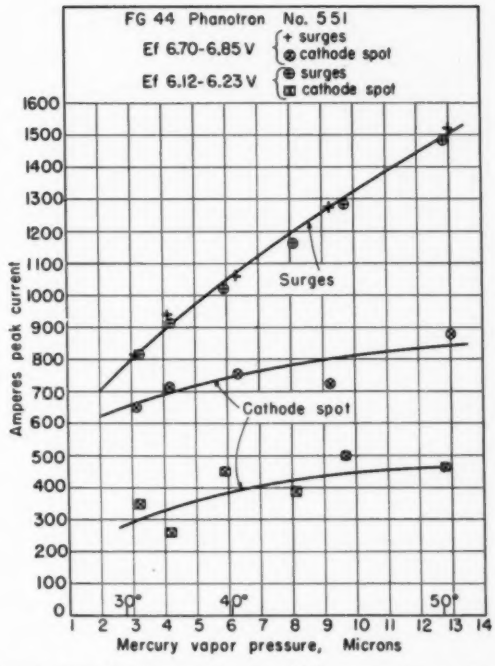

FIG. 5. Overload currents at which surges were observed in FG-44 phanotron. The lower curves give the cathode-emission limits.

data on tube No. 1069. In this case the cathode had ample emission for the maximum overload demanded.

It appears that the surge limit is about 20 percent higher when there is ample emission than when a considerable part is furnished by a cathode spot. A possible explanation of this difference is the inaccessibility of some of the cathode holes to emission originating at a spot, hence incomplete utilization of the holes.

4. INTERPRETATION OF DATA

It is clear from the data of curves 3 to 6 that the limiting current which a tube can carry is a function of vapor pressure, increasing less rapidly than the pressure. A linear relation might have been expected; but back diffusion, magnetostriction, and vapor temperature (influencing density) are all factors which might favor low pressure.

The second parameter limiting current-carrying capacity is cross section of path. The heat shield of the FG-45 cathode is furnished with 40 holes of $\frac{7}{16}$-in. diameter, through which the current emerges. The total area of these holes is 38.8 cm^2. The grid has 20 cm^2 of 0.170-in. holes, and ap-

proximately 185 cm² of 0.060-in. holes, making a total area of about 200 cm². It is probable, therefore, that the vapor scarcity, and the surges induced thereby, will occur first at the cathode heat shield. The limit of 1400 amperes at 41°C, shown on the upper curve *A* of Fig. 4, represents the current-carrying capacity of the 38.8 cm² of holes, and gives a current density of 36 amp. per cm² at 41°C.

The other curves for FG-45 thyratrons give a limiting value 20 percent lower, *viz.*, 28.2 amp./cm² at 41°C. In all of these runs the cathode had insufficient emission for the maximum currents, and the lower current capacity is believed to be caused by inaccessibility of some of the holes.

The cathode of the FG-44 phanotron has the same hole area as the FG-45 thyratron, but the current path between its cathode and anode is otherwise unobstructed. The fact that its surge limit is the same as that of the FG-45 is evidence that the limitation is due to the cathode holes.

The FG-41 tube has a grid consisting of a carbon disk pierced with 44 holes of 0.51-cm diameter, making a total hole area of 9 cm², which constitutes its limitation. From Fig. 3 it is seen that the maximum current capacity at 41°C is 330 amperes, or 36.7 amp./cm². This agrees with the value of 36 amp./cm² found for the FG-45 tube in the condition of full utilization of holes (upper curve, Fig. 4).

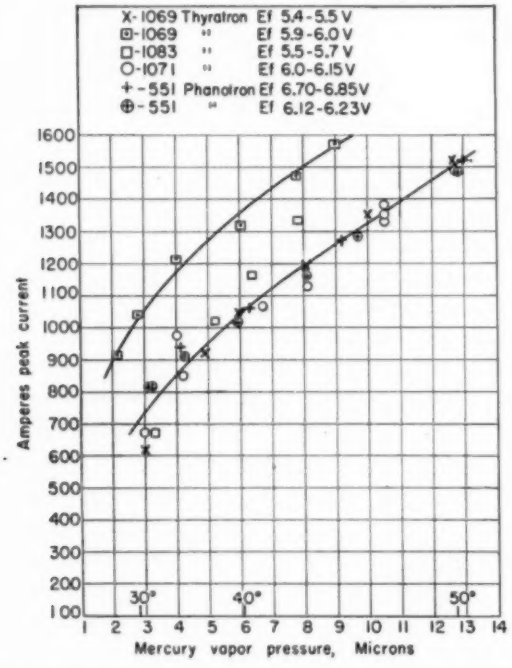

FIG. 6. Comparison of surge limits in FG-44 phanotron and FG-45 thyratrons. This graph includes the data from Figs. 4 and 5, using the same symbols; and values for two additional FG-45 thyratrons.

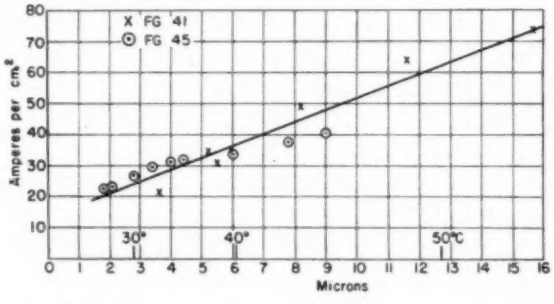

FIG. 7. Maximum current-carrying capacity of mercury vapor as function of pressure. These data are valid for holes of $\frac{1}{8}$-inch to $\frac{1}{2}$-inch diameter in a wall at 500°C.

The FG-118 tube has three grids in series, $\frac{1}{8}$ inch apart, each similar to that of the FG-41. From Fig. 3 it is seen that this multiple grid construction lowers its current capacity approximately 30 percent, compared to the single grid construction of the FG-41. This is probably a temperature effect, the central grid of the three-assembly running considerably hotter than the single grid in the FG-41, and thus lowering the vapor density in its vicinity.

For the case of a single obstruction these experiments yield fairly definite values of maximum current density, as a function of vapor pressure. These are given in Fig. 7, and are the values of maximum current plotted on the upper curves in Figs. 3 and 4, divided by the respective cross sections. These values may be expected to hold for holes between $\frac{1}{8}$-inch and $\frac{1}{2}$-inch diameter in a wall of thickness equal to the hole diameter approximately, when the wall is at a temperature of about 500°C. These values are applicable in both hot-cathode and pool tubes, and are in good agreement with those found in earlier tests,[2] with one exception; *viz.*, the 0.6-cm hole in a 1-cm graphite disk (Fig. 8 and Table V, reference 2), which gave 93 amp./cm² at 6.5 microns (41°C). This was a cold disk at one end of a tube with Hg cathode, and the test current, a single 1/60-sec.

impulse, did not heat it appreciably. Assuming its temperature to be 300°K, and that of the FG-45 cathode shields and FG-41 grid to be 775°K = 500°C, the vapor *densities* in the cold and hot holes, respectively, would be in the ratio 775/300, which is just the ratio 93/36 of the observed currents. Such a cold condition is not likely to be encountered in practice, except transiently; and the 500°C wall temperature may be taken as representative of maximum load operation in practical tubes.

5. CONCLUSION

High voltage surges in apparatus associated with gas discharge tubes are caused by paucity of gas. They can be avoided by using rectifiers of sufficient cross section and pressure to carry the maximum current, including short circuit current, without exceeding the current-carrying capacity of the gas or vapor in the rectifier. Values of mercury vapor current-carrying capacity, in amperes per square centimeter as a function of pressure, are given in Fig. 7.

Eddy Current Type Flaw Detectors for Non-Magnetic Metals

IRWIN VIGNESS, J. E. DINGER, AND ROSS GUNN
Naval Research Laboratory, Washington, D. C.

(Received April 6, 1942)

New developments in an eddy current type flaw detector are discussed. Several types of pick-up units, which contain the exciting coils for inducing eddy currents in the test material and pick-up coils for detecting changes in this eddy current pattern when a flaw is approached, are described. The electric power for the exciting current is supplied by a vacuum tube power oscillator at a frequency of 500 or 1000 cycles/second. The circuit for detecting the changes in the eddy current pattern employs vacuum tube bridge circuits sensitive to both amplitude and phase changes. The use of jigs to guide the pick-up unit, automatic scanning, and automatic recording is discussed.

INTRODUCTION

THE rapid increase in the use and applications of non-ferrous metals has required that non-destructive methods be devised for the location of flaws in them. A review of the various methods of non-destructive testing has been given by others.[1] One described method[2] measures the change, caused by a flaw, of an eddy current pattern induced in the object under test. This method has been successful in locating flaws that cause discontinuities in the electrical resistance of non-magnetic materials. Since the original publication by Gunn,[2] many types of flaw detector units involving eddy current principles have been developed, the useful frequency range of the exciting current has been extended, and electronic devices have been used for the source of exciting current and for the amplification and detection of the flaw detector signal. The use of jigs and automatic scanning devices, to hold the detector unit at a definite orientation and to move the unit at a uniform speed over the material under test, has been found necessary in many cases. Automatic recording of the detector unit unbalance has been found to be practical and necessary when the objects under test are of shapes that cause irregularities in the flaw detector signal. In this latter case the scanning curve of a known sound piece must be compared with scanning curves of other similar pieces.

DESCRIPTION OF APPARATUS

An eddy current type pick-up unit consists of two essential parts: an exciting alternating magnetic field, the purpose of which is to cause an eddy current pattern in the object under test, and a pick-up coil that is adjusted to determine variations in the "normal" eddy current pattern. The

[1] "Symposium on non-destructive testing," J. Inst. Elec. Eng. **84**, 519–596 (May 1939).
[2] Ross Gunn, "An eddy-current method of flaw detection in non-magnetic metals," J. App. Mech. **8**, A22 (1941).

effect of the exciting field on the pick-up coil is balanced so that a zero average current flows through the indicating microammeter when the pick-up unit is placed on a homogenous flat metallic plate. Different arrangements of the exciting and of the pick-up coils, with respect to each other, provide endless variations in the construction and applicability of the flaw detector pick-up units. The variations can be divided into two general types: (a) Those in which the magnetic path within the pick-up unit of the pick-up coil is isolated as much as possible from the magnetic path of the exciting field. An example of this type is shown in Fig. 1a. (b) Those in which the magnetic path within the pick-up unit of the pick-up coil has sections in common with the magnetic path of the exciting field. This second type is illustrated by all units of the first two figures except that shown in Fig. 1a.

There are many good theoretical arguments and physical reasons which indicate that the first type of pick-up unit is much to be preferred. In practice, however, it has been found that the second type can be made as sensitive and nearly as stable as the first. In addition, the second type has the advantage of being able to be constructed in many shapes and of smaller dimensions. Five types of pick-up units (Figs. 1 and 2) are described. Those shown in Fig. 1 are general purpose units, while those shown in Fig. 2 were designed for specific applications. The principal magnetic paths of the exciting fields can be traced from these figures. A non-magnetic specimen that is to be examined for the presence of a flaw is placed so that the external exciting field penetrates into it. If the magnetic field from the induced eddy currents does not affect each of the two pick-up coils in an identical manner an unbalance will result. Among other things a flaw will cause such an unbalance. It is to be noted that a flaw must be scanned with the pick-up unit oriented so that some part of the flaw is brought nearer to the pole of one pick-up coil than to its mate. All of the units illustrated are therefore directional in effect except the axial type (Fig. 2a). If a flaw is approached so that its effect on both pick-up coils is the same, no unbalance will result. Best sensitivity is had when the pick-up unit is oriented so that the direction of scanning is in a plane containing the pick-up coils or in a plane containing the principal magnetic path of the pick-up coils.

Some applications of the pick-up units illustrated in Fig. 2 are given below. These units may be convenient for many other applications. The axial type pick-up unit (Fig. 2a) is included for its properties as a thickness gauge rather than a flaw detector. With it thicknesses of sheet, non-magnetic conducting materials can be determined from one side of the sheet with an accuracy better than 10 percent for thicknesses between 0.01 inch to 0.25 inch. Calibration curves must be used (see Fig. 6). With the spot weld tester (Fig. 2b) cracks and porosities in the weld are detectable; however, the effects of cracks, porosities, dimpling, cavitation, and straining of the weld material by shrinkage are of such magnitude as largely to mask the effects of fusion between the plates. It

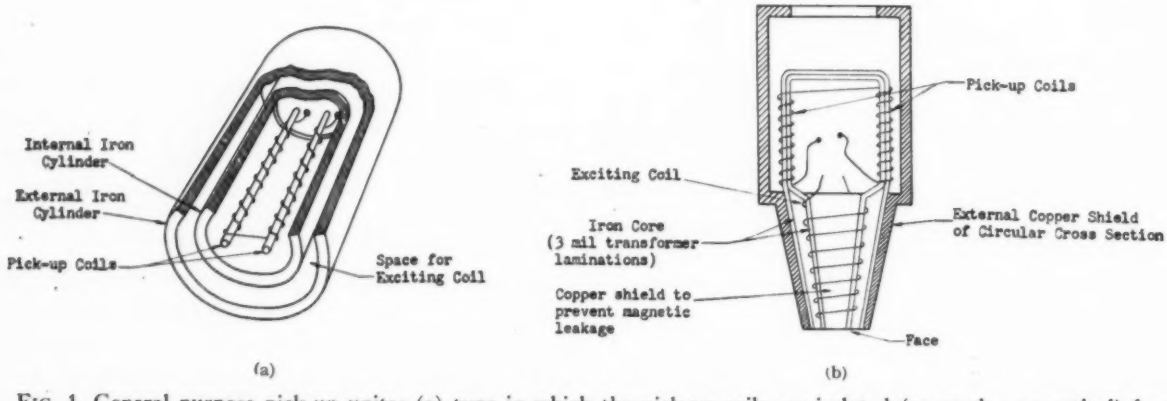

FIG. 1. General purpose pick-up units: (a) type in which the pick-up coils are isolated (as much as practical) from the magnetic path of the exciting field; (b) a pick-up unit can be made to small dimensions and that has little edge effect.

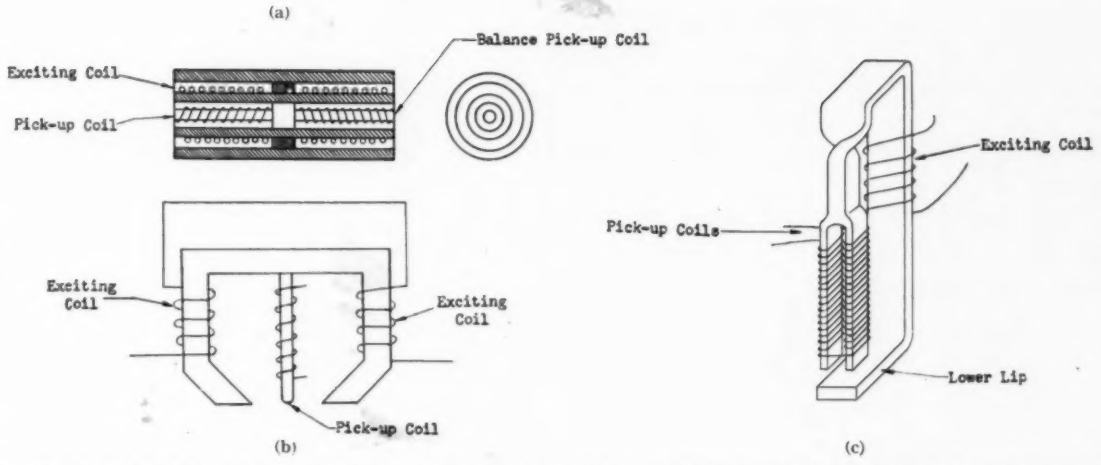

FIG. 2. (a) Axial pick-up coil unit. Voltage induced in the pick-up coil by the exciting field is balanced by a voltage generated in the "balance" pick-up coil. This unit makes an excellent thickness gauge for non-ferrous sheet material and, because of this property, is a poor flaw detector. (b) Spot weld tester type pick-up unit. This unit has excellent sensitivity and edge effects can be reduced by encasing in a thick copper shield. (c) Edge or bar tester type pick-up unit. Type in which no attempt was made to isolate the exciting flux from the pick-up coils. The unit is jacketed by a copper shield when assembled. It has excellent sensitivity.

is not regarded probable that this method can be developed to test the degree of fusion between plates. The edge or bar tester, Fig. 2c, was made to determine the presence of flaws along the edge of a material, such as turbine blades, or in bars. The flaws must be perpendicular to the edge or the bar axis. The material under test is placed between the lower lip and the pick-up coils. The pick-up coil axes are kept perpendicular to the length of the material and a plane containing the two pick-up coils is kept parallel to the length. It is to be noted that the exciting flux penetrates through the material. However, the pick-up unit gives a much better indication of a flaw if the flaw is on the side nearer the pick-up coils.

It is desirable that the source of exciting current provide a power output of about 10 watts of good wave form at a constant frequency in the range between a few hundred to a few thousand cycles per second. Two frequencies, 500 and 1000 cycles per second, have been found to be sufficient.

A convenient source of exciting current consists of a vacuum tube oscillator and power amplifier.* The diagram of Fig. 3 gives the circuit of the oscillator power amplifier. The pentode, 6AC7/1852, serves as an oscillator. The circuit constants C_1, C_2, C_3, R_{15}, R_{16}, R_{17}, which determine the frequency of oscillation, are mounted on a removable plug so that several desired frequencies can be obtained. R_6 varies the output current which is indicated by the milliammeter M_1. Switch S_1 is provided to match an output impedance of 500 or 15 ohms. When the lower impedance is used a shunt is automatically placed across the milliammeter so that the exciting current is about twice that indicated.

It is the function of the detector unit to receive the pick-up signal from the pick-up coil and indicate any change that may occur in this signal as the pick-up unit is passed over a flaw. The amplitude of the pick-up signal and its phase relative to the exciting current are dependent upon the conductivity of the material under test, the position and extent of the flaw in the material, and the particular pick-up unit employed. Figure 4 gives the circuit of a detector which is both amplitude and phase sensitive. The pick-up signal is amplified by tubes T_1 and T_2. The bridge arrangement in the cathode return of T_2 makes it possible to shift the phase of the pick-up signal a desired amount after which the signal is applied in push-pull to tubes T_3 and T_4. Tube T_5 receives a signal from an oscillator in phase with the flaw detector exciting current and produces a signal of nearly square wave form which is then applied to a second pair of grids of tubes T_3 and T_4. This square wave signal gives a valve action that permits tubes T_3 and T_4 to be conducting for one-

* Dr. Ramond Waddel assisted in the design of these vacuum tube circuits.

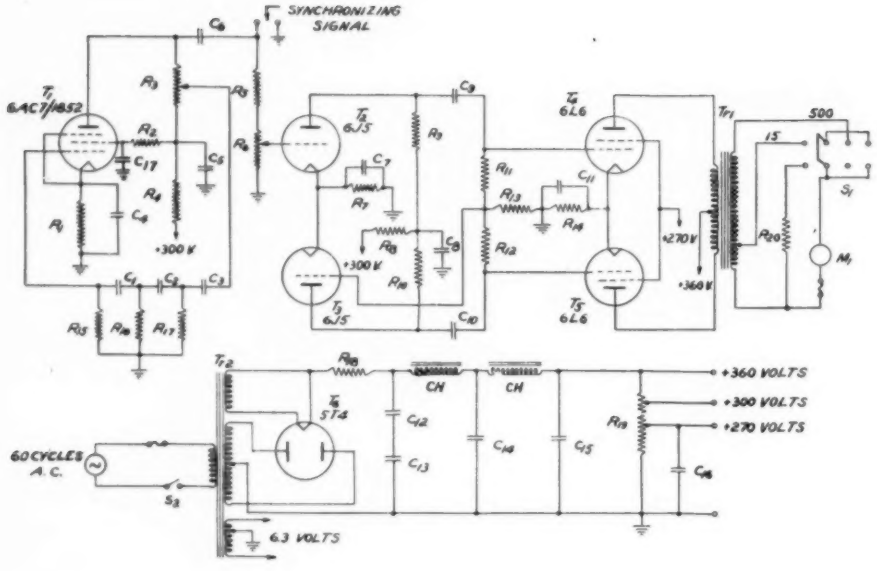

FIG. 3. Oscillator power amplifier.

half of each cycle. The control R_8 in the phase shifting bridge makes possible a phase shift of the pick-up signal with respect to the square wave, so that tubes T_3 and T_4 are conducting during that portion of the pick-up signal cycle which will give the largest and most symmetrical response as a flaw is passed over by the pick-up unit. A change in the amplitude or phase of the pick-up signal thus produces a change in the potential difference between A and B and is indicated by the d.c. microammeter M. The sensitivity of the meter is varied by the shunt R_{15}. S_1 permits the use of meter M or an external meter or recorder. It should be noted that the meter connections are at a potential near that of the plates of T_3 and T_4 so that care should be taken in the using of external connections. The control R_{13} is used to adjust the zero position of the meter. Control R_1 varies the pick-up signal applied to T_1 and serves as a sensitivity control.

It is not necessary that the oscillator shown be the source of power for the flaw detector. Any convenient source of constant and suitable frequency can be used. The same source must supply the flaw detector exciting coil and synchronize the detector circuit valves by being applied through the 6SF5 tube. Sixty-cycle frequency from the power mains has been successfully used.

In the application of the flaw detector to a particular piece of material, it is usually convenient to hold the pick-up unit in a jig especially constructed for the object being examined. The purpose of the jig is to prevent unnecessary tipping of the pick-up unit and to serve as a guide so that scanning will take place with a definite relation to edges and irregular places on the object. With a proper jig it is possible to duplicate the scanning of a particular object and thus obtain a characteristic pattern for the object. If a flaw is present in another identical object, this characteristic pattern will be altered and will thus indicate the presence of the flaw.

It is often advantageous to scan the object automatically. By automatically scanning the object the pick-up unit moves at a uniform speed and in a definite path. It is only by the use of jigs and scanning devices that accurate quantitative work can be obtained. However, in most applications quantitative work is not necessary; in such cases jigs and scanning devices are necessary only when scanning irregularly shaped materials, when scanning near an edge, or when routinely scanning many identical pieces.

Automatic recording of the pick-up coil unbalance as an object is automatically scanned is often useful. If an object of varying curvature is examined, a recording of the scanning-unbalance curve can be compared with a recording of an identical sound object. A flaw can thus be detected by differences in the characteristic scanning curves. Automatic recording has the advantage of providing a permanent record of the

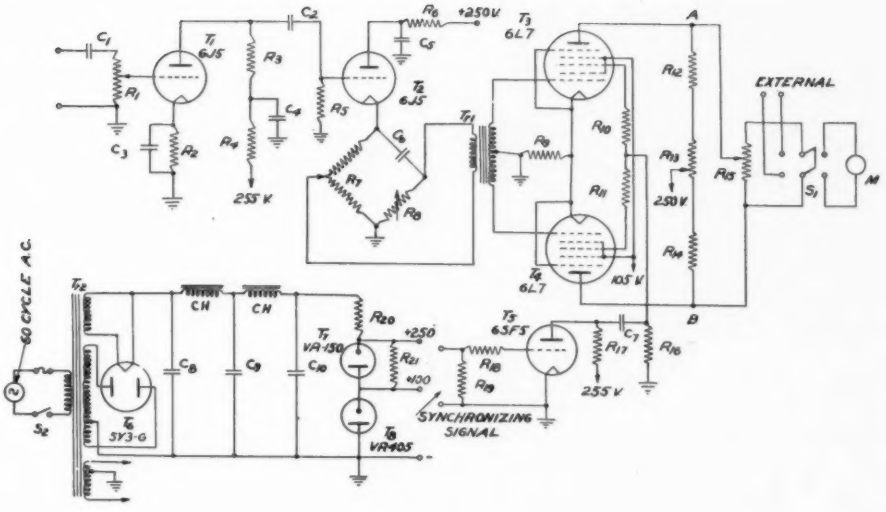

FIG. 4. Detector circuit.

scanning curve. In the case of large regular objects it has not been found advisable to use a recorder unless a permanent record is desired. In such cases a flaw can as easily be detected by observing the indicating microammeter. A photoelectric microammeter recorder, with 10-microamperes full scale deflection, has been found very satisfactory to use with the detector unit.

APPLICATIONS AND RESULTS

All of the units, except the "axial pick-up" type and the "spot weld tester" type, have characteristic curves of unbalance caused by a crack-like flaw similar to those shown in Fig. 5a. The curves are of this shape only when the detector (or rectifier) unit is adjusted to give good rectification of the signal caused by the flaw. If the phase is not adjusted for best sensitivity, then this characteristic curve becomes unsymmetrical and four peaks, rather than two, may be present. It is not necessary, and it is usually not convenient, to keep the phase accurately adjusted for best sensitivity, as this adjustment depends on the pick-up unit used, on the kind and thickness of material being scanned, and on the position and depth of a flaw. It is necessary to recognize that a crack-like flaw may be indicated by an unbalanced curve that may be unlike the characteristic curves illustrated.

The axial type pick-up unit (Fig. 2a) is the only type of unit developed that is non-directional; i.e., a flaw will be indicated in the same manner when it is crossed by the unit regardless of how the unit is oriented with respect to a central axis through its length. The unbalance of this unit is at a maximum when the unit is directly over the flaw and decreases rapidly as the unit is moved away from the flaw. There is, of course, a large change of balance as the unit is moved away from the plate under test. This is its depth gauge effect. A curve showing the unbalance resulting from different thicknesses of sheet copper is given in Fig. 6.

The spot weld tester unit (Fig. 2b) may be made to traverse a weld in a direction of a plane that contains the unit, i.e., the plane of the paper as shown in Fig. 2. In this method the weld is successively passed over by the leading exciting coil, the pick-up coil, and the trailing exciting coil. The unbalance curve is similar to that shown on Fig. 5a. This pick-up unit may also be made to traverse a weld in a direction perpendicular to that described above. In this case the unit is passed over the weld so that the weld is contained between the pick-up coil and an exciting coil when the unit is directly over the weld. The unbalance curve rises to a simple maximum as the unit approaches the weld. When this latter type of scanning is used, troublesome edge effects are to a large extent eliminated. However, more information as to the weld can be obtained by the first method of scanning. The indentation caused by electrode pressure and the different specific resistance of the metal contained in the spot weld usually make the results difficult to interpret.

Figure 5 illustrates the types of results obtain-

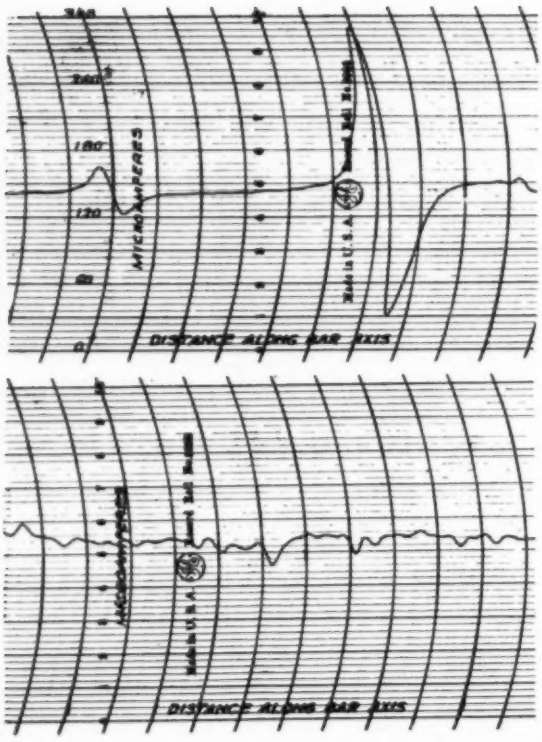

FIG. 5. a (above) Flaw detector recording of two fatigue cracks in an aluminum alloy bar. b (below) Background variations of apparatus. The sensitivity is thirty times that of the top recording.

able with the edge or bar tester type pick-up unit (Fig. 2c). The results would be comparable with any of the units that give this characteristic type curve. The upper curve was caused by two fatigue cracks in an aluminum alloy bar with rectangular cross section of $\frac{7}{8}\times\frac{3}{8}$ inch. The pick-up unit was moved at a uniform speed parallel to the bar axis. A fatigue crack that penetrated about halfway through the bar is indicated by the large microammeter variation. The smaller variation at the left of this curve was caused by a barely noticeable crack that extended around one corner. The lower curve shows the extent of background variations. It should be noted that full scale deflection for the upper curve is equal to thirty full scale deflections for the lower curve.

Variations in electrical conductivity of a metal caused by different degrees of cold working, or different treatment of the metal at different sections, are often very apparent. As the mechanical properties of the metal are also related to its previous history, these electrical variations are a measure of mechanical inhomogeneities.

Figure 7 illustrates flaw detector recordings of a forged aluminum alloy 25ST bar. The surfaces of this bar had been machined smooth. Two different recordings are given to show the ability of the apparatus to duplicate the curves. The sensitivity used was quite high. Any forged material whose electrical conductivity is affected by the mechanical working will be expected to cause a background flaw detector variation that may make the detection of very small flaws difficult. It is not known, as yet, if these variations can be connected with fatigue or tensile properties of the material.

In order that a flaw may be detectable, it is necessary that it be located in such a manner that it will disturb the eddy current flow set up by the exciting field and that this disturbance will affect the two pick-up coils in a similar manner. For most types of detectors the induced eddy current flow is in planes parallel to the surface of the metal being scanned (an exception is the spot weld tester). Flaws that run parallel to the surface will not disturb this eddy current pattern and will, therefore, not be detectable under ordinary conditions.

Rough surfaces or surfaces of short radius of curvature cannot be successfully scanned unless special pick-up units are designed for the particular application, or unless jigs and recorders are used with standard units and the unbalance curves of sound pieces and duplicate curves of similar pieces of unknown quality are compared.

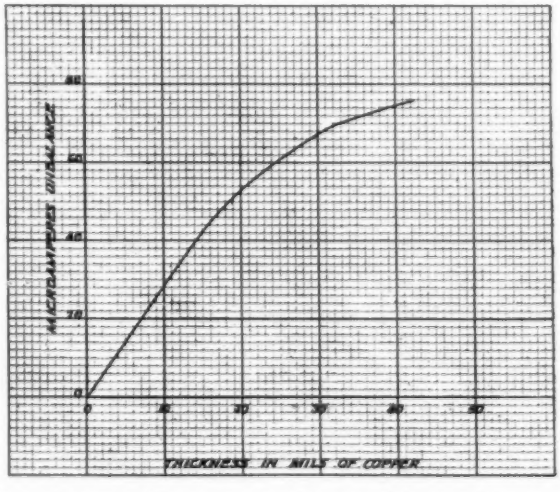

FIG. 6. Calibration curve of axial type pick-up unit used as a thickness gauge.

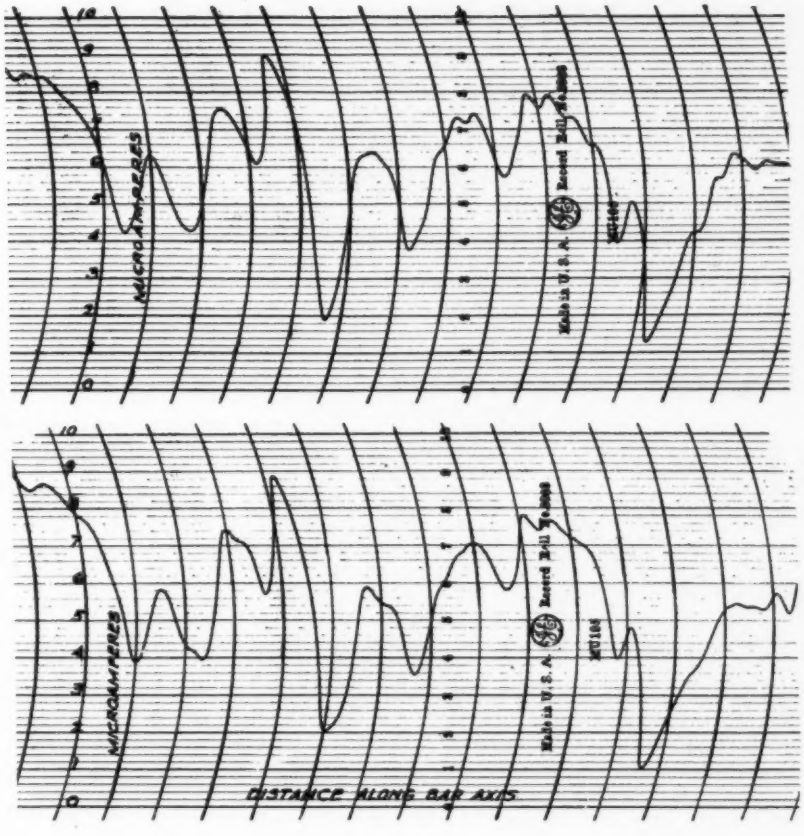

FIG. 7. Recordings of 25ST forged aluminum alloy bar. The two recordings illustrate the ability of apparatus to duplicate the curves.

The flaw detector can best be applied to smooth flat surfaces, or surfaces with large radius of curvature in the direction of scanning. Tubes and rods of uniform cross section are easily tested for transverse cracks. Fatigue cracks are easily noticeable as they usually extend in a plane perpendicular to a surface. Blow holes and occlusions can be detected when they occur near the surface.

Curves showing the sensitivity of the apparatus for flaws of different sizes and under different thicknesses of material and the effects of electrical conductivity on the sensitivity have been given in a previous article.[2] The use of different means of detection and of higher frequencies has greatly improved the stability and ease of operation. The ultimate sensitivity has not changed appreciably for corresponding frequencies. It appears that the higher frequencies (500 to 1000 cycles per second) can be used with advantage under most conditions as the depth of penetration of the exciting field is usually more limited by the geometry of the pick-up unit than by shielding of over-lying material. With the type pick-up units used, no advantage was obtained by using frequencies above 1000 cycles per second.

Transient Temperatures in the Anode of an X-Ray Tube

F. R. ABBOTT*
Vacuum Tube Engineering Department, General Electric X-Ray Corporation, Chicago, Illinois
(Received February 13, 1942)

The rapid heating and cooling cycle of the focal area of a high speed radiographic x-ray tube anode results in short life, although maximum temperatures produced are not excessive. Some objections are found to earlier theoretical investigations of temperature distributions beneath such focal areas. An operational solution is obtained in terms of Bessel functions. From the calculated temperature distribution the mechanism of disruption is explainable.

TRANSIENT TEMPERATURES IN X-RAY TARGETS

MODERN high speed roentgenography presents the x-ray tube designer with a problem in dissipation of heat from the focal area under intense electronic bombardment. Exposure times of the order of 1/20 of a second with loadings of 200 to 400 milliamperes at 60 to 100 kilovolts have become common practice. At the same time, fine detail has demanded small focal spots. With stationary anode tubes, target temperature limits the focal spot size under such loading to about 5.0 mm×5.0 mm. Rotating anode tubes permit reduction in focal spot to about 2 mm×2 mm, or even smaller. These sizes are, of course, the right angle projections of line focal areas, as shown in Fig. 1.

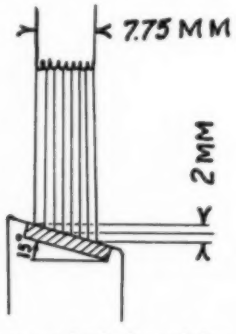

FIG. 1. Line focus method of attaining an effective focal spot width of 2 mm with an electron beam 7.75 mm wide.

Here an electron beam of 7.75-mm width strikes a target tilted at 15°, resulting in a projected focal area width of 7.75 tan 15° = 2 mm.

Loading of 300 milliamperes at 80 kilovolts corresponds to 24,000 watts. A focal area 2 mm×7.75 mm amounts to 0.155 sq. cm. Thus the momentary intensity of heat loading is given by 24,000/0.155 = 155,000 watts/cm².

Little of this heat is dissipated by radiation, for even at the melting point of tungsten, 3400°C, the blackbody radiation according to the Stefan-Boltzmann law amounts to only about 1000 watts/cm². The emissive power of clean tungsten is rather low; thus it is safe to say that less than 1 percent of the heat is lost as radiant heat. Because of the low efficiency of x-ray production (1 percent or less at this kilovoltage) it is evident that almost all the energy must be absorbed by the massive anode of the tube. The total heat involved is not enough to heat the anode excessively. 155,000 watts for 1/20 second corresponds to 1870 calories, which will raise the temperature of a two-kilogram anode only about 10°C. Thus the total heat problem is not serious in this case.

Safe load ratings of tungsten targets have been experimentally determined. Temperatures well below the melting point of tungsten are utilized. In spite of this safe temperature condition, the focal area frequently fails after relatively short life, say 2000 to 4000 exposures. This paper will include a computation of temperatures and a brief discussion of the probable process of anode failure.

COMPUTATION OF TRANSIENT TEMPERATURES

The best that can be hoped for in a computation of this type is a close approximation. The thermal conductivity of the material involved is a variable function of the temperature and direction of flow for non-isotropic material such as rolled tungsten. Furthermore, the specific heat is a function of the temperature. To simplify computations, we have selected mean

* Now with U. S. Navy Radio and Sound Laboratory, San Diego, California.

values of these functions and assumed them constant through the range considered.

The notation employed in the following computation is given below:

k = heat conductivity cal./cm sec. degree; $k_c = 0.9$ = heat conductivity of copper in cal./cm sec. degree; $k_w = 0.3$ = heat conductivity of tungsten in cal./cm sec. degree (mean values approximate to the range 700°–1500°); S = heat capacity of material in cal./cm³; $S_c = 0.9$ = heat capacity

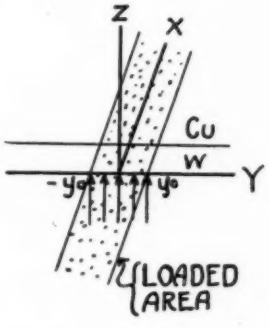

FIG. 2. Rectangular coordinate system with centerline of focal area along the X axis.

per cm³ of copper in cal. per degree; $S_w = 0.75$ = heat capacity per cm³ of tungsten in cal. per degree (mean values for temperatures 700°–1500°C); V = temperature Centigrade; t = time in seconds measured from beginning of exposure; W = power input per cm length of line focus in calories/sec.

In this computation we will consider the line focal area to be long compared to its width. Thus, taking a section perpendicular to the focal line our problem reduces to temperatures in a plane. This will, of course, give computed temperatures appreciably higher than the true values. Errors in this direction are, however, not too objectionable from the safe operation point of view.

We select a rectangular coordinate system in which the target face is the XY plane and the center of the line focus lies along the X axis as shown on Fig. 2. The width of the line focus is represented by $2y_0$. This area of unit length is loaded with a W calories/sec.

The general equation for heat flow is given by

$$\partial V/\partial t = (k/S)\nabla^2 V, \tag{1}$$

in which ∇^2 is the Laplacian operator.

We will be concerned with two forms of this equation.

In cartesian coordinates

$$\frac{\partial V}{\partial t} = \frac{k}{S}\left[\frac{\partial^2 V}{\partial x^2} + \frac{\partial^2 V}{\partial y^2} + \frac{\partial^2 V}{\partial z^2}\right] \tag{2}$$

and in cylindrical coordinates if V is a function of r alone:

$$\frac{\partial V}{\partial t} = \frac{k}{S}\left[\frac{1}{r}\frac{\partial V}{\partial r} + \frac{\partial^2 V}{\partial r^2}\right]. \tag{3}$$

We apply Eq. (2) to the problem as indicated in Fig. 2. Assume that the target is composed of only one material. For a long line focal area, we reduce the problem to two dimensions and Eq. (2) becomes:

$$\partial V/\partial t = k/S[(\partial^2 V/\partial y^2) + (\partial^2 V/\partial z^2)]. \tag{4}$$

Our solution is subject to the boundary conditions.

$$V = 0 \quad \text{for} \quad t = 0,$$
$$V = 0 \quad \text{for} \quad y = \infty,$$
$$V = 0 \quad \text{for} \quad z = \infty.$$

The last two conditions are inexact but greatly simplify the solution. Since we introduce W calories of heat at $z = 0$ between y_0 and $-y_0$, we have the additional condition

$$(\partial V/\partial z)_{z=0} = \frac{-W}{2y_0 k} \quad \text{for } -y_0 < y < y_0 \text{ and } t > 0$$

and

$$(\partial V/\partial z)_{z=0} = 0$$

for absolute values of y greater than y_0 and all values of time.

The simplest Fourier series solution of this problem would be extremely unwieldy. Seeliger[1] obtained a Fourier's integral solution for Eq. (4).

Bowers[2] has discussed Seeliger's solution under these boundary conditions. In our nomenclature it becomes:

$$V = \frac{W}{2k\pi}\int_0^{4a^2t} \frac{\exp(-z^2/\tau)}{2y_0\sqrt{\tau}}\,d\tau \int_{y-y_0/\sqrt{\tau}}^{y+y_0/\sqrt{\tau}} \exp(-\xi^2)\,d\xi,$$

in which $a = (k/S)^{\frac{1}{2}}$.

[1] R. Seeliger, Physik. Zeits. **27**, 35 (1926).
[2] A. Bowers, Zeits. f. tech. Physik **8**, 271 (1927).

There are several objections to this type of solution. (1) It requires graphical integration. (2) It cannot well be modified to apply to a double layer such as copper faced with tungsten. (3) The second and third boundary conditions at $V=0$ for infinite y or z are quite inexact. In most physical cases the copper is maintained at low temperature at only a few centimeters distance from the loaded area.

There are other sources of error which cannot well be avoided in any theoretical treatment of this problem. An example is in the selection of a suitable constant value for the thermal conductivity. Bowers chose $k_w=0.4$. Recently Osborn[3] has found $k_w=0.28$ at 1100°C. This supports our average value of $k_w=0.3$.

A compensating error in Bowers' treatment of the problem is the neglect of end effects. In x-ray application the length of the line focal area is, in general, about three times the width. A two-dimensional analysis will thus give higher temperatures than actually exist. After consideration of these factors, it was decided to attempt a solution in cylindrical coordinates.

PART II. OPERATIONAL SOLUTION OF TRANSIENT HEAT FLOW FROM A LINE SOURCE

We begin by assuming that the loaded area is of semi-cylindric form of infinite length normal to the paper as shown in Fig. 3.

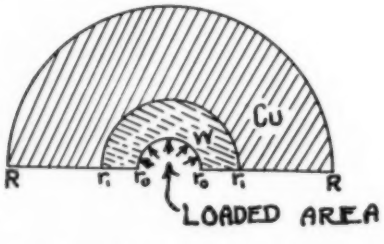

FIG. 3. Section through an infinite semi-cylinder of tungsten and copper with radial outward heat flow.

The heat load per unit length W is uniformly applied to the semi-circumferential area given by πr_0. The first conducting material extends to $r=r_1$. This would represent tungsten, for example. The second material, say copper, would then extend to $r=R$, where a constant temperature is maintained.

[3] R. H. Osborn, J. Opt. Soc. Am. **31**, 428–32 (1941).

We now employ Eq. (3):

$$\partial V/\partial r=k/S[(1/r)(\partial V/\partial r)+(\partial^2 V/\partial r^2)]. \quad (3)$$

Heaviside's operational method facilitates determination of constants in the solution of this type of equation.[4] Introducing the time derivative operator p and the substitution

$$-pS/k=\alpha^2. \quad (4)$$

Values in the second medium will be distinguished by primes; for example k', α'.

Equation (3) becomes:

$$(d^2V/dr^2)+(1/r)(dV/dr)+\alpha^2 V=0. \quad (5)$$

This has the general solution in one medium:

$$V(\alpha r)=AJ_0(\alpha r)+BN_0(\alpha r) \quad (6a)$$

and similarly in the second medium:

$$V(\alpha' r)=A'J_0(\alpha' r)+B'N_0(\alpha' r), \quad (6b)$$

in which A, A', B, and B' are functions of α and α', while $J_0(-r)$ and $N_0(-r)$ are Bessel's functions of the first and second (Neumann's) kind, respectively, and of zero order.

The physical boundary conditions determine an infinite number of values of α.

We specify:

$$V=0 \quad \text{at} \quad r=R, \quad (7)$$

$$V=0 \quad \text{for} \quad t\gtrless 0. \quad (8)$$

The impressed load at $r=r_0$ for positive t requires that: (for $r=r_0$)

$$-k\pi r(dV/dr)=W. \quad (9)$$

Furthermore, continuity of temperature and of heat flow at the boundary r_1 introduces two additional conditions. Expressions (6a) and (6b) assume the same value:

$$[V(\alpha r)]_{r=r_1}=[V(\alpha' r)]_{r=r_1} \quad (10)$$

and

$$k\left[\frac{dV(\alpha r)}{dr}\right]_{r=r_1}=k'\left[\frac{dV(\alpha' r)}{dr}\right]_{r=r_1}. \quad (11)$$

Equations (7), (9), (10), and (11) constitute four equations from which constants A, B, A', and B' may be eliminated.

[4] S. Goldstein, Zeits. f. angew. Math. Mech. **12**, 234 (1932).

We arrive at rather cumbersome expressions, $V(\alpha, \alpha', r_0, r_1, R, W, r)$ and dV/dr in the two media.

For the sake of brevity we will present the subsequent analysis only for a single component target. We need apply only conditions (7) and (9) to obtain an operational expression for the temperature gradient.

$$\frac{dV}{dr}=\frac{W}{k\pi r_0}\left[\frac{N_0(\alpha R)J_1(\alpha r)-J_0(\alpha R)N_1(\alpha r)}{N_0(\alpha R)J_1(\alpha r_0)-J_0(\alpha R)N_1(\alpha r_0)}\right], \quad (12)$$

in which $J_1(\alpha-)$ and $N_1(\alpha-)$ are Bessel functions of the first order.

This expression can be expanded by the Heaviside expansion theorem. Using the notation of van der Pol,[5] given a fractional form $f(p)/F(p)$, in which the order of $F(p)$ is at least as great as that of $f(p)$, and provided that $F(p)=0$ has n distinct zeros, $p_1, p_2\cdots, p_r\cdots, p_n$, then

$$\frac{f(p)}{F(p)}\doteqdot\frac{f(0)}{F(0)}+\sum_{r=1}^{n}\left[\frac{f(p)e^{pt}}{p(dF/dp)}\right]_{p=p_r}. \quad (13)$$

Since from (4) $p=-k\alpha^2/S$

and

$$p\frac{dF}{dp}=\frac{\alpha}{2}\frac{dF(\alpha)}{d\alpha}, \quad (14)$$

Eq. (13) in terms of α assumes the form:

$$\frac{f(p)}{F(p)}\doteqdot\frac{f(0)}{F(0)}+\sum_{r=1}^{n}\left[\frac{f(\alpha)\exp\left(-\frac{k}{S}\alpha^2t\right)}{\frac{\alpha}{2}\frac{dF(\alpha)}{d\alpha}}\right]_{\alpha=\alpha_r}, \quad (15)$$

in which $\alpha_1, \alpha_2, -\alpha_r, -\alpha_n$ are roots of $F(\alpha)=0$.

Applying relation (15) to expression (12), we note:

$$f(\alpha)=\frac{W}{k\pi r_0}[N_0(\alpha R)J_1(\alpha r)-J_0(\alpha R)N_1(\alpha r)] \quad (16a)$$

and

$$F(\alpha)=N_0(\alpha R)J_1(\alpha r_0)-J_0(\alpha R)N_1(\alpha r_0). \quad (16b)$$

The equation $F(\alpha)=0$ has an infinite number of roots.

For a typical physical case of $R=20r_0$, Eq. (16) assumes the form:

$$\frac{J_0(20\alpha r_0)}{N_0(20\alpha r_0)}=\frac{J_1(\alpha r_0)}{N_1(\alpha r_0)}. \quad (17)$$

The first six roots of (17) are given by Jahnke and Emde, *Tables of Functions* (1938), pp. 207–209.

$$\alpha r_0=0,\ 0.122,\ 0.279,\ 0.439,\ 0.600,\ 0.777 \quad (18)$$
$$\alpha R=20\alpha r_0=0,\ 2.44,\ 5.58,\ 8.78,\ 12.00,\ 15.4 \quad (19)$$

and for a typical physical case where $r_0=0.15$ and $R=3.0$, we find

$$\alpha=0,\ 0.815,\ 1.86,\ 2.92,\ 4.00,\ 5.17 \quad (20)$$

and

$$\alpha^2=0,\ 0.665,\ 3.47,\ 8.58,\ 16.00,\ 26.7. \quad (21)$$

From (16) we obtain for substitution in (15)

$$\frac{\alpha}{2}\frac{dF}{d\alpha}(\alpha)=\frac{\alpha R}{2}[J_1(\alpha R)N_1(\alpha r_0)-N_1(\alpha R)J_1(\alpha r_0)]$$
$$-\frac{\alpha r_0}{2}[J_0(\alpha R)N_0(\alpha r_0)-N_0(\alpha R)J_0(\alpha r_0)]. \quad (22)$$

After reduction of the first term (15) is expressible as:

$$\frac{\partial V}{\partial r}=\frac{f(p)}{F(p)}\doteqdot\frac{W}{k\pi}\left\{\frac{R}{r}-\sum_{r=1}^{n}\left[\frac{N_0(\alpha R)J_1(\alpha r)-J_0(\alpha R)N_1(\alpha r)}{\frac{\alpha}{2}\frac{dF(\alpha)}{d\alpha}}\exp\left(-\frac{k}{S}\alpha^2t\right)\right]_{\alpha=\alpha_r}\right\} \quad (23)$$

and

$$V=\frac{W}{k\pi}\left\{\log\frac{R}{r}-\sum_{r=1}^{n}\left[\frac{N_0(\alpha R)J_0(\alpha r)-J_0(\alpha R)N_0(\alpha r)}{\frac{\alpha^2}{2}\frac{dF(\alpha)}{d\alpha}}\exp\left(-\frac{k}{S}\alpha^2t\right)\right]_{\alpha=\alpha_r}\right\}. \quad (24)$$

[5] L. A. Pipes, J. App. Phys. **10**, 258 (1939).

To compensate for end effects we introduce a factor E less than unity. To estimate a reasonable value for E, the steady state temperatures were computed for a hemispherical area and a semicylindrical area under the same load density.

It was found that the temperature of the hemispherical area would be about 60 percent of that for the semicylindrical area. In our physical case the length of loaded area was about 2.9 times the width. From this reasoning and to obtain agreement with experimental measurements of surface temperature, a value of 0.75 was selected for E. The factor outside the brackets in (24) thus becomes:

$$WE/k\pi.$$

Introducing our previously selected values for tungsten:

$$k_w = 0.3,$$
$$S_w = 0.75,$$

so for tungsten

$$k/S = 0.4$$

and assuming a loading W of 3000 cal./sec. per linear cm

$$WE/k_w\pi = (3000 \times 0.75)/0.3\pi = 2390 \text{ degrees.}$$

Further introducing values from (18), (19), (20), (21) to evaluate (22) and substituting in (24) we have for tungsten an infinite series solution of which only the first two terms are shown:

$$V = 2390\begin{bmatrix} \log R/r - [1.24J_0(0.815r) + 0.04N_0(0.815r)]e^{-.266t} \\ \quad - [0.54J_0(1.86r) \ + 0.03N_0(1.86r) \ ]e^{-1.39t} \\ \quad - [\ \cdot\ \cdot\ \cdot\ \cdot\ \cdot\ \cdot\ \cdot\ \cdot\ \cdot\ ] \\ \quad - \ \cdot\ \cdot\ \cdot\ \cdot\ \cdot\ \cdot\ \cdot\ \cdot\ \cdot \end{bmatrix}. \tag{25}$$

For extremely short times it was found necessary to evaluate ten terms of this series. Computed temperatures are shown in Fig. 4.

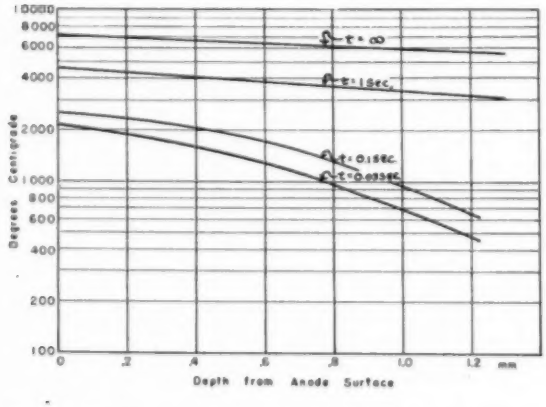

FIG. 4. Temperatures near the surface of tungsten under line heat loading. Typical standard loading condition 3000 calories per second per centimeter length on a line of 4.7-mm width. Thermal conductivity of tungsten 0.3 cal. cm^{-1} $degree^{-1}$.

It is interesting to compare these curves with those of Bowers. His assumed load density was 200 watts/mm^2. Ours was 270 watts/mm^2. The temperatures should compare in the ratio $270/200 = 1.35$. At the surface of the tungsten:

At 1 second, he finds	$T = 4050.$
Our value is	$T = 4600.$
At 0.1 second, he finds	$T = 2920.$
Our value is	$T = 2560.$

The correspondence is as close as could be expected. For such short times he employed an approximate expression which is probably as accurate as other factors justify. His high assumed thermal conductivity of tungsten no doubt compensated for his disregard of end effects.

The maximum abscissa shown is about 1.5 millimeter. In the physical case considered, the tungsten face over the massive copper was over 3 millimeters thick. Thus from a transient standpoint, the effect of the copper may be ignored. The more involved expressions for the two-component case are thus omitted. It will suffice to remember that the copper backing will only slightly reduce computed temperatures, for fractional second loading. The steady state effect of the copper would, however, be important. Steady state computations are quite simple and are not treated herein. Figure 5 shows

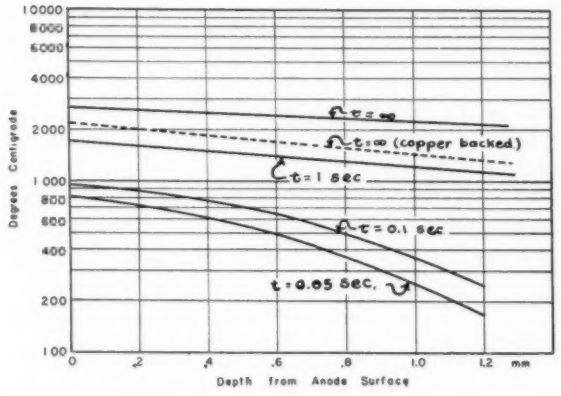

FIG. 5. Temperatures near surface of tungsten under line heat load of 10,000 watts/cm². Thermal conductivity 0.3 cal. cm^{-1} $degree^{-1}$.

transient temperatures near the surface of a tungsten target under line loading of 10 kw per cm². The steady state temperatures for a tungsten button backed with copper are shown dotted for purposes of comparison.

These curves facilitate the application of results here obtained to estimate temperatures in targets under other loading conditions. For example, under a loading of 20 kw per cm² temperatures will be approximately twice the values shown. The degree of approximation will, of course, depend on size, shape, and physical characteristics of the loaded area.

Figure 6 gives temperature as related to time for a load of 10 kw per cm². Conditions at the surface, ½ mm, and 1 mm beneath the surface are indicated. These curves facilitate selection of a safe operating time under a specified load.

ANALYSIS OF RESULTS

Equation (24) shows that the temperature is a linear function of the loading. On Fig. 5, the curve of $t=0.1$ second thus indicates that the assumed load is about 75 percent of the loading to produce melt (2550°/3400°). Other effects due to excess loading might show up due to recrystallization. F. Brech[6] has briefly discussed this process. The annealing temperature for tungsten is generally given as about 1000°C. Thus it would be expected that repeated loading of the magnitude considered would lead to ultimate disruption of the surface. The effect would probably be exaggerated if only a thin film on the surface were heated. In this case, to the depth heated to 1000°C or higher, the thermal stresses would be partially relieved while hot. On cooling, tensile stress would be set up, tending to cause fracture. Because of the grain structure parallel to the surface of rolled tungsten sheet, failure would probably be in shear and would result in peeling. This has been confirmed by experiments. The noteworthy observation was that failure was much more rapid under 0.05-second loading than under 0.1-second loading. From this, it would appear that improved life would result if a considerable depth of tungsten could be heated to the annealing temperature.

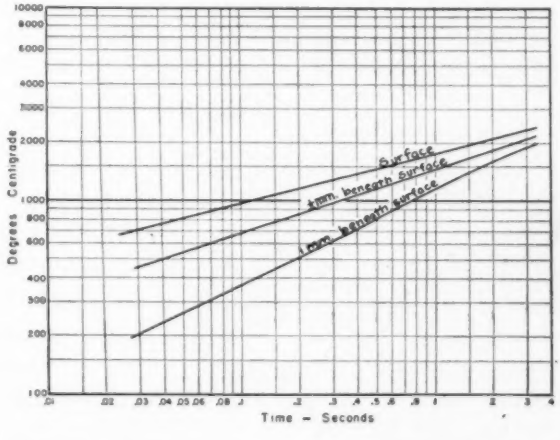

FIG. 6. The temperatures near the surface of tungsten under a load of 10 kw per cm² as a function of the time of loading.

This analysis constituted one phase of an extensive engineering program by the Vacuum Tube Engineering Department of the General Electric X-Ray Corporation of increasing the operating life of diagnostic x-ray tubes. The writer gratefully acknowledges the cooperation of Mr. Z. J. Atlee, in charge of the program, who presented the problem and experimental records which provided point checks on calculated values, and of the departmental staff engineers, who checked performance efficiency under revised loadings as suggested by the analytical results.

[6] F. Brech, J. Sci. Inst. **18**, 101–2 (1941).

The Vector Potential and Inductance of a Circuit Comprising Linear Conductors of Different Permeability*

THOMAS JAMES HIGGINS†
The Tulane University of Louisiana, New Orleans, Louisiana
(Received January 19, 1942)

Formulas are derived for the vector potential and inductance of a circuit comprised of a long linear cylinder enveloped by a return conductor of eccentric-annular cross section, the two cylinders and the surrounding medium each being of different permeability. The restriction to very long cylinders rendering the problem two-dimensional, a familiar scheme of analysis can be employed. A plane cross section is mapped conformally on a rectangle of infinite length and of breadth 2π, the perimeters of the conductors going over into line segments parallel to the short sides. In each of the three resulting rectangular regions of different permeability the vector potential A is expressed as a sum of appropriate infinite double series of trigonometric functions with constant coefficients, these latter being determined in accordance with the known boundary conditions—continuity of the normal component of induction and of the tangential component of field intensity on the perimeters of the conductors. The magnetic field energy is obtained by evaluating $W=\frac{1}{2}\int_S wA\,dS$; whence the inductance follows from $W=\frac{1}{2}LI^2$. The resulting expression for the inductance yields known formulas for certain special cases of the general problem, thus verifying the analysis. As the symbol for the vector potential is capable of physical reinterpretation as temperature, the foregoing analysis also furnishes solutions to certain heat problems of technical interest.

1. PRELIMINARY REMARKS

IN this paper we are concerned with the following problem: to determine the vector potential and the inductance of a circuit constructed of a long linear cylinder enveloped by a return conductor of eccentric-annular cross section, the two cylinders and the surrounding medium each being of different permeability. The required analysis is, however, capable of various interpretations; and others may find certain hydrodynamical, geophysical, or heat renderings of greater interest. For example, physically re-identifying the various quantities—the vector potential as the temperature, the permeability as the reciprocal of thermal conductivity, and $-4\pi w$ as the rate of heat generation per unit volume—one obtains the temperature distribution for the cylindrical arrangement specified, the heat generated therein being lost by conduction to the surrounding medium. By varying the thermal constants, the radii, and the eccentricity of the cylinders the solutions of numerous problems of considerable engineering or physical interest are obtained. Other renderings come readily to mind.

The problem here treated is complimentary to another lately considered by the writer. Both were prompted by an observation of the late A. G. Webster[1] *re* a problem now of much interest—by virtue of the fast increasing use of steel wire for transmitting electric energy in rural areas.

> The treatment of the magnetic field due to currents even in straight conductors where inductivity is different from that of the surrounding medium, except in the case of concentric cylinders, is a problem of considerable complexity, and the results given by Maxwell for the case of two wires, Art. 685 are [as Rayleigh noted some thirteen years after publication of Maxwell's text] only approximately correct.

A rigorous solution of Maxwell's problem—to determine the inductance per unit length of a circuit constructed of two long linear conductors of unlike permeability, the two contained in a medium of yet different permeability—was given by MacDonald[2] a half century ago. Certain misprints appearing in the latter's paper were indicated by the present writer in a recent treatment[3] of a very general problem of which Maxwell's is a special case: the determination of the vector potential and the inductance of a

* Based upon one chapter of a thesis submitted by Thomas James Higgins to the Faculty of Purdue University in partial fulfillment of the requirements for the degree of Doctor of Philosophy (June, 1941).

† Assistant Professor of Electrical Engineering, The Tulane University of Louisiana, New Orleans.

[1] A. G. Webster, *The Theory of Electricity and Magnetism* (Macmillan, 1897), p. 466.

[2] H. M. MacDonald, Proc. Camb. Phil. Soc. **7**, 259 (1889–1892).

[3] To be published in a forthcoming issue of the J. Math. Phys.

circuit comprising two long linear conductors of eccentric-annular cross section; each conductor, each internal space, and the external space, being of different permeability.

2. THE FORMAL SOLUTION

With reference to Fig. 1, we seek A which

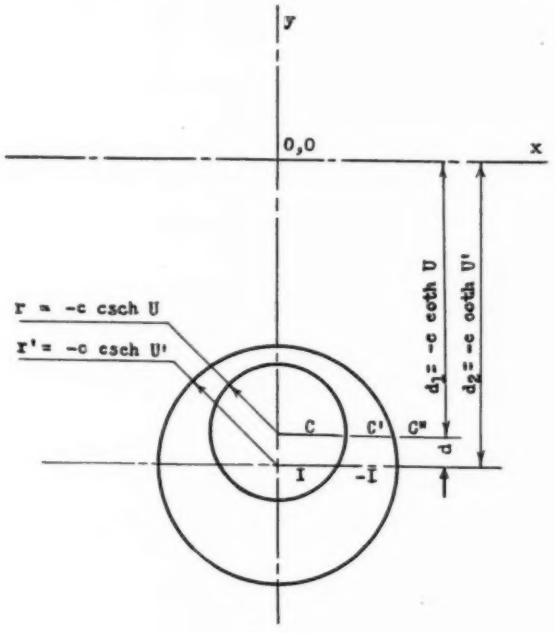

FIG. 1.

satisfies the differential equations

$$\nabla^2 A = -4\pi\mu w \quad \text{over } C, \tag{1}$$

$$\nabla^2 A' = -4\pi\mu' w' \quad \text{over } C', \tag{2}$$

$$\nabla^2 A'' = 0 \quad \text{outside } C', \tag{3}$$

and the boundary conditions

$$A = A' \text{ and } (1/\mu)(\partial A/\partial n) = (1/\mu')(\partial A'/\partial n) \text{ on the perimeter of } C, \tag{4}$$

$$A'' = A' \text{ and } (1/\mu'')(\partial A''/\partial n) = (1/\mu')(\partial A'/\partial n) \text{ on the perimeter of } C', \tag{5}$$

$$A'' = \text{a constant} \quad \text{at infinity.} \tag{6}$$

The boundary conditions are obtained as follows: (4) and (5) from knowledge that the vector potential and the tangential component of magnetic intensity must be continuous at each point in the interface between two media of different permeability; (6) from knowledge that the vector potential vanishes at infinity except for an arbitrary constant.

To determine the vector potential, we find particular solutions of (1) and (2), and add to them solutions of $\nabla^2 A = 0$ such that the boundary conditions are satisfied. To facilitate this task, we make a change of variables. The conformal transformation

$$f(z) = -i \log \frac{-z+ic}{z+ic} = v+iu; \qquad z = c \tan \tfrac{1}{2}(v+iu) \tag{7}$$

maps the (x, y) plane on the (v, u) plane as shown in Fig. 2. The scale factor is

$$|dw/dz| = \frac{1}{c}(\cosh u + \cos v); \tag{8}$$

the old coordinates in terms of the new are

$$x = c\frac{\sin v}{\cosh u + \cos v} \quad \text{and} \quad y = c\frac{\sinh u}{\cosh u + \cos v}. \tag{9}$$

In the new coordinates (1), (2), and (3) become

$$\nabla^2 A = -4\pi\mu w c^2/(\cosh u + \cos v)^2 \qquad -\infty \le u \le U, \tag{10}$$

$$\nabla^2 A' = -4\pi\mu' w' c^2/(\cosh u + \cos v)^2 \qquad U \le u \le U', \tag{11}$$

$$\nabla^2 A'' = 0 \qquad U' \le u \le \infty, \tag{12}$$

while (4), (5), and (6) yield

$$A = A' \qquad u = U, \tag{13}$$

$$A'' = A' \qquad u = U', \tag{14}$$

$$(1/\mu)(\partial A/\partial \mu) = (1/\mu')(\partial A'/\partial u) \qquad u = U, \tag{15}$$

$$(1/\mu'')(\partial A''/\partial u) = (1/\mu')(\partial A'/\partial u) \qquad u = U', \tag{16}$$

$$A'' = \text{a constant} \qquad u = 0,\ v = \pm\pi. \tag{17}$$

A well-known particular solution[4] of (1) is

$$-\pi\mu w[x^2 + (y - c\coth U)^2 + K], \tag{18}$$

where K is an arbitrary constant. Substituting (9) in (18) and setting $K = c^2$, we obtain

$$-\pi\mu w c^2\left[\frac{2\sinh(U-u)}{\sinh U(\cosh u + \cos v)} + \coth^2 U\right]. \tag{19}$$

[4] This is the familiar solution, $-\pi\mu w(x^2+y^2)$, transferred into the coordinates $x = x$, $y = y - c\coth U$.

The second term in (19) being a constant, the first is a particular solution of (10). Hence, as particular solutions of (10) and (11), we have

$$\frac{2\pi\mu wc^2}{\sinh U}\frac{\sinh(u-U)}{\cosh u+\cos v}, \tag{20}$$

$$\frac{2\pi\mu' w'c^2}{\sinh U}\frac{\sinh(u-U)}{\cosh u+\cos v}. \tag{21}$$

To find solutions of $\nabla^2 A=0$ which, added to (20) and (21), enable the boundary conditions (13) to (17), inclusive, to be satisfied, we note that the vector potential is symmetrical about the axis of u, and is finite over the conductor C, thus finite at the point $u=-\infty$, the center of C. These considerations, together with the observation that the vector potential is finite everywhere, and is equal to a constant at infinity, lead to the following expressions:

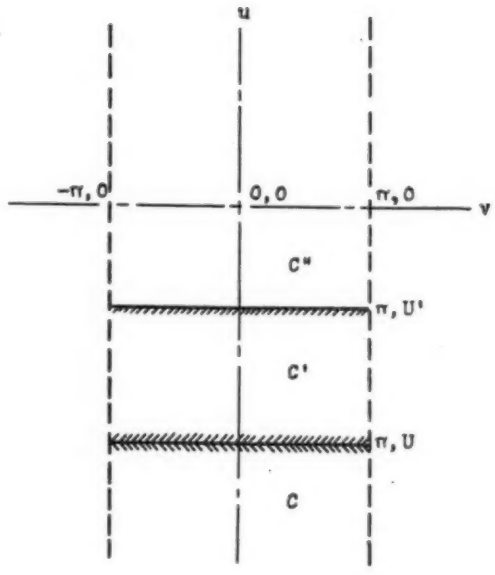

FIG. 2.

$$A=\frac{2\pi\mu wc^2}{\sinh U}\frac{\sinh(u-U)}{\cosh u+\cos v}+\sum_{n=0}^{\infty}P_n\epsilon^{nu}\cos nv, \tag{22}$$

$$A'=\frac{2\pi\mu' w'c^2}{\sinh U}\frac{\sinh(u-U)}{\cosh u+\cos v}+Tu+\sum_{n=0}^{\infty}(R_n\epsilon^{nu}+S_n\epsilon^{-nu})\cos nv, \tag{23}$$

$$A''=\sum_{n=0}^{\infty}Q_n\epsilon^{-nu}\cos nv. \tag{24}$$

To obtain the unknown coefficients, we apply the boundary conditions. From (13) to (16), inclusive, we have:

$$\sum_{n=0}^{\infty}P_n\epsilon^{nU}\cos nv=TU+\sum_{n=0}^{\infty}(R_n\epsilon^{nU}+S_n\epsilon^{-nU})\cos nv, \tag{25}$$

$$\sum_{n=0}^{\infty}Q_n\epsilon^{-nU'}\cos nv=TU'+\frac{2\pi\mu' w'c^2\sinh(U'-U)}{\sinh U(\cosh U'+\cos v)}+\sum_{n=0}^{\infty}(R_n\epsilon^{nU'}+S_n\epsilon^{-nU'})\cos nv, \tag{26}$$

$$\frac{1}{\mu}\left[\frac{2\pi\mu wc^2}{\sinh U(\cosh U+\cos v)}+\sum_{n=0}^{\infty}nP_n\epsilon^{nU}\cos nv\right]$$

$$=\frac{1}{\mu'}\left[\frac{2\pi\mu' w'c^2}{\sinh U(\cosh U+\cos v)}+T+\sum_{n=0}^{\infty}n(R_n\epsilon^{nU}-S_n\epsilon^{-nU})\cos nv\right], \tag{27}$$

$$-\frac{1}{\mu''}\sum_{n=0}^{\infty}nQ_n\epsilon^{-nU'}\cos nv=\frac{1}{\mu'}\left[\frac{2\pi\mu' w'c^2}{\sinh U}\cdot\frac{\cosh(2U'-U)+\cos v\cosh(U'-U)}{(\cosh U'+\cos v)^2}\right.$$

$$\left.+T+\sum_{n=0}^{\infty}n(R_n\epsilon^{nU'}-S_n\epsilon^{-nU'})\cos nv\right]. \tag{28}$$

Now $(\cosh u+\cos v)^{-1}$ can be expanded in a Fourier series of the form

$$\tfrac{1}{2}b_0+\sum_{n=1}^{\infty} b_n \cos nv, \tag{29}$$

where,[5] for $u<0$,

$$\begin{aligned} b_n &= \frac{2}{\pi}\int_0^{\pi} \frac{\cos nv}{\cosh u+\cos v}dv \\ &= -\frac{2(-1)^n\epsilon^{nu}}{\sinh u}. \end{aligned} \tag{30}$$

Hence,

$$(\cosh U+\cos v)^{-1} = -\frac{1}{\sinh U}\left[1+2\sum_{n=1}^{\infty}(-1)^n\epsilon^{nU}\cos nv\right]. \tag{31}$$

Similarly, $(\cosh u+\cos v)^{-2}$ can be expanded in a Fourier series of the form

$$\tfrac{1}{2}b_0+\sum_{n=1}^{\infty} b_n \cos nv, \tag{32}$$

where,[6] for $u<0$,

$$\begin{aligned} b_n &= \frac{2}{\pi}\int_0^{\pi} \frac{\cos nv}{(\cosh u+\cos v)^2}dv \\ &= \frac{2(-1)^n(n\sinh u-\cosh u)\epsilon^{nu}}{\sinh^3 u}. \end{aligned} \tag{33}$$

Hence,

$$(\cosh U'+\cos v)^{-2} = -\frac{\cosh U'}{\sinh^3 U'}\left[1+2\sum_{n=1}^{\infty}(-1)^n\epsilon^{nU'}\cos nv\right]+\frac{1}{\sinh^2 U'}\left[2\sum_{n=1}^{\infty}n(-1)^n\epsilon^{nU'}\cos nv\right]. \tag{34}$$

Substituting (31) and (34) in (25) to (28), inclusive, and collecting terms, we have

$$\sum_{n=0}^{\infty} P_n\epsilon^{nU}\cos nv = TU+\sum_{n=0}^{\infty}(R_n\epsilon^{nU}+S_n\epsilon^{-nU})\cos nv, \tag{35}$$

$$\sum_{n=0}^{\infty} Q_n\epsilon^{-nU'}\cos nv = -\frac{2\pi\mu' w' c^2\sinh(U'-U)}{\sinh U\sinh U'}\left[1+2\sum_{n=1}^{\infty}(-1)^n\epsilon^{nU'}\cos nv\right]$$

$$+TU'+\sum_{n=0}^{\infty}(R_n\epsilon^{nU'}+S_n\epsilon^{-nU'})\cos nv, \tag{36}$$

$$\frac{1}{\mu}\left\{-\frac{2\pi\mu w c^2}{\sinh^2 U}\left[1+2\sum_{n=1}^{\infty}(-1)^n\epsilon^{nU}\cos nv\right]+\sum_{n=0}^{\infty}n(P_n\epsilon^{nU}\cos nv)\right\}$$

$$=\frac{1}{\mu'}\left\{-\frac{2\pi\mu' w' c^2}{\sinh^2 U}\left[1+2\sum_{n=1}^{\infty}(-1)^n\epsilon^{nU}\cos nv\right]+T+\sum_{n=0}^{\infty}n(R_n\epsilon^{nU}-S_n\epsilon^{-nU})\cos nv\right\}, \tag{37}$$

[5] D. Bierens de Haan, *Nouvelles d'Intégrales Définies* (Leyden, 1867), Table 65, No. 3.
[6] Reference 5, Table 66, No. 5.

$$\frac{1}{\mu''}\sum_{n=0}^{\infty} nQ_n\epsilon^{-nU'}\cos nv=\frac{1}{\mu'}\Bigg\{+\frac{2\pi\mu' w'c^2}{\sinh^2 U'}+\frac{4\pi\mu' w'c^2}{\sinh^2 U'}\sum_{n=1}^{\infty}(-1)^n\epsilon^{nU'}\cos nv$$

$$+\frac{4\pi\mu' w'c^2\sinh(U'-U)}{\sinh U\sinh U'}\sum_{n=1}^{\infty} n(-1)^n\epsilon^{nU'}\cos nv-T-\sum_{n=0}^{\infty} n(R_n\epsilon^{nU'}-S_n\epsilon^{-nU'})\cos nv\Bigg\}. \quad (38)$$

Equating in each equation the coefficients of the like values of cos (nv) and utilizing the identities

$$r=-c\,\mathrm{csch}\,U,\quad r'=-c\,\mathrm{csch}\,U',\quad d=c\frac{\sinh(U'-U)}{\sinh U\sinh U'},$$

we obtain from (35) to (38), inclusive,

$$P_0=(R_0+S_0)+TU, \quad (39)$$

$$Q_0=(R_0+S_0)+TU'-2\pi\mu' w'dc, \quad (40)$$

$$-2\pi wr^2=T/\mu'-2\pi w'r^2, \quad (41)$$

$$0=T/\mu'-2\pi w'r'^2, \quad (42)$$

$$P_n=R_n+S_n\epsilon^{-2nU}, \quad (43)$$

$$Q_n=R_n\epsilon^{2nU'}+S_n-4\pi\mu' w'dc(-1)^n\epsilon^{2nU'}, \quad (44)$$

$$P_n(n/\mu)=R_n(n/\mu')-S_n(n/\mu')\epsilon^{-2nU}-4\pi w'r'^2(-1)^n, \quad (45)$$

$$Q_n(n/\mu'')=-R_n(n/\mu')\epsilon^{2nU'}+S_n(n/\mu')+4\pi w'(r'^2+ndc)(-1)^n\epsilon^{2nU'}. \quad (46)$$

Although we thus obtain eight equations, but seven of these are linearly independent. This, however, is to be expected; for (6) is equivalent to stating that the expression for the vector potential contains an arbitrary constant. Accordingly, taking (R_0+S_0) as this arbitrary constant, we can solve the above set of equations for the remaining unknowns.

From (39) to (42), inclusive, we obtain at once

$$P_0=(R_0+S_0)+2\pi\mu' w'r'^2U, \quad (47)$$

$$Q_0=(R_0+S_0)+2\pi\mu' w'r'^2U'-2\pi\mu' w'dc, \quad (48)$$

$$T=2\pi\mu'(w'-w)r^2=2\pi\mu' w'r'^2. \quad (49)$$

Solving (43) to (46), inclusive, by means of determinants, we have

$$P_n=\frac{1}{n}\frac{k'\left(\frac{1}{\mu''}-\frac{1}{\mu}\right)(-1+\epsilon^{-2n(U'-U)})+2nk''\frac{1}{\mu'}\left(\frac{1}{\mu''}+\frac{1}{\mu'}\right)}{\left(\frac{1}{\mu''}+\frac{1}{\mu'}\right)\left(\frac{1}{\mu}+\frac{1}{\mu'}\right)-\left(\frac{1}{\mu''}-\frac{1}{\mu'}\right)\left(\frac{1}{\mu}-\frac{1}{\mu'}\right)\epsilon^{2n(U-U')}}, \quad (50)$$

$$Q_n=\frac{\epsilon^{2nU'}}{n}\left[\frac{k'\left[\left(\frac{1}{\mu}+\frac{1}{\mu'}\right)-\frac{2}{\mu'}\epsilon^{2n(U-U')}\right]}{\left(\frac{1}{\mu''}+\frac{1}{\mu'}\right)\left(\frac{1}{\mu}+\frac{1}{\mu'}\right)-\left(\frac{1}{\mu''}-\frac{1}{\mu'}\right)\left(\frac{1}{\mu}-\frac{1}{\mu'}\right)\epsilon^{2n(U-U')}}\right.$$

$$\left.-\frac{2nk''\left[\left(\frac{1}{\mu''}+\frac{1}{\mu'}\right)\left(\frac{1}{\mu}+\frac{1}{\mu'}\right)+\frac{1}{\mu'}\left(\frac{1}{\mu}-\frac{1}{\mu'}\right)\epsilon^{2n(U-U')}\right]}{\left(\frac{1}{\mu''}+\frac{1}{\mu'}\right)\left(\frac{1}{\mu}+\frac{1}{\mu'}\right)-\left(\frac{1}{\mu''}-\frac{1}{\mu'}\right)\left(\frac{1}{\mu}-\frac{1}{\mu'}\right)\epsilon^{2n(U-U')}}\right], \quad (51)$$

$$R_n=\frac{1}{n}\frac{k'\left[\left(\frac{1}{\mu}+\frac{1}{\mu'}\right)+\left(\frac{1}{\mu''}-\frac{1}{\mu'}\right)\epsilon^{2n(U-U')}\right]}{\left(\frac{1}{\mu''}+\frac{1}{\mu'}\right)\left(\frac{1}{\mu}+\frac{1}{\mu'}\right)-\left(\frac{1}{\mu''}-\frac{1}{\mu'}\right)\left(\frac{1}{\mu}-\frac{1}{\mu'}\right)\epsilon^{2n(U-U')}}$$

$$+\frac{k''\left(\frac{1}{\mu''}+\frac{1}{\mu'}\right)\left(\frac{1}{\mu}+\frac{1}{\mu'}\right)}{\left(\frac{1}{\mu''}+\frac{1}{\mu'}\right)\left(\frac{1}{\mu}+\frac{1}{\mu'}\right)-\left(\frac{1}{\mu''}-\frac{1}{\mu'}\right)\left(\frac{1}{\mu}-\frac{1}{\mu'}\right)\epsilon^{2n(U-U')}}, \quad (52)$$

$$S_n=-\frac{\epsilon^{2nU}}{n}\frac{k'\left(\frac{1}{\mu''}+\frac{1}{\mu}\right)+nk'\left(\frac{1}{\mu''}+\frac{1}{\mu'}\right)\left(\frac{1}{\mu}-\frac{1}{\mu'}\right)}{\left(\frac{1}{\mu''}+\frac{1}{\mu'}\right)\left(\frac{1}{\mu}+\frac{1}{\mu'}\right)-\left(\frac{1}{\mu''}-\frac{1}{\mu'}\right)\left(\frac{1}{\mu}-\frac{1}{\mu'}\right)\epsilon^{2n(U-U')}}, \quad (53)$$

where, for convenience,

$$k'=4\pi w'r'^2(-1)^n, \quad (54)$$

$$k''=4\pi\mu' w'dc(-1)^n. \quad (55)$$

The vector potential being completely determined, we now turn to determining L, the inductance per unit length of line, from the condition that W, the energy stored in the electromagnetic field per unit length of line, equals $\frac{1}{2}LI^2$. From well-known theory we have

$$W=\tfrac{1}{2}\int\int_C Awdvdu+\tfrac{1}{2}\int\int_{C'}A'w'dvdu$$

$$=\frac{wc^2}{2}\int_{-\infty}^{U}\int_{-\pi}^{\pi}\frac{Advdu}{(\cosh u+\cos v)^2}+\frac{w'c^2}{2}\int_{U}^{U'}\int_{-\pi}^{\pi}\frac{A'dvdu}{(\cosh u+\cos v)^2}$$

$$=wc^2\int_{-\infty}^{U}\int_{0}^{\pi}\frac{Advdu}{(\cosh u+\cos v)^2}+w'c^2\int_{U}^{U'}\int_{0}^{\pi}\frac{A'dvdu}{(\cosh u+\cos v)^2}. \quad (56)$$

To evaluate W we require the following integrals:[7]

$$c^3\int_{-\infty}^{U}\int_0^{\pi}\frac{\sinh(u-U)}{(\cosh u+\cos v)^3}dvdu=\frac{\pi r^3}{8}, \tag{57}$$

$$c^2\int_{-\infty}^{U}\int_0^{\pi}\frac{\epsilon^{nu}\cos nv}{(\cosh u+\cos v)^2}dvdu=\frac{\pi r^2(-1)^n}{2}\epsilon^{2nU}, \tag{58}$$

$$c^2\int_{-\infty}^{U}\int_0^{\pi}\frac{1}{(\cosh u+\cos v)^2}dvdu=\frac{\pi r^2}{2}, \tag{59}$$

$$c^4\int_{U}^{U'}\int_0^{\pi}\frac{\sinh(u-U)}{\sinh U(\cosh u+\cos v)^3}dvdu=\frac{\pi}{2}(d_1d_2r'^2-c^2r'^2-\tfrac{3}{4}r'^4-\tfrac{1}{4}r^4), \tag{60}$$

$$c^2\int_{U}^{U'}\int_0^{\pi}\frac{\epsilon^{nu}\cos nv}{(\cosh u+\cos v)^2}dvdu=\frac{\pi(-1)^n}{2}(r'^2\epsilon^{2nU'}-r^2\epsilon^{2nU}), \tag{61}$$

$$c^2\int_{U}^{U'}\int_0^{\pi}\frac{\epsilon^{-nu}\cos nv}{(\cosh u+\cos v)^2}dvdu=\frac{\pi(-1)^n}{2}(r'^2-r^2+2ndc), \tag{62}$$

$$c^2\int_{U}^{U'}\int_0^{\pi}\frac{u}{(\cosh u+\cos v)^2}dvdu=\frac{\pi}{2}(r'^2U'-r^2U-dc), \tag{63}$$

$$c^2\int_{U}^{U'}\int_0^{\pi}\frac{1}{(\cosh u+\cos v)^2}dvdu=\frac{\pi r'^2}{2}. \tag{64}$$

Substituting (22) and (23) in (56) and carrying out the required integration by aid of (57) to (64), inclusive, we obtain

$$\begin{aligned}2W=&\tfrac{1}{2}\pi^2\mu w^2r^4+2\pi^2\mu' ww'r^2r'^2U+2\pi^2\mu' w'^2r'^2(r'^2U'-r^2U-dc)+\pi wr^2(R_0+S_0)+\pi w'(r'^2-r^2)(R_0+S_0)\\&+2\pi^2\mu' w'^2(d_1d_2r'^2-c^2r'^2-\tfrac{3}{4}r'^4-\tfrac{1}{4}r^4)+\pi w\sum_{n=1}^{\infty}(-1)^nP_n(r^2\epsilon^{2nU})\\&+\pi w'\sum_{n=1}^{\infty}(-1)^nR_n(r'^2\epsilon^{2nU'}-r^2\epsilon^{2nU})+\pi w'\sum_{n=1}^{\infty}(-1)^nS_n(r'^2-r^2+2ndc),\end{aligned} \tag{65}$$

the values of P_n, R_n, and S_n for any particular problem being determined from (50), (52), and (53), respectively.

Finally, L can be determined from

$$L=2W/I^2 \text{ abhenries per centimeter of line.} \tag{66}$$

3. SPECIAL CASES OF THE GENERAL PROBLEM

As a check on the correctness of the foregoing work, we now obtain explicit expressions for certain cases of general interest.

I. We have $\mu=\mu'=\mu''$. Accordingly, from (50), (52), and (53) we obtain

$$P_n=k'', \tag{67}$$

$$R_n=(\mu k'/2n)+k'', \tag{68}$$

$$S_n=-(\mu k'/2n)\epsilon^{2nU}. \tag{69}$$

We note that

$$P_n=R_n+S_n\epsilon^{-2nU}. \tag{70}$$

Now

$$\coth u=(\epsilon^u+\epsilon^{-u})(\epsilon^u-\epsilon^{-u})^{-1}. \tag{71}$$

Expanding the right-hand side of (71) by use of

[7] See the Appendix for evaluation of these integrals.

the binomial theorem, we have, for $u<0$,

$$-2\sum_{n=1}^{\infty}\epsilon^{2nu}=1+\coth u. \tag{72}$$

Integrating each member of (72) we obtain

$$\sum_{n=1}^{\infty}\frac{\epsilon^{2nu}}{n}=-[U+\log\sinh(-u)]. \tag{73}$$

Substituting (67), (68), and (69) in (65) and then evaluating the infinite series thus obtained by aid of (72) and (73), we obtain after collecting terms

$$W=2\pi^2\mu w'^2r'^4\log(r'/r)-\mu\pi^2w'^2r'^2(r'^2-r^2)+2\mu\pi^2w'^2d^2r'^2. \tag{74}$$

Finally, from (66) we have

$$L=\frac{2\mu r'^4}{(r'^2-r^2)^2}\log\frac{r'}{r}-\frac{\mu r'^2}{r'^2-r^2}+\frac{2\mu d^2r'^2}{(r'^2-r^2)^2}. \tag{75}$$

II. We have $\mu=\mu'=\mu''$ and, in addition, $d=0$. We have at once from (75)

$$L=\frac{2\mu r'^4}{(r'^2-r^2)^2}\log\frac{r'}{r}-\frac{\mu r'^2}{r'^2-r^2}. \tag{76}$$

This is the well-known solution for this particular problem, and our above work is thus verified.

4. RÉSUMÉ OF THE FOREGOING ANALYSIS

We mention briefly some of the more important results or applications of the foregoing development. These include:

(a) Explicit expressions for the vector potential and inductance of all configurations to be obtained by varying the parameters (μ, w, d, r) associated with Fig. 1;

(b) Implicit equations for the lines of induction and the flux density associated with these configurations, the same to be obtained, respectively, from $A=$arbitrary constant and curl $\mathbf{A}=\mathbf{B}$;

(c) Explicit expressions for the temperatures associated with the configurations to be obtained by varying the parameters (μ, w, d, r) of Fig. 1, these variables taking on the physical interpretations stated in Section 1.

(d) Implicit equations for the isothermals, the rate of heat flux density, and the rate of heat flux associated with these configurations, the same to be obtained, respectively, from $A=$arbitrary constant, grad $\mathbf{A}=u\mathbf{V}$, and

$$F_r=\int_s A\frac{\partial A}{\partial n}ds,$$

the integral being taken over the lateral area of interest.

APPENDIX

To obtain (57) we first evaluate the inner integral. Thus,[8]

$$c^3\int_{-\infty}^{U}\int_0^{\pi}\frac{\sinh(u-U)}{(\cosh u+\cos v)^3}dvdu=c^3\int_{-\infty}^{U}\sinh(u-U)du\int_0^{\pi}\frac{1}{(\cosh u+\cos v)^3}dv=\frac{\pi c^3}{2}\int_{-\infty}^{U}\frac{3+2\sinh^3 u}{\sinh^5 u}\sinh(u-U)du.$$

Expanding $\sinh(u-U)$ and evaluating the resulting integrals,[9] we have

$$c^3\int_{-\infty}^{U}\int_0^{\pi}\frac{\sinh(u-U)}{(\cosh u+\cos v)^3}dvdu=\frac{\pi c^3}{8\sinh^3 U}=\pi r^3/8.$$

To obtain (58) we first evaluate the inner integral. Thus[10]

$$c^2\int_{-\infty}^{U}\int_0^{\pi}\frac{\epsilon^{nu}\cos nv}{(\cosh u+\cos v)^2}dvdu=c^2\int_{-\infty}^{U}\epsilon^{nu}du\int_0^{\pi}\frac{\cos nv}{(\cosh u+\cos v)^2}dv=\pi c^2(-1)^n\int_{-\infty}^{U}\frac{(n\sinh u-\cosh u)\epsilon^{2nu}}{\sinh^3 u}du.$$

Integrating by parts, we have

$$c^2\int_{-\infty}^{U}\int_0^{\pi}\frac{\epsilon^{nu}\cos nv}{(\cosh u+\cos v)^2}dvdu=\frac{\pi c^2(-1)^n\epsilon^{2nU}}{2\sinh^2 U}=\frac{\pi r^2(-1)^n}{2}\epsilon^{2nU}.$$

Noting in (59) and (64) that the integrand is the unit of area in the (x, y) plane, we have by inspection

$$c^2\int_{-\infty}^{U}\int_0^{\pi}\frac{1}{(\cosh u+\cos v)^2}dvdu=\frac{\pi r^2}{2}.$$

We obtain (60) from (57) by noting that

$$c^4\int_{U}^{U'}\int_0^{\pi}\frac{\sinh(u-U)}{\sinh U(\cosh u+\cos v)^3}dvdu=c^4\int_{-\infty}^{U'}\int_0^{\pi}\frac{\sinh(u-U)}{\sinh U(\cosh u+\cos v)^3}dvdu-c^4\int_{-\infty}^{U}\int_0^{\pi}\frac{\sinh(u-U)}{\sinh U(\cosh u+\cos v)^3}dvdu=\frac{\pi}{2}(d_1d_2r'^2-c^2r'^2-\tfrac{3}{4}r'^4-\tfrac{1}{4}r^4).$$

Again, (61) is similarly obtained from (58).

To obtain (62) we first evaluate the inner integral.

[8] Reference 5, Table 66, No. 2.

[9] H. B. Dwight, *Tables of Integrals and Other Mathematical Data* (Macmillan, 1934), No. 673.20 and No. 688.19.

[10] Reference 5, Table 66, No. 3.

Thus,[11]

$$c^2\int_U^{U'}\int_0^{\pi}\frac{\epsilon^{-nu}\cos nv}{(\cosh u+\cos v)^2}dvdu$$
$$=c^2\int_U^{U'}\epsilon^{-nu}du\int_0^{\pi}\frac{\cos nv}{(\cosh u+\cos v)^2}dv$$
$$=\pi c^2(-1)^n\int_U^{U'}\frac{n\sinh u-\cosh}{\sinh^3 u}du.$$

Evaluating as indicated[12] we obtain

$$c^2\int_U^{U'}\int_0^{\pi}\frac{\epsilon^{-nu}\cos nv}{(\cosh u+\cos v)^2}dvdu$$
$$=\frac{\pi c^2(-1)^n}{2}\left(\operatorname{csch}^2 U'-\operatorname{csch}^2 U-2n\frac{\sinh(U-U')}{\sinh U'\sinh U}\right)$$
$$=\frac{\pi(-1)^n}{2}(r'^2-r^2+2ndc).$$

[11] Reference 5, Table 66, No. 2.
[12] Reference 9, No. 671.20 and No. 688.12.

Finally, for (63) we have

$$c^2\int_U^{U'}\int_0^{\pi}\frac{u}{(\cosh u+\cos v)^2}dvdu$$
$$=c^2\int_U^{U'}udu\int_0^{\pi}\frac{1}{(\cosh u+\cos v)^2}dv$$
$$=-\pi c^2\int_U^{U'}\frac{u\cosh u}{\sinh^3 u}du.$$

Integrating by parts, we find

$$c^2\int_U^{U'}\int_0^{\pi}\frac{u}{(\cosh u+\cos v)^2}dvdu$$
$$=\frac{\pi c^2}{2}\left(\frac{U'}{\sinh^2 U'}-\frac{U}{\sinh^2 U}+\coth U'-\coth U\right)$$
$$=\frac{\pi}{2}(r'^2U'-r^2U-dc)$$

An Improved X-Ray Tube for Diffraction Analysis

R. R. MACHLETT
Machlett Laboratories, Inc., Springdale, Connecticut
(Received March 12, 1942)

A new x-ray tube for diffraction analysis has been produced which affords much greater x-ray beam intensity than has been possible with previous designs. In addition the purity of the x-ray spectrum is insured. The new tube employs thin sheets of malleable beryllium, produced by additions of minute amounts of titanium, for windows in the metal tube wall. The low inherent absorption of such windows and their electrical and mechanical sturdiness are factors in the improvement in beam intensity .A shockproof form of the new diffraction analysis tube is also described.

BERYLLIUM metal of a high degree of purity in very thin vacuum-tight sections, which has recently become available,[1] has made possible the construction of an improved design of x-ray diffraction tube, the first sealed-off x-ray tube to be constructed with thin beryllium for window material. This tube meets an insistent demand for an improved instrument in this field.

The principal objects of the new design are: (1) To increase the beam intensity; (2) to minimize inherent filtration; (3) to provide against the contamination of the spectrum by tungsten from the cathode condensed on the target surface; (4) to incorporate the features of shockproof and rayproof design found in modern radiographic x-ray tubes.

Some steps toward the achievement of these objectives were made in Europe just prior to the war. The present design, however, accomplishes the desired results to a considerably greater degree than the most advanced of the European tubes[2] so far as is known.

The construction of the tube is shown in Figs. 1 and 2. The grounded water-cooled anode is directly connected to a metal enclosure forming the shockproof shield. The tube is energized through a shockproof cable which is readily removable. The insert tube is removable from the shockproof casing for easy replacement, and may be employed without the shockproof shield where desired, as shown in Fig. 1a.

Figure 3 illustrates an installation of the tube in the form shown in Fig. 1a as applied to existing diffraction analysis apparatus.

[1] G. E. Claussen and J. W. Skehan, "Malleable beryllium," Metals and Alloys (April, 1942).

[2] J. E. DeGraff and W. J. Oosterkamp, J. Sci. Inst. 15, 293 (1938).

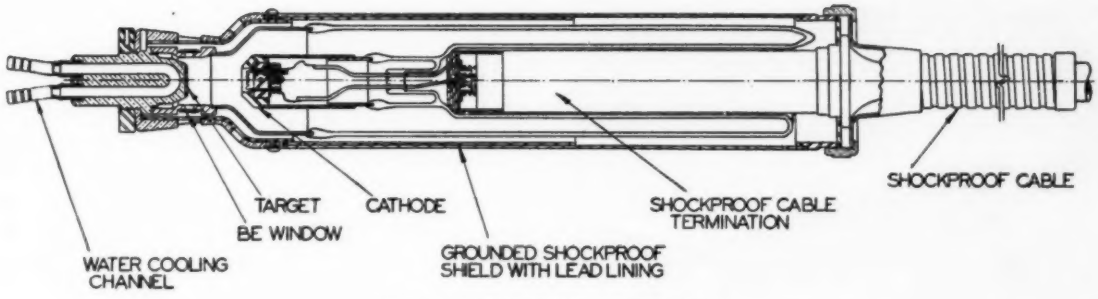

FIG. 1. Shockproof tube complete.

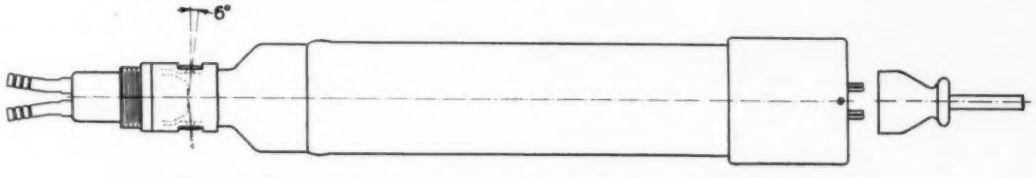

FIG. 1a. X-ray tube only for use without shockproof shield and cable.

1. INCREASED BEAM INTENSITY

Large increases in beam intensity are achieved by means of the following features in the construction of the tube:

(a) Beryllium Windows

Heretofore, diffraction tubes have commonly been provided with windows of materials such as aluminum foil or Lindemann glass, the use of aluminum ordinarily being confined to tubes operating under continuous pumping. Lindemann glass, when used in windows for such tubes, must be spaced a substantial distance from the focal spot, because it would otherwise be under heavy secondary electron bombardment with accompanying danger of gas liberation and possible melting of the glass. Windows of glass become negatively charged during operation and their mechanical and electrical fragility is such that the camera equipment must be kept a considerable distance from their exterior because of the danger of electrical puncture or mechanical damage. Various shielding means have been suggested to reduce the amount of secondary bombardment to which such windows are subjected, but these expedients do not permit the desired close approach to the source of the x-rays.

The new tube is provided with windows of metallic beryllium, mounted on a grounded section of the tube envelope. This metallic window material being a fair heat and electrical conductor, the windows do not become over-heated and charged by the secondary bombardment. Hence, it becomes possible to place the windows very close to the focal spot, so that the diameter of the tube at the windows is very small, being limited in this respect only by the length of the focal spot itself. The small diameter permits a very close approach of the aperture of the camera equipment to the focal spot, thus making possible a great increase in beam intensity by virtue of the inverse square law.

The low absorption coefficient of the beryllium in itself further contributes to increased beam intensity. This factor is elaborated below.

(b) Focal Spot Design

The tube is provided with a line focus 1.2 mm wide and about 12 mm long. It is square in projection at an angle of 6° from the target surface. These dimensions are the optimum values for maximum specific loading capacity. The highest possible specific loading of the focal spot becomes an important factor in improving the beam intensity in view of the small apertures usually found in the collimators associated with diffraction cameras.

2. LOW INHERENT FILTRATION

As mentioned above, probably the most frequently used materials for windows in diffraction tubes have been aluminum and Lindemann glass. Aluminum windows have been frequently used in pump-connected tubes where it is possible to

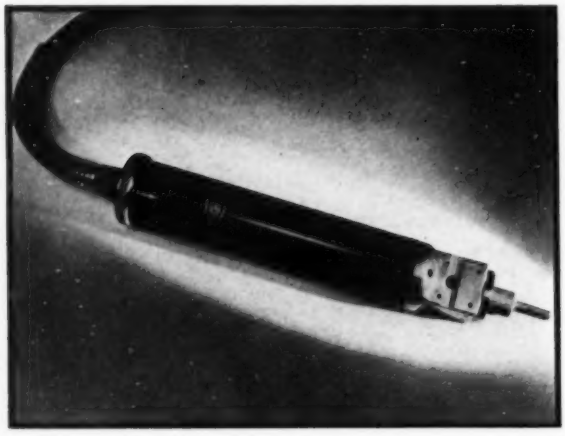

FIG. 2. Photograph of complete shockproof assembly.

make them very thin. Most commercial diffraction tubes of the sealed-off type have used Lindemann glass windows, the thickness varying between 0.005 and 0.010″. Beryllium windows used in the present design have a thickness of the order of 0.010″.

To give some idea of the improvement in inherent filtration, there are given in Table I the absorption coefficients of beryllium, aluminum, and Lindemann glass.

The low inherent filtration and shockproof features of this new tube also make it highly applicable to the recently developed technique of microradiography.[3] For this work operation at very low voltages (4 to 10 kv) is required, and hence, unless the inherent filtration is very low, the x-ray output is greatly diminished by the filtration of the window. It is believed that the present tube has lower inherent filtration than has previously been achieved in a commercially produced sealed-off x-ray tube. These same characteristics, plus the very fine effective focal spot, make the tube especially suitable for radiographic inspection of very thin sections of light weight structures, as, for example, spot welds of thin aluminum sheets.

3. TARGET CONTAMINATION

It has long been recognized that tungsten vapor originating from the cathode filament and condensing on the surface of the target may in time produce radiation of a troublesome character in diffraction work. In the present tube this effect is minimized by the long anode-cathode spacing and small diameter of the discharge chamber. The beryllium windows are completely shielded from condensation of tungsten vapor by means of the recesses in the discharge chamber wall wherein they are located.

A new type of cathode-beam focusing device has also been devised which is being adapted experimentally to this tube and by means of which all possibility of target contamination is expected to be eliminated.

The structure of the new cathode is shown in Fig. 4. It consists of a helical filament, indicated at *A*, surrounded by an electrostatic focusing shield *B*. The anode-cathode spacing in this tube is considerably greater than is usually employed in line focus tubes.

With the usual line focus construction great difficulty is encountered in accurately controlling spot size and electron distribution when the spacing to the anode is increased. The difficulty involved is due to the fact that two separate electron bundles originate from the helical filament, one from the front face and one from the face furthest removed from the target. The latter electrons must completely change direction in order to emerge, and thus they enter the anode

FIG. 3.

[3] G. L. Clark, *Applied X-Rays* (McGraw-Hill, 1940), third edition, p. 180.

field at lower speed. They are, therefore, more influenced by the electrostatic forces than those on the bundle originating from the front face of the helix. When the anode and cathode are spaced a considerable distance apart the focusing of these diverse electron bundles on a spot of predetermined size on the anode involves a degree of accuracy in the cathode structure which is very difficult, if not impossible, to achieve.

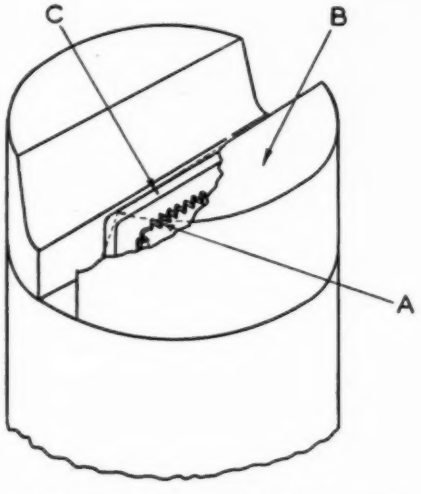

FIG. 4. Schematic diagram of cathode structure.

It has been found, however, that such focusing is considerably simplified by placing a shield *C*, which may take the form of a flattened wire of about the same dimensions as the cathode helix, in front of the same. This shield performs two functions. In the first place it tends to make the electrical conditions influencing the electrons originating from the cathode helix more uniform and thus simplifies the focusing problem so that long anode-cathode spacings may be employed. In the second place, the vaporized tungsten from the cathode helix is influenced by the electrical field within the tube and tends to move in straight lines outward from its origin. Thus the shield in effect casts a shadow on the portion of the anode occupied by the focal spot. As a result of this expedient the contaminating effect of the tungsten vapor is substantially eliminated.

4. SHOCKPROOF FEATURES

The shockproof features of the new design impart a great deal of flexibility to the diffraction tube. It is possible, for example, to bring the tube to existing large structures which may be spaced a very considerable distance from the high voltage generator and control. American manufacturers of x-ray equipment have not hitherto had a shockproof tube available and it is, therefore, expected that new equipment which may appear on the market in the future will be influenced by this feature.

TABLE I. Absorption coefficients of beryllium, aluminum, and Lindemann glass.*

Wave-length in angstroms	Absorption coefficient** Be	Al	Lind. gl.	Ratio Al-Be	Ratio LG-Be
0.710 ($K\alpha$ for Mo)	0.582	14.1	2.24	24.2	3.85
1.54 ($K\alpha$ for Cu)	2.96	132.0	19.5	44.7	6.6
1.934 ($K\alpha$ for Fe)	5.64	252.0	38.4	44.8	6.8

* The composition in Lindemann glass varies somewhat. The values used in making these computations are given by W. Espe and M. Knoll, *Werkstoffkunde der Hochvacuumtechnik* (Julius Springer, Berlin, 1936).
** Absorption coefficient taken from tables in A. H. Compton and S. K. Allison, *X-Rays in Theory and Experiment* (D. Van Nostrand Company, 1935).

APPENDIX

It is apparent that the principal advantages of the design described herein depend upon the availability of beryllium metal, which must be of a high purity, vacuum-tight in thin sections, and hermetically brazable to the body of the tube. The principal problem encountered, therefore, in the evolution of this design was in the development of suitable beryllium metal and brazing techniques.

The material employed was developed at this laboratory by Claussen[1] and others and consists of an alloy containing less than 0.2 percent of titanium. The process of purification and of alloying the material is carried out in a vacuum furnace of special design, the final step being the formation of an ingot approximately 5″ long and 1″ in diameter. From this ingot disks are cut by high speed abrasive wheels and the material is then hot-rolled between plates of nickel or stainless steel to any desired thickness.

This material is believed to be the first substantially pure beryllium possessing hot malleability. Beryllium as previously available, including samples which were distilled in high vacuum, developed cracks and fissures in subsequent working. The difficulty with all such prior efforts appears to be due to the presence of very thin oxide films. These films appear to be reduced by the addition of a very small percentage of titanium.

Numerous difficulties were encountered in developing a successful technique for brazing the thin beryllium sheets to the metallic body of the tube. Such brazed joints must be capable of withstanding high temperatures and rapid changes in temperature. In the present design several subsequent brazing operations must be carried out with relatively high temperature alloys, for example, 50–50 silver-copper, and the beryllium window joint may not approach its melting point during such operations.

A successful technique has been developed and it is intended to report it in detail in the near future.

Rubber in Vibration

S. D. GEHMAN
The Goodyear Tire & Rubber Company, Akron, Ohio
(Received April 9, 1942)

A machine is described which has been used for determining the vibration properties of various types of rubber mountings used for the isolation of mechanical vibrations. The vibrations are excited by oppositely rotating eccentric weights and are recorded on a tape. It was found that resonance curves for various types of rubber vibrations such as shear, torsion, and compression are, except for some minor deviations, adequately accounted for by the equation which contains a damping term proportional to the velocity and inversely proportional to the frequency. The apparent static modulus of rubber in compression depends upon the shape of the piece, more explicitly, on the ratio of load area to the free area. The same is true for the dynamic modulus. It was found that pieces of similar shape have identical values for the dynamic modulus and also for the internal friction. Some curves are given showing the dependence of dynamic modulus and internal friction on the shape factor. The dynamic stiffness shows the largest deviation from the static values at high shape factors. The internal friction has a linear relationship to the dynamic modulus when the shape factor is varied. This results in damping which is practically independent of the shape. The effect of temperature on the vibration properties of mounting stocks for a range $-10°$F to 160°F was studied and curves are included showing the temperature dependence in this range.

INTRODUCTION

IN most of the uses to which rubber is put, it is subjected to deformations which are relatively small compared to the ultimate deformation of which the rubber is capable. For many products, such as vehicle tires, motor mountings, and belts, the deformations are periodic. There is, therefore, a great deal of interest attached to the physical properties of rubber as measured under vibratory, as contrasted to static, conditions.

The use of rubber in mountings for the absorption or isolation of vibration, with which this paper is principally concerned, has led to a number of systematic investigations of its static properties from the standpoint of the engineer who might be interested in employing it for such purposes. As representative of such contributions may be cited the work of Keys,[1] Smith,[2,3] Brown,[4] Haushalter,[5] Hirshfeld and Piron,[6] and Kimmich.[7] The principal concern was to determine the rules which govern the deformation of rubber pieces of varying size, shape, and hardness. Related questions of permanent set, creep, and the effect of temperature also came into the discussion. The importance of dynamic measurements was realized, but information on this phase of the subject was beyond the scope of the work.

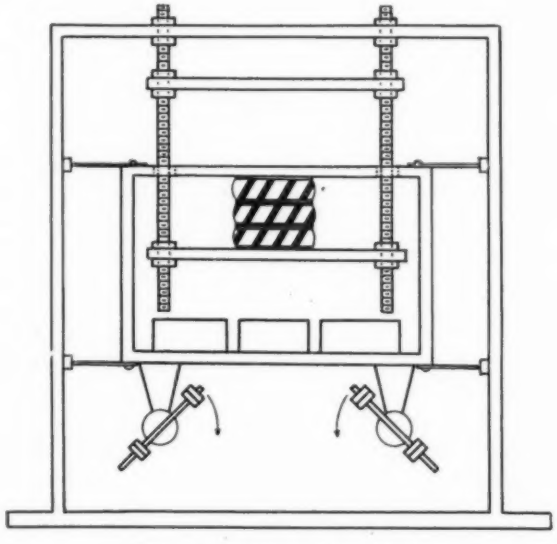

FIG. 1. Diagram of machine.

Published investigations on the vibration properties of rubber, with a few exceptions, have not had much direct connection with the design of mountings. Usually they have been carried out on relatively small, standardized test pieces, the principal interest being the comparison of the properties of different rubber compositions for

[1] W. C. Keys, Mech. Eng. **59**, 345 (1937).
[2] J. F. D. Smith, Trans. Am. Soc. Mech. Eng. **5**, A13 (1938).
[3] J. F. D. Smith, Ind. Rubber World **100**, No. 5, 48 (1939).
[4] R. Brown, J. S. A. E. **47**, 432 (1940).
[5] F. L. Haushalter, Trans. Am. Soc. Mech. Eng. **61**, 149 (1939).
[6] C. F. Hirshfeld and E. H. Piron, Trans. Am. Soc. Mech. Eng. **59**, 471 (1937).
[7] E. G. Kimmich, Ind. Rubber World **103**, No. 3, 45 (1940).

the purpose of developing compounds with improved dynamic properties. In some cases the work has been of a fundamental research character on the nature of rubber elasticity. The following references, if consulted, will give a fairly comprehensive picture of what has been done, although they are by no means a complete bibliography. Vogt[8] has reviewed the work of Bouasse, Wiegand, Gerke, Meyer and Ferri, and others dealing with cyclic extensions and contractions of stretched rubber. Kosten has discussed the general character of the dynamic results which have been observed when rubber is subjected to periodic vibrations and has extended the data by his own investigations.[9–12] Roelig[13] has reported extensive results on dynamic tests carried out with forced vibrations. Naunton and Waring[14,15] used electrical methods for driving the rubber sample and measuring the dynamic properties. Yerzley[16,17] employed a system where free oscillations occurred. Gehman, Woodford, and Stambaugh[18] studied the effect of pigment loadings on the vibration properties.

Rubber mountings are now generally made with the rubber molded and adhered to metal during vulcanization. The rubber may act in compression, tension, shear, or torsion. Frequently there are complicated combinations of such superposed stresses in a mounting. The mountings which have been designed and developed for specific purposes show an almost infinite variety in geometrical design, size, shape, and type of action.

The work here reported will describe equipment which is useful for observing and studying such mountings under vibration and will give some of the more general results of such studies.

[8] W. W. Vogt, in Davis and Blake's *Chemistry and Technology of Rubber* (Reinhold Publishing Company, New York, 1937), p. 332.
[9] C. W. Kosten, Proc. Rubber Technology Conf. (London, 1938), p. 987.
[10] C. W. Kosten and C. Zwikker, Physica **4**, 221 (1937).
[11] C. W. Kosten, and C. Zwikker, Physica **4**, 843 (1937).
[12] C. W. Kosten, De Ingenieur **54**, W128 (1939).
[13] H. Roelig, Proc. Rubber Technology Conf. (London, 1938), p. 821.
[14] W. J. S. Naunton, and J. R. S. Waring, Proc. Rubber Technology Conf. (London, 1938), p. 805.
[15] W. J. S. Naunton, and J. R. S. Waring, Trans. Inst. Rubber Ind. **14**, 340 (1939).
[16] F. L. Yerzley, Proc. A. S. T. M. **39**, 1180 (1939).
[17] F. L. Yerzley, Trans. A. S. M. E. **62**, 469 (1940).
[18] S. D. Gehman, D. E. Woodford, and R. B. Stambaugh, Ind. Eng. Chem. **33**, 1032 (1941).

DESCRIPTION OF APPARATUS AND PROCEDURES

The principles of the machine used for exciting the vibrations are apparent from the diagram of Fig. 1. The central carriage, held in place by centering springs of negligible stiffness, is set into vertical vibration by the opposite rotation of two geared shafts carrying eccentric weights at each end, a well-known device. The centering system consists of thin horizontal cantilever blades, one of which is attached at each corner of the carriage as indicated in Figs. 1 and 2. The shafts are driven by a horizontal belt from a variable speed d.c. motor. The amplitude of vibration reaches large values only in the neighborhood of the resonance frequency which is determined by the stiffness of the rubber mountings and the mass of the vibrating carriage. From the resonance frequency, the dynamic stiffness can be calculated and from the amplitude of vibration at resonance a value of the damping can be computed.

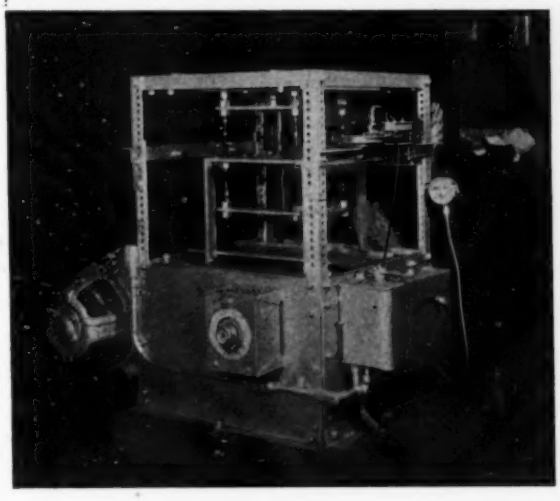

FIG. 2. Photograph of machine.

A photograph of the machine is shown in Fig. 2. The platens on which the test pieces are mounted are fourteen inches square and capable of a separation of about eight inches so that by use of suitable fittings all types of rubber mountings of ordinary size can be accommodated. This includes mountings for which the rubber vibrates in tension, compression, shear, or torsion under various superposed static stresses. In the photo-

graph, the test pieces are mounted for vibration in shear. In this arrangement, the test pieces under the platen are subjected to a greater static load than those above, because of the weight of the carriage. When the weight of the carriage is small compared to the total static load, this inequality of static load is not objectionable. In many cases, however, it is preferable and simpler

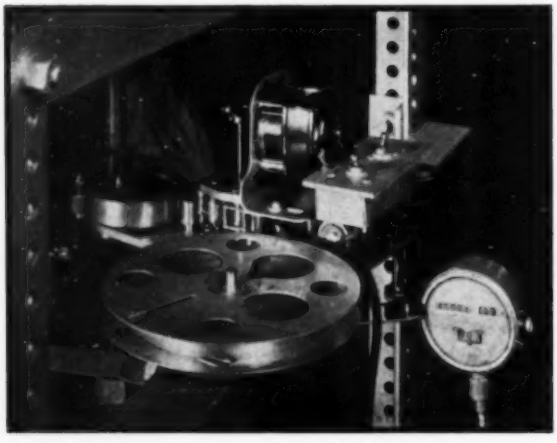

Fig. 3. Photograph of recorder used for registering vibrations.

not to have the double test piece, but to use the weight of the carriage to impress the static load on a test piece under the platen. The weight of the carriage is normally 174 pounds, but it can be readily varied in the range from 140 to 400 pounds by the removal or addition of weights. There is usually little difficulty in arranging things so as to secure resonance at a speed of about 600 r.p.m. If a particular rubber mounting is too stiff, it is often possible to use two or more of the units in series; if it is too soft, several can be used in parallel. Thus it has been found as a rule to be even simpler to adjust the stiffness than it is to adjust the weight of the carriage. This restriction to approximately the same frequency assists in the comparison of results and insures operation of the machine at a speed such that reactions through the frame are completely negligible.

Figure 3 is a photograph of the recorder used for registering the vibrations. It was constructed with the aid of parts from a moving picture projector. Standard 16-mm film is moved around a horizontal drum at a constant speed by a synchronous motor. Exposed film is used from which the gelatine has been removed by soaking in warm, dilute hydrochloric acid. The film is scratched by a stylus attached to the vibrating carriage. Sample records are reproduced in Fig. 4. The procedure for securing records was as follows: The speed controlling rheostats were left at one setting until the speedometer (shown at the right in Fig. 3) indicated that a constant speed had been attained. The recorder was then started and six or eight inches of record secured. The recorder was stopped and the speed of the machine changed by an amount shown by the speedometer and a short record at this speed secured. In this way, step by step, the resonance peak was passed through. The time required to secure a record is about five minutes.

The amplitudes are measured by projecting the record on graph paper using the optical system of a microphotometer which was available. The magnification can be checked by measuring the notches in the film. The frequency corresponding to a given amplitude is determined by measuring the length of ten waves, making use of the micrometer screw which moves the platform of the microphotometer. A considerable amount of time is required to measure a complete record. Usually it is sufficient to measure four or five points near the resonance peak. For this, ten or fifteen minutes are ample.

After the record is measured, a few simple calculations are necessary. There are four rotors, each carrying two equal masses w at radii r_1 and r_2 from the center. The driving force for the vibration is, therefore, the centrifugal force:

$$F=(16\pi^2/32.2)w(r_1-r_2)(\text{r.p.m.})^2/3600, \quad (1)$$
$$w=0.441 \text{ lb.}$$

The units for r_1 and r_2 are feet and for F, lb.

Each mass w consists of two nuts screwed against each other on a threaded rotor. It is frequently desirable to change the value of the driving force. This is done by always keeping r_1 fixed and changing r_2 on each rotor by bringing the nuts up against spacer blocks which locate the nuts accurately with reference to the axles. The spacers, of course, are then removed. To determine the position of the weights for dynamic balance of the machine, resonance amplitudes, for a given mounting, were plotted against the values of (r_1-r_2) as determined by the spacer

blocks. This plot is shown in Fig. 5. The intercept of the straight line with the axis gives the point of dynamic balance. By use of Eq. (1), a chart was then plotted, each curve of which gave F as a function of the r.p.m. for one of the spacer blocks. Thus the value of the driving force at a given r.p.m. can be read from the chart. Since the r.p.m. is proportional to the reciprocal of the wave-length which is measured on the record, it is also convenient to read the r.p.m. values from a plotted curve. In this way, corresponding values of r.p.m. driving force, and amplitude can be easily secured.

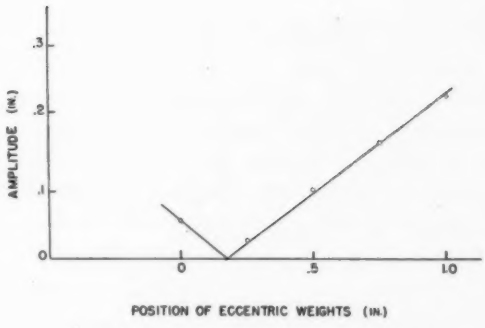

FIG. 5. Dynamic balance of machine.

THEORY

The procedure which has been described has the effect of correcting the results to an exciting force independent of the frequency and thus reducing the interpretation of the results to the simple one degree of freedom system, the analysis of which is given in every text book on vibration.

The equation of motion is

$$M\ddot{x}+\alpha\dot{x}+sx=F\cos pt; \tag{2}$$

M—mass (lb./32.2);
x—displacement from equilibrium position (ft.);
α—constant of proportionality between the internal frictional resistance of the rubber and the velocity (lb./ft. per sec.);
s—stiffness of rubber (lb./ft.);
F—maximum value of sinusoidal driving force (lb.);
p—angular frequency, 2π(r.p.m.)/60.

The steady state solution of Eq. (2) is,

$$x=\frac{F\cos(pt-\theta)}{[(s-mp^2)^2+\alpha^2p^2]^{\frac{1}{2}}}, \tag{3}$$

$$\tan\theta=\alpha p/(s-mp^2). \tag{4}$$

The value of p for the maximum amplitude of vibration is given by

$$p^2=s/M-\alpha^2/2M^2. \tag{5}$$

Usually the second term can be neglected so that, at resonance

$$p_n^2=s/M, \tag{6}$$

$$x_{\max}=F/\alpha p_n. \tag{7}$$

These equations serve to determine s, the dynamic stiffness of the rubber and α, its internal damping coefficient. It is known, however, that for most materials, including rubber, α is a function of the frequency.[9,14,18,19] At resonance, x/F is given by $1/\alpha p_n$ in accordance with Eq. (7). Finite amplitudes at resonance are observed at all frequencies so that it can be seen, in a general way, that as p increases α will diminish and vice versa. As a matter of fact, the amplitude at resonance for rubber vibrations, as the mass of the system is varied and F held constant, is, to a first approximation, independent of frequency so that the product αp is very nearly constant.

This type of internal friction has been designated by Kimball[19,20] as solid friction. Kimball

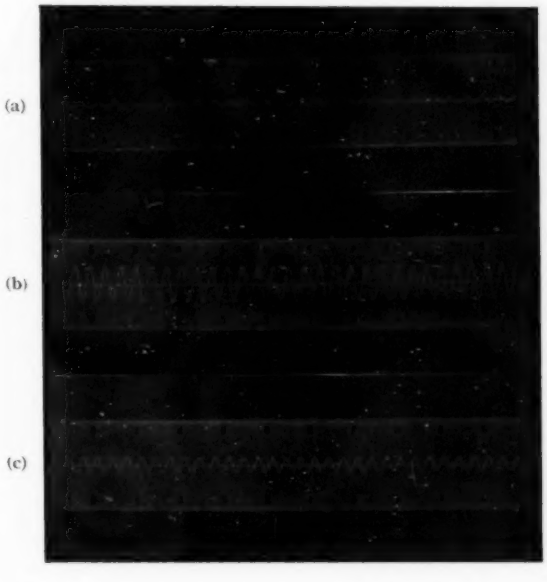

FIG. 4. Reproduction of portions of typical record (torsional vibrations). (a) Speed below resonance; (b) resonance; (c) speed above resonance.

[19] A. L. Kimball, Trans. A. S. M. E. **51**, 227 (1929).
[20] A. L. Kimball, *Vibration Prevention in Engineering* (John Wiley and Sons, New York, 1932), p. 119.

has developed the theory in terms of the stress and strain per unit volume of the vibrating medium and has defined the quantity η, the coefficient of normal viscosity, as the constant of proportionality between the velocity damping force and the time rate of change of the strain.

The logarithmic decrement for free vibrations is shown to be

$$\delta = \pi\eta p_n/E; \tag{8}$$

E—Young's modulus of the material.

Since observation showed δ to be independent of frequency, Kimball concluded that ηp was invariant.

Illustrating still another viewpoint, Kosten[9] has pointed out that the quantity $\alpha p_n/s$ is analogous to tan δ in alternating current theory, where δ is the angle of loss and should not be confused with the logarithmic decrement given by Eq. (8). Kosten has expressed his results for rubber in terms of this angle.

The logarithmic decrement is connected with α by the relationship

$$\delta = \pi\alpha/(sM)^{\frac{1}{2}} = \pi\alpha/Mp_n = \pi\alpha p_n/s. \tag{9}$$

It is general practice to use an approximate relation for the logarithmic decrement, *viz.*:

$$\delta = \Delta W/2W = \Delta y/y. \tag{10}$$

Here W is the vibrational energy and y is the amplitude. Δ represents the change in these quantities for two successive free vibrations. $\Delta W/W$ is the damping.

In the case of rubber the damping is sometimes so large that the above approximations are inaccurate. Hence, it is preferable to define a quantity called the dynamic resilience as the percent of the vibrational energy remaining in the second of two successive free vibrations.[18] This is given by

$$\begin{aligned} R &= 100 \exp\left[-2\pi\alpha/Mp_n\right] \\ &= 100 \exp\left[-2\pi\alpha p_n/s\right] \\ &= 100 \exp\left[-2\pi p(\eta/E)\right]. \end{aligned} \tag{11}$$

The percent damping is $(100-R)$.

Although it has been found expedient to work up the data in such a way as to correct for the variation of the exciting force with frequency, it is worthwhile to give some consideration to the theory underlying the actual response when, as in this case, the amplitude of the force varies with the square of the frequency.

TABLE I. Characteristics of resonance curves.

	Constant force amplitude	Force amplitude proportional to p^2
1.	$x \to F/s$ as $p \to 0$	$x \to 0$ as $p \to 0$
2.	Maxima shift to lower frequencies as damping increases	Maxima shift to higher frequencies as damping increases
3.	$x \to 0$ as $p \to \infty$	$x \to mr/M = mrp_n^2/s$ as $p \to \infty$

A general analysis for such a system has been given by Bernhard.[21]

The amplitude is,

$$x = \frac{mrp^2 \cos(pt-\theta)}{\left[(s-Mp^2)^2+\alpha^2p^2\right]^{\frac{1}{2}}}; \tag{12}$$

m—eccentric rotating mass,
r—eccentricity.

The characteristics of the resonance curves from Eq. (12) in comparison with those from (3) are stated in Table I.

These characteristics have been observed for resonance curves secured in this work with rubber.

When rubber mountings are used for the isolation of vibrations, the fundamental principle is that the natural period of any mode of vibration of the system should be lower than that of any impressed frequency which will excite the mode in question or any mode coupled with it.

For a system with one degree of freedom, the transmitted force is given by,

$$F_t = F\left[\frac{1+\left[2(\alpha/\alpha_c)\cdot(p/p_n)\right]^2}{(1-p^2/p_n^2)^2+\left[2(\alpha/\alpha_c)p/p_n\right]^2}\right]^{\frac{1}{2}}; \tag{13}$$

F_t—transmitted force;
α, p, and F are defined as in Eq. (3);
p_n—natural frequency of system;
α_c—critical damping $= 2Mp_n$.

For zero damping,

$$F_t = \frac{F}{1-(p/p_n)^2}. \tag{14}$$

[21] R. K. Bernhard, J. App. Phys. **12**, 866 (1941).

The relationships involved in these formulas are analyzed by den Hartog[22] and need not be repeated here. It is sufficient to point out that in accordance with Eq. (14), rubber mountings are carefully designed to avoid resonance conditions during operation. This does not detract from the expediency of using resonance conditions to study the vibrational properties of the mountings.

For vibration isolation, the natural frequency of the system is set below the resonance frequency. If it is set too low, the system will develop instability for static loads, transient accelerations, etc. Hence a balance must be struck in the design between vibration isolation and static stability. Usually it is desirable to provide some type of snubbing to preclude excessive transient deflections.

TEST OF VIBRATION THEORY AS APPLIED TO RUBBER VIBRATIONS

In Fig. 6 are compared observed and calculated resonance curves for both shear vibrations and compression vibrations. Sandwiches of rubber adhered to metal were used in the test. The durometer hardness of the rubber was 30, size of the sandwiches $2''\times4''\times1''$. As ordinate is plotted the amplitude per pound of driving force and as abscissa, the r.p.m. of the driving force. The calculated curves were obtained from Eq. (3) and were fitted to coincide with the experimental curves at the resonance peak. A small systematic deviation between the calculated and observed curves occurs on the low frequency side of the resonance peak, observed values of the amplitudes falling below the calculated ones. This is due to the fact that s in Eq. (2) is not strictly a constant. The known variation of α with frequency cannot account for this deviation because, at the base of the peak, where the deviation is largest, the amplitude is practically independent of α and is determined by the term $(s-mp^2)$ in Eq. (3).

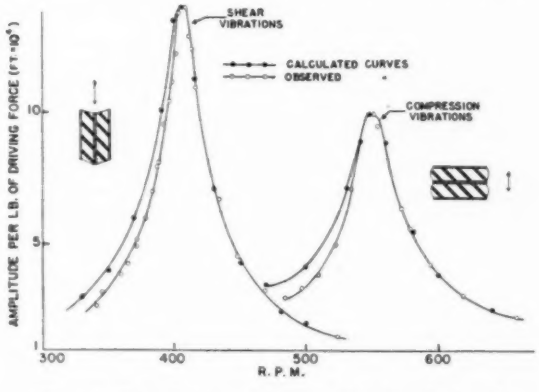

FIG. 6. Comparison of observed and calculated resonance curves.

Although the deviation from the theoretical curve is rather small, it seemed worthwhile to find the cause for what light it might throw on any peculiarity of the dynamic properties of rubber or the accuracy of the work.

A variation of s could be shown by calculating s for different points of the experimental curve using, instead of Eq. (6), an equation derived from Eq. (3), *viz.*:

$$s^2=\left(\frac{p_2^2}{a_1^2}-\frac{p_1^2}{a_2^2}\right)\left(\frac{1}{p_2^2-p_1^2}\right)+p_1^2p_2^2M^2. \quad (15)$$

Here p_1 and p_2 are frequencies for two points selected for the calculation and a_1 and a_2 are the corresponding x/F values or unit amplitudes from the curve for the two points. It was found that the value of s depended somewhat upon the two points selected for the calculation. If this variation of s were due to a dependence upon frequency, there should be a deviation from the theoretical curve on the high frequency as well as on the low frequency side of the resonance peak.

The remaining possibility is that s varies with the amplitude in such a way that it is larger for small amplitudes than it is for large ones. Because of the way in which the vibrations were excited, by centrifugal force, the amplitudes were larger on the high frequency side of the resonance peak than they were on the low frequency side, although the amplitudes per unit force, which are plotted in Fig. 6, do not show this. This accounts for the appearance of the deviation between the observed and calculated curves on the low frequency side of the peak and not on the high frequency side.

If the centering springs of the vibrating carriage had any influence on the observed value of s, the opposite effect would be expected and s become greater as the amplitude increased.

[22] J. P. den Hartog, *Mechanical Vibrations* (McGraw-Hill, New York, 1940).

The variation of s with amplitude can also be shown directly by securing resonance curves using different driving forces so as to obtain different amplitudes at resonance. Two such curves are shown in Fig. 7. The test pieces were two parallel rubber cylinders adhered at the ends to metal, 30-durometer hardness, height $1\frac{3}{8}$ inch, diameter 2 inches. For the lower amplitude, the resonance peak is displaced to a higher frequency relative to the peak secured at the higher amplitude. For gum stock, under ordinary circumstances, this dependence of stiffness on amplitude is negligible. When the hardness of the rubber is increased by the addition of appreciable volumes of carbon black or other pigments, the effect can become very pronounced.

Figure 8 shows the large deviation which occurs between calculated and observed resonance curves for a tire tread stock containing about 25 volumes of gas black. Here the test piece was a rectangular block, $1''\times1''\times2''$, vibrated lengthwise in compression. The effect of the dependence of modulus on amplitude is to give a much sharper resonance peak than is predicted by the simple theory. The internal friction, as determined by the quantity α in Eq. (7), decreases with increase of amplitude in such a way that calculated values of resilience increase with increase of amplitude. Naunton and Waring[14] and Gehman, Woodford, and Stambaugh[18] also observed a dependence of modulus and resilience on amplitude for tread stocks, at much higher frequencies than those here used. Kosten,[9] on the other hand, for smaller amplitudes and probably a smaller range of amplitudes, reported that both the angle of loss and the stiffness were independent of amplitude.

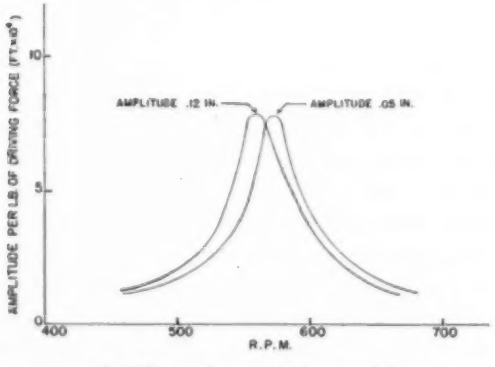

FIG. 7. Effect of amplitude on stiffness.

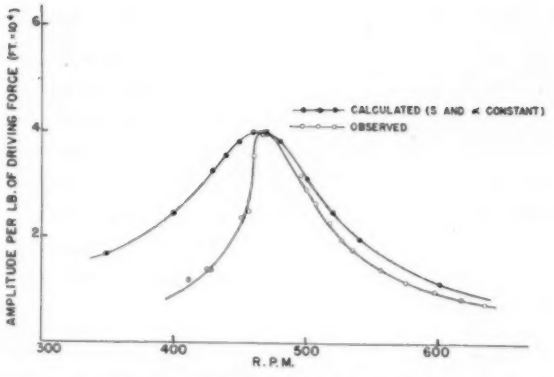

FIG. 8. Calculated and observed resonance curves for tread stock.

The reason for the dependence of the stiffness on the amplitude is somewhat obscure. The heat generation in the test piece is proportional to the square of the amplitude of vibration. Temperature changes on this account would be in the proper direction to account for the results. One of the reasons for not dismissing the dependence of s and R on the amplitude as being entirely due to the temperature rise is that the temperature rise in these experiments was so small. For the test piece for which the curve of Fig. 8 was secured, the temperature rise as measured by a needle thermocouple inserted into the test piece did not exceed 5°C. Another reason is that observed values of s are independent of frequency. A heating effect should also occur for frequency variation. Results of Weber and Goeder[23] give some indication that an increase in modulus for small stresses may be a very general property of materials.

The dynamic modulus for rubber is generally observed to be somewhat higher than the static modulus. Also, the dynamic modulus is independent of the frequency. The question now arises as to how low the frequency would have to be in order for the dynamic modulus to decrease and approach the static value. This is somewhat of a dilemma since the greater dynamic values are observed at the lowest frequencies which could be reached in this work, 250 to 300 cycles per minute. If there were a true dependence of the dynamic modulus on amplitude, i.e., not caused by temperature rise, it

[23] R. L. Weber and F. P. Goeder, Phys. Rev. **61**, 94 (1942).

could be said that the dynamic modulus approaches the static modulus as the amplitude increases, regardless of the frequency. For this reason, the dependence of dynamic modulus on amplitude is of some theoretical interest. The points raised here require further carefully designed and controlled experiments for full understanding. The deviation of the dynamic from the static stiffness for rubber has never been satisfactorily explained. The most probable basis for an explanation appears to lie in the elastic imperfections of rubber described by such words as hysteresis, creep, relaxation, set, "memory," etc. It is possible that a mathematical formulation of rubber vibrations in terms of the relaxation theory of Maxwell or the "memory"

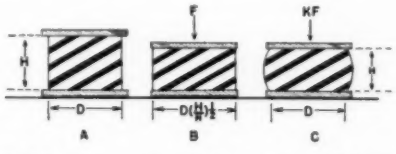

FIG. 9. Rubber in compression. (A) Original cylinder; (B) lubricated end plates; (C) no sliding at end plates.

theory of Boltzmann would account for these dynamic effects. The decrease of s with amplitude is a favorable factor in the performance of rubber mountings for the isolation of vibration as it tends to shift the natural frequency to lower values as vibration amplitude builds up. But the effect is a small one.

PROPERTIES OF RUBBER VIBRATING IN COMPRESSION

Rubber shows peculiar characteristics when placed under compressive stress. When equal uniform stresses are applied to two opposed parallel faces of a block of rubber, instead of compressing in the ordinary sense, the rubber undergoes a deformation without appreciable change in volume. The rubber bulges out at the sides and a complicated, non-uniform stress distribution is set up in the rubber. The stiffness depends not only on the modulus of the rubber but on the shape of the piece and on the friction between the rubber and the end plates. The static effects have been thoroughly studied.[6]

For test pieces similar in shape but varying in size, a given stress produces the same percentage compression. For pieces with different shapes, the stress required to do this is dependent on the ratio of the area of the loaded surface to the area of the free surfaces but otherwise practically independent of the shape. When the stress required for a constant percent compression is plotted against the shape factor, load area/free area, a smooth curve is obtained. A family of such curves for rubber compositions of different hardnesses gives the empirical information required for the static design of rubber compression mountings.

In contrast to the results for rough end plates or for test pieces in which the rubber is adhered to the end plates, are those for lubricated end plates. In this case, as compressive stress is applied, the sides of the rubber remain straight, a uniform condition of stress exists throughout the rubber, and a value for a compression modulus characteristic of the rubber composition can be obtained. Even so, the calculated modulus is constant only if the calculation is based on the actual cross section, which increases with the stress. Figure 9 illustrates, for a cylindrical test piece, the effect which is being discussed.

For the case of no slipping at the end plates and low shape factors, the calculated modulus approaches the value secured with lubricated end plates. This is the lowest value. For relatively high shape factors, such as 2.5, no slipping, the calculated modulus may exceed, by a factor of ten or more, the modulus for lubricated end plates.

The fundamental principle which has come out of the static tests is that rubber test pieces, similar in shape but varying in size, subjected to the same compressive stress, undergo the same percentage deformation. It might be taken for granted that this same rule applies for the dynamic stiffness, especially since some evidence to this effect already exists.[9] Nevertheless, it

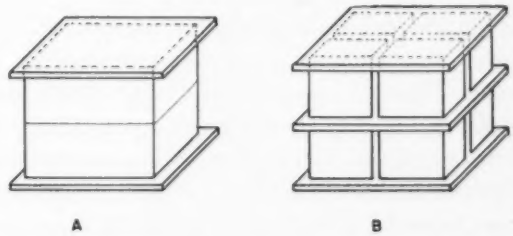

FIG. 10. Arrangement of test pieces for test of principle of dynamic similarity.

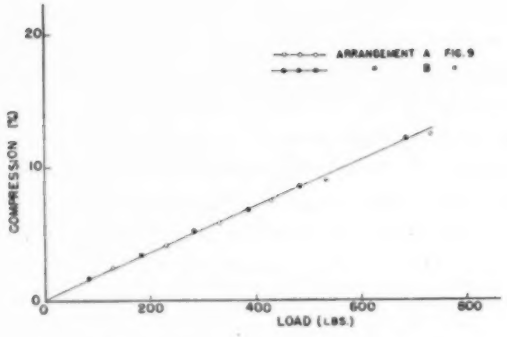

FIG. 11. Static results of similarity test.

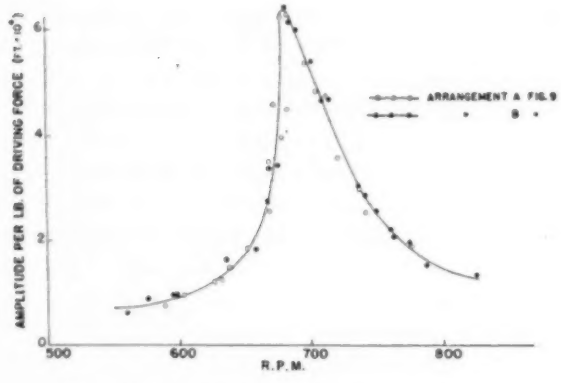

FIG. 12. Dynamic results of similarity test.

seemed worthwhile to make a carefully controlled experiment to test the applicability of this principle under dynamic conditions.

In carrying out the experiment, it was desirable that test pieces of identical composition and cure, of the same shape but of different size, be subjected to the same percentage static compression, set into vibration with the same resonance frequency and the same percentage amplitude. The test pieces were cut from a slab of rubber, thickness 1.25 inch. The durometer hardness of the rubber was 40. Two squares were cut three inches on a side. These were cemented together to give a rectangular block of dimensions $3\times3\times2.5$ inches. Eight small blocks were cut from the slab with dimensions $1.5\times1.5\times1.25$ inches. The eight small pieces, when mounted as shown in Fig. 10, should have, according to the above principle, the same stiffness as the single large block. All of the end surfaces of the blocks were loaded against fine sandpaper to avoid slipping at the ends. The static stiffnesses of the single large block and the eight small blocks were found, in fact, to be identical. The results of this Olsen machine test are shown in Fig. 11.

The resonance curves obtained for the large block and the eight small blocks were also the same, as shown in Fig. 12. This indicates that both the dynamic stiffness and the internal friction were essentially identical in the two cases.

From this and similar experiments, it became apparent that relative effects caused by changes of size, without change of shape, of rubber mountings vibrating in compression could be very simply expressed. The same rule of similarity applies for the dynamic stiffness as for the static stiffness.

As regards the internal friction, if α in Eq. (2) is multiplied by the factor h/A, where h is the height of the rubber and A the loaded area, a value for the internal friction is obtained which is independent of the size of the rubber test piece but which depends upon the composition and the shape. This value of the internal friction will be designated by η. It corresponds to the coefficient of normal viscosity discussed by Kimball.[19] In the same way, a value for the dynamic modulus can be calculated which will be valid for a given shape of test piece. This is given by

$$E=sh/A. \tag{16}$$

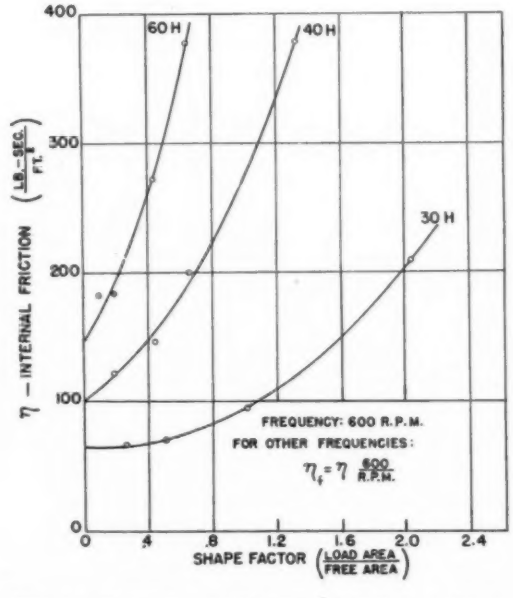

FIG. 13. Dependence of internal friction on shape.

Strictly, this modulus will apply only for the same percentage compression, but in many cases the stress-strain curve is sufficiently linear over the limited range of use that any curvature can be ignored.

The usefulness of these principles lies in the fact that the determination of E and η for small test pieces in vibration enables the dynamic properties of full size mountings of similar shape to be calculated. Furthermore, it can safely be assumed that the scale effect for more complicated rubber deformations, such as, for instance, the radial deflections of cylindrical bushings can be handled in the same way.

The effect of shape on the dynamic properties of rubber mountings vibrating in compression is more complicated than the effect of size. Nevertheless, by the use of the shape factor, previously defined and discussed, it is possible to describe the effects in a relatively simple way.

Figure 13 is a plot of η, as determined by experiment, against the shape factor for stocks of different durometer hardness. From the curves, the value of η can be read for any desired shape. By use of the relation that the product of η and frequency is constant, which is true at least to a first approximation, the value of η for any frequency can be obtained.

Figure 14 shows curves for E, the dynamic modulus, which is independent of frequency. Curves for the static modulus are also given in Fig. 14 for comparison with the dynamic values. The dynamic and static values of the modulus diverge from each other both as the shape factor and durometer hardness increase. Since the design of a mounting usually requires the greatest static stiffness or stability consistent with effective vibration isolation, this deviation of dynamic from static stiffness is in the unfavorable direction and should be taken into account.

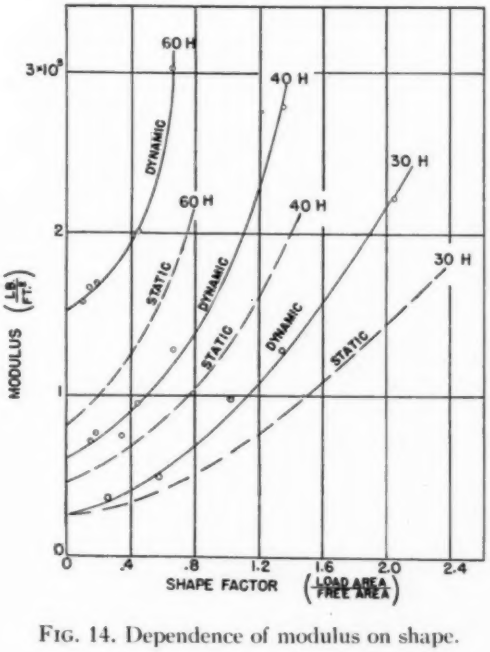

FIG. 14. Dependence of modulus on shape.

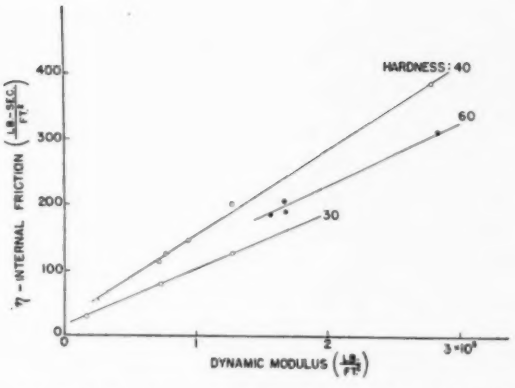

FIG. 15. Relation between dynamic modulus and internal friction.

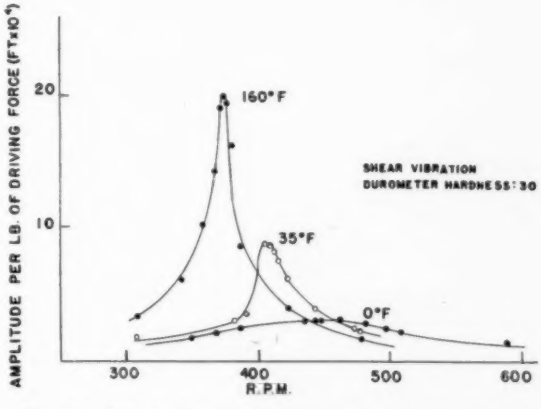

FIG. 16. Effect of temperature on resonance curves.

Figure 15 is a plot of the internal friction against the dynamic modulus. The relationship between η and E is linear. It should be kept in mind that the variations in η and E are caused by changes in shape of the vibrating piece as shown in the Figs. 13 and 14. It thus appears that the increase in modulus with increase in shape factor and the increase in internal friction are both associated with the more complicated stress distribution which occurs at higher shape factors.

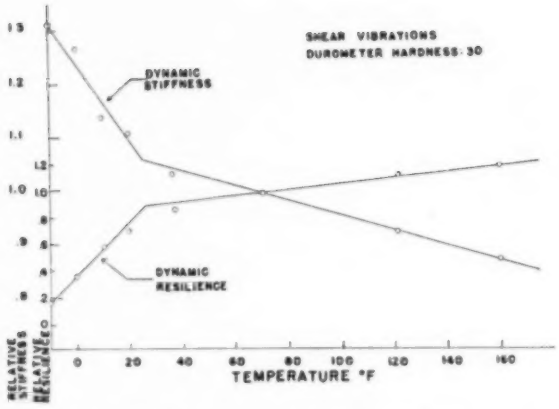

FIG. 17. Effect of temperature on dynamic properties.

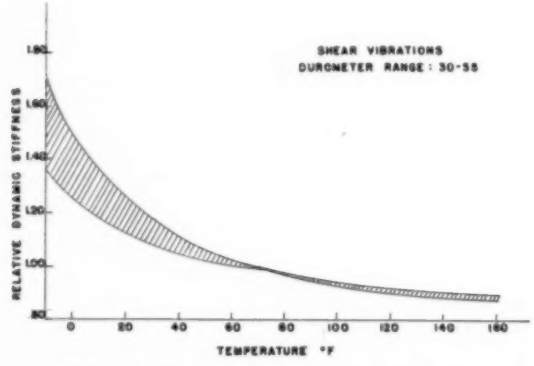

FIG. 18. Effect of temperature on dynamic stiffness of different rubber compositions.

E and η have also been shown to have a linear interdependence for different pigment loadings.[18] In this case also a complicated stress distribution about the pigment particles may be the controlling factor. Both cases may be illustrations of the broad general relationship between modulus and viscosity formulated by Gemant[24] on a basis of molecular theory.

From Eq. (12) and the linear relationship between η and E, it follows that the dynamic resilience is relatively insensitive to shape factor.

EFFECT OF TEMPERATURE ON RUBBER VIBRATIONS

One of the most important variables affecting the use of rubber mountings is the temperature. Rubber mountings are frequently expected to function over an extended temperature range so that it is important to know the variations of stiffness and resilience which are to be expected.

[24] A. Gemant, J. App. Phys. **12**, 680 (1941).

Rubber-like elasticity for any material is always displayed in a limited temperature range. Vulcanization has the effect of extending this range for raw rubber at both ends; that is, to both lower and higher temperatures. It is thus apparent that a great deal of variation may be expected in the effect of temperature on a rubber composition, depending not only upon the added ingredients such as pigments, softeners, etc., but also upon the vulcanization process; that is, the vulcanizing ingredients used and the extent of the cure. In spite of this variation, it does seem possible to find some rather general relationships which may be useful.

Figure 16 shows the resonance curves secured for shear vibrations of a commercial mounting stock of 30-durometer hardness not especially compounded in regard to temperature effects.

Figure 17 shows the temperature dependence of dynamic resilience and dynamic stiffness for this same stock. The values are plotted in such a way as to show the relative changes from those at 70°F. The data for both dynamic resilience and stiffness are fairly well represented by two straight lines of different slopes, one for the low temperature range and one for the high temperature range. For large shear deformations, where appreciable molecular orientation occurs, an actual stiffening may be observed as the temperature is raised, analogous to effects with rubber in tension.

Figure 18 is a similar plot of dynamic stiffness including data secured with commercial mounting stocks with durometer hardnesses in the range 30 to 55. All the values measured fell in the

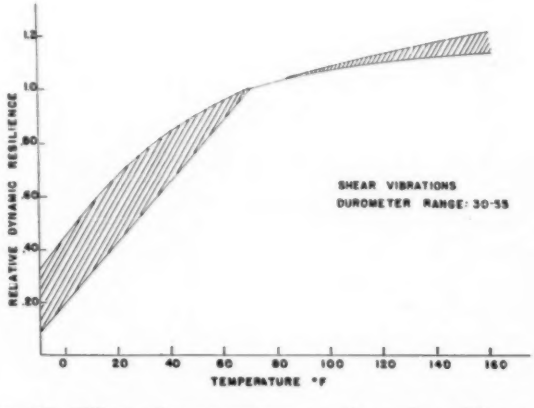

FIG. 19. Effect of temperature on dynamic resilience of different rubber compositions.

shaded area. The various compositions show a much greater spread in relative temperature effect at low temperatures than at high temperatures. Figure 19 is the same type of plot for dynamic resilience. It is apparent that variations in dynamic properties of a mounting caused by low temperatures are likely to be of greater magnitude than those caused by high temperatures. The decrease in resilience and increase in stiffness at low temperature may be even greater than shown here if the rubber is held at the low temperature for a prolonged period of time.

ACKNOWLEDGMENT

It is a pleasure to acknowledge the assistance of Mr. M. Wendt in the design of the machine and of Dr. J. E. Field in the design and construction of the recorder. I also wish to express my thanks to Dr. L. B. Sebrell, Manager of the Research Department at Goodyear, for permission to publish this work.

New Instrument Booklets

The W. M. Welch Scientific Company has recently issued an interesting booklet on "Welch Duo-Seal Pumps and Vacuum Technique." Fourteen of the twenty-nine pages of this booklet give technical information on the design and use of vacuum systems. Copies may be obtained by writing to the W. M. Welch Manufacturing Company, 1515 Sedgwick Street, Chicago, Illinois.

The February issue of *The General Radio Experimenter* contains articles entitled "Measurement and Analysis of Linear and Torsional Vibrations with Electronic Instruments" and "A 100-Watt Output Power Meter." The March issue is devoted to a paper, "How Good Is an Iron-Cored Coil?" by P. K. McElroy and R. F. Field. The April issue features an article entitled "Increased Power-Factor Range for the Capacitance Bridge." Issued monthly by the General Radio Company, 30 State Street, Cambridge A, Massachusetts.

"Priorities and Pyrometers" is the title of Defense Bulletin Number One issued by the Wheelco Instruments Company, Harrison and Peoria Streets, Chicago, Illinois. Substitutes are listed for various materials now in use and properties of both are compared. Many tips on pyrometer care are also given to aid in maintaining present equipment.

The winter issue of *The Educational Focus*, published by the Bausch & Lomb Optical Company of Rochester, New York, contains the following articles: "Using the Microprojector," "Your Eyes and How They Function," "Preparation of Metallurgical Specimens for Microscopical Examination," as well as an editorial dealing with the optical industry in relation to the war. Articles of particular interest in the spring issue are: "Basic Factors in Vision" by W. B. Rayton and "Isaac Newton, 1642–1942" by E. W. Melson.

Two new technical information bulletins entitled "Lumetron Photoelectric Colorimeter" and "Lumetron Photoelectric Fluorescence Meter" have recently been released by the Photovolt Corporation, 95 Madison Avenue, New York, New York. These bulletins contain sketches of each instrument and give detailed instruction regarding their use and care.

Recent improvements in Micromax CO_2 recording equipment are described in a revised catalog issued by Leeds & Northrup Company. Heavy-walled glass tubing in shock-absorber mountings now brings the continuously flowing flue-gas sample from primary filter to cell assembly. Three-way cock for check purposes and condensate drain, previously of metal and external to the cabinet, are now of glass and housed in a separate compartment. Because the flue-gas sample comes in contact only with glass from the time it leaves the stack until it is automatically analyzed, maintenance due to corrosion is eliminated. To receive a copy of this illustrated catalog, write to Leeds & Northrup Company, 4934 Stenton Avenue, Philadelphia, Pennsylvania, for Catalog N-91-163.

The October issue of *Cenco News Chats*, occasional publication of the Central Scientific Company, 1700 Irving Park Road, Chicago, Illinois, discusses "The priorities situation of scientific apparatus," and contains descriptions of many new and improved pieces of apparatus now being offered by this company. More recent issues of this bulletin have been released in January and March of this year.

The July, 1941 issue of *Tin and Its Uses*, quarterly review of the Tin Research Institute, examines the various trends in tin consumption in the United States in the present emergency. The relative merits of tin and the suggested alternatives are discussed. Other articles in this issue include a description of an Australian test of the Institute's process for protecting tinplate against sulphur-staining by foodstuffs; a review of the use of tin in printing metals; an account of further improvements in tinfoil; and a pictorial record of special uses of canned foods in wartime England. The March, 1942 issue features an article on "Tin and War in the Pacific," analyzing the present supply of and demand for tin, and the measures which are necessary to control its use. Also appearing in this issue are reports on research for improved solder fluxes and improvements in the smoothness of tin coatings on tinplate. *Tin and Its Uses* is obtainable free of charge from the Tin Research Institute, Fraser Road, Greenford, Middlesex, or, in the United States, from the Battelle Memorial Institute, 505 King Avenue, Columbus, Ohio.

The Frontier for December, 1941, publication of the Armour Research Foundation, Chicago, Illinois, presents articles on the following topics: "The Cultivation of Guayule Rubber," "Casein Textiles Reach Commercial Status," "Research Finds New Aluminum Sources," and "Gasoline Deodorized by New Process."

Volume XVII, Number 4, of the *Bausch & Lomb Magazine* features an article of special interest entitled, "Anti-Reflection Film on Glass" by A. F. Turner. Volume XVIII, Number 1, released in April, reprints two articles from the spring issue of *The Educational Focus:* "With MacArthur's Men" and "Sir Isaac Newton, 1642–1942." Published by Bausch & Lomb Optical Company, Rochester, New York.

"Prospecting for Knowledge" by Charles F. Kettering is the leading article of the January issue of *The Bakelite Review*. Other articles include "Evolution of Industrial Design," "Designing Molded Plastic Parts," "Unique Properties of Plastics," and short items on new developments and uses of Bakelite products. Published quarterly by the Bakelite Corporation, unit of Union Carbide and Carbon Corporation, 30 East 42 Street, New York, New York.

List CEC, issued by the Cambridge Instrument Company, Inc., 3732 Grand Central Terminal, New York, New York, describes industrial models of analyzers, indicators and recorders. Recording gas analyzers together with ρH and other equipment for precise measurements are featured.

A new 16-page catalog listing over a thousand stock items in rheostats, resistors, tap switches, chokes, and attenuators has been issued by the Ohmite Manufacturing Company. A free copy of Catalog 18 may be obtained by writing to the Ohmite Manufacturing Company, Department 7C, 4835 Flournoy Street, Chicago, Illinois.

Small oil circuit breakers designed for use on alternating current circuits in industrial plants and power houses where interrupting capacities of 50,000 kva are required are described and illustrated in a 12-page catalog released in April by the Roller-Smith Company, Bethlehem, Pennsylvania. The catalog discusses various methods of tripping, describes attachments that can be supplied, gives the characteristics of each size of breaker, and shows dimensions and typical control diagrams.

For industrial, central station, laboratory, and general use, portable switchboard and miniature panel instruments are described in a 34-page booklet B-3013 which may be secured from Department 7-N-20, Westinghouse Electric and Manufacturing Company, East Pittsburgh, Pennsylvania. The new publication lists all instrument types for specific applications on an instrument selector chart. Special features, specification data, and full-scale range of standard ratings are included.

Nickel Steel Topics for March, 1942, presents an interesting leading article describing methods used by the Caterpillar Tractor Company in reclaiming nickel from steel scraps. Published by the International Nickel Company, 67 Wall Street, New York, New York.

Nickel Cast Iron News, Volume 13, Number 1, contains articles dealing with the properties of martensitic cast irons and the heat treatment of alloy cast irons. This is a quarterly publication of the International Nickel Company, Inc., 67 Wall Street, New York, New York.

Other booklets recently received include the followng:

Bulletin 1705 issued by the James G. Biddle Company, 1211–1213 Arch Street, Philadelphia, Pennsylvania, describing their Jagabi "Lubri-tact" laboratory rheostats which feature graphite lubricated contacts to eliminate wear and provide smooth adjustment.

The Ohmite News for February, March, and April, 1942, issued monthly by the Ohmite Manufacturing Company, 4835 Flournoy Street, Chicago, Illinois.

Nickelsworth, Volume IX, Number 1, quarterly publication of the International Nickel Company, Inc., 67 Wall Street, New York, New York.

Bulletin B-103 of the Coleman Electric Company, 318 Madison Street, Maywood, Illinois, describing their Electronic Photofluorometer used for vitamin determinations and *Bulletin T-108*, a strictly technical publication which is a résumé of Vitamin B_1 and B_2 analytical technics to date.

Wheelco Comments, issues of February-March, 1942 and April, 1942, published by the Wheelco Instruments Company, Harrison and Peoria Streets, Chicago, Illinois.